MELISSA HORVAT, BSc

# Biochemical Characterization of Hydratases

**MASTERARBEIT**

zur Erlangung des akademischen Grades

Diplom-Ingenieur

Masterstudium Biotechnologie

eingereicht an der

**Technischen Universität Graz**

Supervisors:

Assoc.Prof. Dipl.-Ing. Dr.techn. Harald PICHLER

Mag. Dr. Tamara Wriessnegger

Institute of Molecular Biotechnology,

Graz, 2016

# AFFIDAVIT

I, Melissa HORVAT, declare that this thesis titled, "Biochemical Characterization of Hydratases" and the work presented in it are my own. I declare that I have authored this thesis independently, that I have not used other than the declared sources/resources, and that I have explicitly indicated all material which has been quoted either literally or by content from the sources used. The text document uploaded to TUGRAZonline is identical to the present diploma thesis.

Signed:

Date:

GRAZ UNIVERISTY OF TECHNOLOGY

# *Abstract*

Institute of Molecular Biotechnology

Master of Science

**Biochemical Characterization of Hydratases**

by Melissa HORVAT

The highly selective production of tertiary alcohols by enzyme catalysis makes kievitone hydrolysis an interesting research target. Three kievitone hydratase (KHS) gene sequences were identified in the organisms *Aspergillus terreus (Ate), Fusarium solani (Fso), Nectria haematococca (Nha)*. Limited biochemical characterization necessitated further investigations of activity, stability, 3D-structure and reaction mechanism of KHSs. The objective of the present work was the discovery of an alternative substrate -apart of kievitone- for investigating biochemical attributes of KHSs. Due to low amounts of KHS proteins in the recombinant host *E. coli*, our focus shifted to their secretory overexpression in *Pichia pastoris*, providing a more natural, i.e. fungal, expression environment. Further, a prenylated plant compound was chosen as the model substrate for further enzyme characterization. In order to propose a reaction mechanism, crystallization experiments were successfully performed and a 3D-structure was proposed. Finally, for large-scale production and characterization of the *P. pastoris* expression strain, a benchtop fed-batch bioreactor cultivation and purification of KHS were performed.

TECHNISCHE UNIVERSITÄT GRAZ

# *Zusammenfassung*

Institut für Molekulare Biotechnologie

Diplom-Ingenieurin

**Biochemische Charakterisierung von Hydratasen**

von Melissa HORVAT

Aufgrund der sehr selektiven biokatalytischen Produktion von tertiären Alkoholen ist die enzymatische Hydrolyse ein interessantes Forschungsgebiet. Drei Kievitone-Hydratase- (KHS) Genesequenzen wurden in den Organismen *Aspergillus terreus (Ate), Fusarium solani (Fso), Nectria haematococca (Nha)* identifiziert, exprimiert und Experimente zur Bestimmung der Aktivität, Stabilität, 3D-Strucktur und des Reaktionsmechanismus von KHSs wurden durchgeführt. Das Ziel dieser Masterarbeit war alternative Substrate -zusätzlich zu Kievitone- für die Charakterisierung von biochemischen Eigenschaften der KHS zu entdecken. Infolge von geringen Mengen an exprimierten KHS-Protein im rekombinanten Expressionssystem *E. coli* wurde der Fokus auf ein natürlicheres, pilzliches, Expressionssystem gelegt. Weiteres wurde ein prenylierter Pflanzeninhaltsstoff als Modelsubstrat für die nachfolgenden Enzymcharakterisierungen verwendet. Um den Reaktionsmechanismus lösen zu können, wurden kristallografische Experimente erfolgreich durchgeführt und eine 3D-Struktur wurde vorgeschlagen. Abschließend wurde eine Fed-Batch Bioreaktorkultivierung durchgeführt um die Ausführbarkeit einer Large-Scale Produktion zu testen und den *P. pastoris* Expressionsstamm weiter zu charakterisieren.

# *Danksagung*

Ohne die tatkräftige und vielseitige Unterstützung, welche ich während meines Studiums erhalten habe, wäre ich nie in der Lage gewesen diese Arbeit zu beginnen wie auch zu beenden, daher möchte ich mit diesen Zeilen meinen herzlichen Dank an folgende Menschen richten:

- Der Technischen Universität Graz, dem Austrian Centre of Industrial Biotechnology und unserem Firmenpartner DSM, welche es mir ermöglichten meine Masterarbeit an diesem Projekt durchzuführen.
- TAMARA WRIESSNEGGER für das immer offene Ohr, die ausgezeichnete Betreuung und Hilfe meine Ideen umzusetzen.
- HARALD PICHLER, welcher mir mit Ratschlägen, Ideen und Lösungsvorschlägen tatkräftig zur Seite stand.
- Der Karl Gruber's Arbeitsgruppe für Strukturbiologie der Karl-Franzens-Universität.
- Gernot Strohmeier's Expertise im Bezug auf HPLC-MS Analytik sowie für die Extraktion und Aufreinigung von Substrat und Produkt.
- Hansjörg Weber, für die Unterstützung durch die NMR-Analyse.
- Den Arbeitsgruppenkollegen Matthias, Anita, Steffi, Eva, Sandra, Simon und Tamara für viele lustige, frustrierende und lehrreiche Stunden im Labor.
- Meinen größten Dank möchte ich jedoch meiner Schwester Marisa, wie auch meinen Eltern widmen. Ohne sie wäre es nie möglich gewesen meine Ausbildung erfolgreich zu beenden. Meine langen erholsamen Wochenenden wie auch frequentierte Telefongespräche gaben mir die nötige Energie und Aufmunterung um auch schwerere Zeiten durchzustehen.

# Contents

# List of Abbreviations

| Abbreviation | Describtion |
|---|---|
| **8-PN** | **8-P**renyl**n**aringenin |
| **ACN** | **Ac**eto**n**itrile |
| ***Ate*** | *Aspergillus **te**rreus* |
| **BMGY** | **B**uffered **G**lycerol- complex **M**edia |
| **BMMY** | **B**uffered **M**ethanol- complex **M**edia |
| **bp** | **B**ase **p**air |
| **CFE** | **C**ell **F**ree **E**xtract |
| **conc.** | **conc**entrated |
| **CV** | **C**olumn **V**olumes |
| **CDW** | **C**ell **D**ry **W**eight |
| **CWW** | **C**ell **W**et **W**eight |
| **d$H_2O$** | **d**eionized **W**ater |
| **dd$H_2O$** | **d**ouble **d**eionized **W**ater |
| **DMSO** | **D**i**m**ethyl**s**ulf**o**xide |
| **DWP** | **D**eep **W**ell **P**late |
| **EC** | **E**nzyme **C**lass |
| **EVC** | **E**mpty **V**ector **C**ontrol |
| **EtBr** | **Et**hidium **Br**omide |
| **EtOH** | **Et**hanol |
| **FA** | **F**ormic **A**cid |
| ***Fso*** | ***F**usarium **so**lani* |
| **HCDC** | **H**igh **C**ell **D**ensity **C**ultivation |
| **HPLC-MS** | **H**igh **P**ressure **L**iquid **C**hromatography- **M**ass **S**pectrometry |
| **HPLC-UV** | **H**igh **P**ressure **L**iquid **C**hromatography- **U**ltra **V**iolet |
| **IPTG** | **I**so**p**ropyl-$\beta$-D-**t**hio**g**alactopyranosid |
| **KHS(s)** | **K**ievitone **H**ydrata**se(s)** |
| **MeOH** | **Me**thanol |
| **Met** | **Met**hionine |
| ***Nha*** | *N**aectria ha**ematococca*** |
| **Ni-NTA column** | **Ni**ckel **N**i**T**riloriaceti**c**Acid purification system |
| **NMR** | **N**uclear **M**agnetic **R**aesonance |
| **nosig** | **No sig**nal sequence |
| **OD** | **O**ptical **D**ensity |

| Continuation of Table | |
|---|---|
| **Abbreviation** | **Describtion** |
| ***OhyA*** | **O**leate **hy**drat**a**se |
| **PCR** | **P**olymerase **C**hain **R**eaction |
| **PMSF** | **P**henyl**m**ethyl **s**ulfonyl**f**luorid |
| ***P. pastoris*** | *Pichia pastoris* |
| **RT** | **R**oom **T**emperature |
| **SCOP** | **S**tructural **C**lassification **O**f **P**roteins |
| **SDS-PAGE** | **S**odium **D**odecyl **S**ulfate - **P**olyacryl **A**mide **G**el **E**lectrophoresis |
| **SIM** | **S**elected **I**on **M**onitoring |
| **SN** | **S**uper**n**atant |
| **TCA** | **T**ri**c**hloracetic **A**cid |
| $\mathbf{T_m}$ | **M**elting **T**emperature |
| **UV- VIS** | **U**ltra **V**iolet **V**isible light |
| **w/oS** | **W**ith**o**ut **S**ubstrate |
| **w/S** | **W**ith **S**ubstrate |
| **WT** | **W**ild **T**ype |
| **XN** | **X**a**n**thohumol |
| **XN-OH** | **X**a**n**thohumol-hydrate |
| **YPD** | **Y**east **P**eptone **D**extrose Medium |

*Dedicated to my family and partner...*

# Chapter 1

# Introduction

Currently, sythesis of secondary and tertiary alcohols is mainly limited to acid catalyzed hydration (see FIGURE 1.1). However, the chemical approaches require complex catalysts [9] or strong nucleophiles [51]. Enantioselective additions of water to $\alpha, \beta$ -unsaturated carbonyl groups (Michael addition) have rarely been documented and represent a challenge [32]. However, limited substrate scope and low yields of regio- and stereoselective alcohols are rational causes for a lack of large scale production processes. So far, only the addition of water to acrolein had been used on an industrial scale. Low conversion rates asked for an improvement of the process. Hence, a biocatalytic approach has been chosen [49]. The energetically inefficient chemical processes without catalyst as well as the limitations of chemical catalysts render alternative approaches highly attractive.

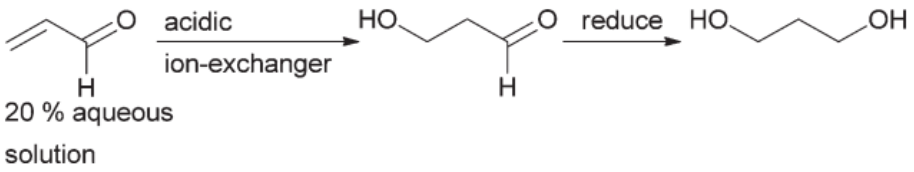


FIGURE 1.1: Addition of water to isolated C=C bonds with acid catalyst (Michael addition). Water added to acrolein, reduction of 3-hydroxypropanal to 1,3-propanediol. [49].

In biological systems, the addition of water, "the liquid of life", to an isolated or conjugated carbon-carbon double bond is needed on a regular basis and is a specialty of enzymes. The class of enzymes (EC) conducting hydrations is known as lyases and can be further classified as hydro-lyases or hydratases (EC 4.2.1), subclass of carbon-oxygen lyases [17]. Addition of water to conjugated carbon-carbon bonds by hydratases allows mild transformation conditions, reduced manufacturing costs and high selectivity of the reaction. In comparison to acid hydration, the selectivity of reactions with biocatalysts is a unique advantage. These benefits have been discovered, implemented and used for large scale productions. Especially over the last 20 years, the interest in hydratases has been growing immensely. Enzymes such as fumarase, malease, citraconase, aconitase, nitrile hydratases and enoyl-CoA hydratase are being used for their highly treasured (regio-

and stereo-) selective attributes [11]. High selectivity, however, comes with a burden of limited substrate scopes.

To explore and broaden the possibilities of hydratases, the glycoenzyme kievitone hydratase was chosen for investigation of reaction mechanism and substrate scope. Up to now, only minimal knowledge of kievitone and kievitone hydratase have been gained. Kievitone is an abundant isoflavonoid synthesized by *Phaseoli vulgaris*, or also known as French bean, when attacked by pathogens. The enzyme (EC 4.2.1.95) reported is secreted by *Fusarium solani f. sp. phaseoli* and detoxifies kievitone, a phytoalexin, by catalyzing the Michael addition to the carbon-carbon double bond of the prenyl-group [46]. The detoxification results in kievitone-hydrate (FIGURE 1.2), which is more polar and a less fungal pathogenic compound [39].

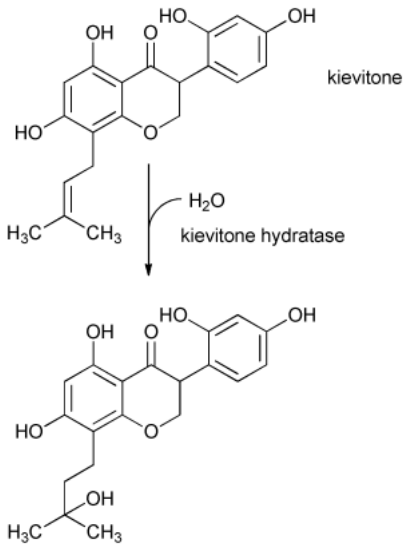


FIGURE 1.2: Kievitone hydratase detoxifies its natural substrate kievitone into a *tert* alcohol [17].

The highly selective production of tertiary alcohols proposes a lucrative field of application for this enzyme category and is immensely fascinating. The investigation of the kievitone hydratases had been tackled following the concept of expression, purification and characterization of oleate hydratase originating from *Elizabethkingia meningoseptica* by Matthias Engleder [21]. Previously, three KHS gene sequences were identified in the organisms *Aspergillus terreus (Ate), Fusarium solani (Fso), Nectria haematococca (Nha)*. Two different overexpression hosts were chosen, *E. coli* as well as *P. pastoris*, for cloning the three different *khs* genes. The aim was to gain sufficient amounts of KHSs for further characterization. Initially, a detection method for kievitone and kievitone-hydrate levels and an activity assay were established. For the purposes of crystallization experiments, muteins

supposedly lacking N-glycans were created. Moreover, variants with mutated and masked native signal sequences were generated to gain insight into the importance of signal sequences [12].

Biochemical knowledge about KHS [7] is limited and further investigations of protein activity, stability, 3D-structure, reaction mechanism as well as broadening the substrate scope are desired. The objective of the present work was to find alternative substrates -apart of kievitone- for investigation of biochemical attributes of KHSs. Due to low amounts of KHS protein in the host *E. coli*, the focus was shifted to secretory overexpression in *P. pastoris*, providing a more natural environment for the fungal enzymes. After identifying two alternative substrates, 8-prenylnaringenin (PN) and xanthohumol (XN), the latter was chosen to be the model substrate for further characterization studies. Hence, optimizations of XN conversion based on ideal physical parameters for *Nha*-KHS, such as pH, temperature- and incubation optima, storage conditions, $T_m$, influences of organic solvents as well as stabilizing the mass balances, were performed. A confirmation of xanthohumol hydrated by NMR was obtained. Kinetics of XN were experimentally determined and reproduced. Also, the role of N-glycosylation sites as well as modified signal sequences of the KHS protein were analysed with expression, thermostability as well as activity-related experiments. In order to propose a reaction mechanism, crystallization experiments were successfully performed and a 3D-model with substrate docking mode was proposed in collaboration with the structural biology group of Karl Gruber. Finally, a benchtop fed-batch bioreactor cultivation and subsequent protein purification were performed to up-scale the *P. pastoris* expression strain and make large quantities of purified *Nha*-KHS for further studies.

# Chapter 2

# Materials and Methods

In the Appendix sections, all instruments and reagents, strains, genes and plasmid descriptions as well as tools for molecular cloning are listed and described.

## 2.1 General methods

### 2.1.1 Agarose gel electrophoresis

Agarose gel electrophoresis was performed with 1% agarose gels containing 0.25 $\mu$g mL$^{-1}$ of EtBr in TAE buffer. Analytical gels were run at 120 V for 45 min whereas preparative gels were run at 90 V for 90 min. Sizes of separated DNA were ascertained by comparison to GeneRuler$^{TM}$ DNA Ladder Mix.

### 2.1.2 DNA gel and PCR purification

DNA fragments in standard 1% agarose gel were purified using the Wizard® SV Gel and PCR Clean UP System. Thirty $\mu$L of dd$H_2O$ preheated to 65°C were used to elute the purified DNA.

### 2.1.3 Preparative DNA restriction

For preparative DNA restriction, a total of 30$\mu$L of purified DNA was incubated with restriction enzyme(s) and appropriate buffer(s) at recommended concentrations for at least 2 h or overnight, at 37°C.

### 2.1.4 Determination of DNA concentration

One $\mu$L of purified DNA was used for measuring the absorbance at 260 nm with the NanoDrop 2000 UV-Vis spectrophotometer to determine the concentration.

### 2.1.5 DNA ligation

Vector backbone and insert were mixed in a molar ratio 1:3 for ligation. Two $\mu$L of ligase buffer as well as 1 $\mu$L of T4-ligase [10 U $\mu L^{-1}$] were added to the DNA and adjusted with $ddH_2O$ to a final volume of 15 $\mu$L. The reaction was incubated at 37°C for at least 30 min. Following inactivation at 72°C for 10 min, the ligation mix was further used for transformation into *E. coli* or stored at -20°C.

### 2.1.6 Transformation of electrocompetent *E. coli* cells

For transformation of ligated vectors, 80 $\mu$L of electrocompetent *E. coli* TOP10 F' cells were mixed with 2 $\mu$L of plasmid, transferred to pre-chilled electroporation cuvettes and incubated on ice for 10 min. Transformation was performed by electroporation (program EC2; electric pulse of 4-5 msec at 2.5 kV) using a MicroPulser electroporator. The addition of 1 mL SOC-medium was performed immediately after transformation. For regeneration of cells, cultures were incubated at 600 rpm and 37°C for 45 min. Then, cells were plated onto LB supplied with appropriate antibiotics and incubated over night at 37°C.

### 2.1.7 Plasmid isolation and control cut

Three selected transformants were chosen, streaked out onto adequate and grown over night. Vectors of chosen clones were isolated using Gene Jet™ Plasmid Miniprep Kit. Control restrictions were performed with FastDigest™ restriction enzymes. After confirmation of successful cloning, vectors were stored at -20°C or further used for transformation into *P. pastoris*.

### 2.1.8 Determination of total protein concentrations via Bio-Rad protein assay

For determination of protein concentrations, a 96-well deep well plate (DWP) protocol, established by A. El-Heliebi [8], was used. Therefore, 10 $\mu$L of suitably concentrated protein samples were transferred to 96-well standard microtiter plates. $ddH_2O$ was used as blank. Calibration was performed with 10 $\mu$L of bovine serum albumin (BSA) ranging from 0.065 mg $mL^{-1}$ to 1.0 mg $mL^{-1}$. The Bio-Rad reagent was diluted 1:5 and 200 $\mu$L of diluted reagent was added to each well. Afterwards, the reactions were incubated for 10 min under moderate shaking. Absorbance was measured at 595 nm. All samples were measured in triplicates.

### 2.1.9 Determination of purified protein concentrations via UV-Vis spectroscopy

In order to determine concentrations of purified enzyme, dilutions of the purified enzymes were performed with 50 mM citrate buffer, pH 6.0, to ensure measurements within the linear range of the spectrophotometer. The dilutions were transferred into semi micro quartz cuvettes and the absorbance was measured in a range from 250 nm to 1000 nm by a Specord 205/BU spectrophotometer. After recoding the spectra, protein concentrations were determined using the absorbance at 280 nm and the respective extinction coefficient $\varepsilon_{280}$. Further, values and the molecular weight of the protein were taken for protein concentration determination[mg $mL^{-1}$] using Beer's law.

$$E = \varepsilon \cdot c \cdot d \tag{2.1}$$

### 2.1.10 SDS-PAGE

Protein samples were denatured by addition of SDS-loading dye (consisting of NuPage ® LDS Sample Buffer (4x) and NuPage ® Sample Reducing Agent (10x)) and by incubation at 37°C for 10 to 20 min. Ten $\mu$L of sample as well as 5 $\mu$L of Novex® Sharp Pre-Stained Protein Standard were loaded onto an SDS-polyacrylamide gel. After running the gels at 125 V and 30 mA for approximately 90 min, gels were further prepared for Western Blot analysis (see next subsection) or stained with Coomassie Blue. Moreover, gels were incubated with Coomassie Brilliant Blue staining solution for approx. 10 min under moderate shaking at RT. Then, gels were destained by applying 10% acetic acid over night at RT.

#### Selfmade gels

SDS-gels were prepared as follows. For separation gels (12.5%), 9.43 mL of dd$H_2O$, 7.03 mL of Tris-HCl(1.5 M, pH 8.8), 11.25 mL of Acrylamid/Bis (30%), 281.25 $\mu$L of SDS (10% w/v), 187.50 $\mu$L ammonium persulfate (APS, 10% w/v) and 28.13 $\mu$L of TEMED were poured and covered with n-butanol. After solidification of the gels and removal of n-butanol with filter papers, the stacking gels (4%) were prepared. Therefore, 11.45 mL of dd$H_2O$, 4.70 mL of Tris-HCl (0.5 M, pH 6.8), 2.45 mL of Acrylamid/Bis (30%), 187.50 $\mu$L of SDS (10% w/v), 93.75 $\mu$L APS (10% w/v), 18.75 $\mu$L of TEMED as well as 10 $\mu$L of phenol-blue were mixed and poured onto the separation gels. Then, 15-well combs were applied. After solidification, gels were stored in Tris-HCl at 4°C.

**NuPage ® SDS-PAGE Gel System**

Ready-to-use NuPage ® SDS from Life Technologies were directly used after removal of the 15-well comb. Denatured protein samples in SDS-Loading Dye as well as ladder standard (Novex® Prestained Protein Ladder) were loaded. The gels were run in 1x MES SDS-Running Buffer at maximum voltage, maximum power and 110 mA for 45 min and further used for Coomassie Blue staining or Western blotting.

### 2.1.11 Immunoblotting - Western Blot

For detailed expression analyses of strains, Western Blots were performed. Therefore, an unlabeled primary antibody (H1029; anti-His antibody from mouse) binds to the antigen ($His_{10}$-tag of the target protein) and a secondary antibody (A4416; Anti- mouse IgG) binds the primary antibody. The secondary antibody amplifies the signal and can be detected by chemiluminenscence (using the SuperSignal® WestPico Chemiluminescent Substrate kit). The protocol was adapted from Haid *et al.* [13].

SDS-PAGE separated proteins were transferred electrophoretically onto nitrocellulose membranes. In order to blot the proteins onto the membranes, a blotting sandwich soaked with 1x transfer buffer was prepared. The setup of the blotting sandwich was as follows starting at the cathode: 3 blotting pads, 2 filter papers, SDS-gel, nitrocellulose membrane, 2 filter papers and 3 blotting pads (anode). Formation of air bubbles was avoided by carefully soaking the pads and filter papers with transfer buffer. After setup, the blotting sandwich was placed into the blotting unit and the inner chamber filled up with buffer. The outer chamber of the *SureLock*® cell and the blotting module was filled with a mixture of water and ice to prevent overheating of the system. Blotting was conducted for 1 h at a current of 125 mA, maximum voltage and maximum power. To confirm the successful transfer of proteins, the membrane was stained with PonceauS (0.1% w/v, in acetic acid 5%) in a plastic box for 2 min. Then, the membrane was destained with dd$H_2O$.

In order to avoid unspecific binding of the primary antibody to the membrane, blocking was performed with 50 mL of TBST- milk for 1 h under moderate shaking at RT. After pouring off the blocking solution, the primary antibody solution (H1029; 1:2000 dilution in TBST with 1% BSA) was applied under moderate shaking over night at 4°C. Afterwards, the membrane was washed for 5x10 min with TBST, followed by incubation with the secondary antibody solution (A4416 in TBST- milk) under moderate shaking at RT for 1 h. The membrane was rinsed for 5x5 min with TBST and transfered to a plastic bag for immunodetection using Bioimager

G:Box HR16. To start the chemiluminenscence reaction, peroxide and enhancer solution were mixed in a 1:1 ratio and applied onto the membrane. After incubation for 2 min, images were taken with the GeneSnap software after 30 s, 4 min, 10 min and 30 min for signal detection.

## 2.2 *E. coli* cultivation for recombinant protein expression

### 2.2.1 Recombinant protein expression in LB-medium

*E. coli* BL21 Star™ (DE3)[pET26b(+)_*Nha*-KHS_$His_{10}$] as well as an empty vector control (EVC) were streaked out directly from glycerol stocks and plated onto LB-Kanamycin and grown over night at 37°C. Overnight cultures (ONCs) were inoculated with a single colony and cultivated in 5 mL of LB-Kanamycin at 130 rpm and 28°C for 12-16 h. The main cultures were prepared by inoculating 50 mL of LB-Kanamycin in 250 mL baffled shaking flasks, with 0.1 $OD_{600}$ units of the ONC and incubation at 130 rpm and 28°C. Cultures were induced with 20 $\mu$M isopropyl-$\beta$-D-thiogalactopyranosid (IPTG) after reaching an $OD_{600}$ of 0.8-1.0 and cultivated for another 6 h until harvest of either 10 or 50 $OD_{600}$ units for resting cells assays or the whole cell pellets for cell free extract (CFE) assays.

### 2.2.2 Preparation of CFEs containing recombinantly expressed protein

For the preparation of CFEs, harvested cell pellets of *E. coli* BL21 Star™ (DE3) [pET26b(+)_*Nha*-KHS_$His_{10}$] as well as an EVC were resuspended in 25 mL of 50 mM potassium phosphate, pH 7.0, and 25 $\mu$L of 1 M PMSF and disrupted by sonification for 2x4 min under 80% duty cycle and an output control level of 8 under extensive cooling. The whole cell lysates were centrifuged at 20,000 rpm and 4 °C for 40 min using a JA-25.50 rotor. Afterwards the CFEs, were used for further analyses.

## 2.3 *P. pastoris* cultivation for recombinant protein expression

Due to low amounts of protein recovery in *E. coli*, *P. pastoris* was applied for recombinant expression of KHSs. To facilitate secretion of KHSs into the culture supernatant (SN), an expression cassette encoding *S. cerevisiae* $\alpha$ -mating factor signal sequence was chosen. Simultaneously, expression from a construct without a signal sequence was assessed.

### 2.3.1 Recombinant protein expression in BMGY/BMMY-medium

Ten mL of BMGY were inoculated with a respective *P. pastoris* strain from a YPD-plate. The ONCs were grown at 170 rpm and 28 °C with 80% humidity. The main culture was prepared by inoculation of 25 mL of BMGY in 250 mL baffled shaking flasks with 0.1 $OD_{600}$ units of the ONC and grown at 130 rpm and 28 °C for 24 h. Then, 25 mL of BMMY with 1% of methanol (MeOH) were added to a final concentration of 0.5% of MeOH. Cultures were induced for 48 h, every 12 h with 1% of MeOH, before harvest.

Cultivations for purification of recombinantly expressed protein, were performed in 200 mL of BMGY and 200 mL of BMMY in 2 L baffled shaking flasks at 100 rpm and 28 °C. The procedure was adapted from the *Pichia* Expression Kit, Invitrogen™ by life techonolgies™.

### 2.3.2 Riezman cell disruption and TCA-precipitation

Cells were disrupted using an adaption of the protocol established by Riezman and Horvath [15]. After harvest of 6 $OD_{600}$-units by centrifugation at 3,500 rpm for 5 min, SN was discarded and the pellet was resuspended in 300 $\mu$L of 1.85 M NaOH and 7.5% (w/v) of $\beta$- mercaptoethanol. The suspension was incubated on ice for 10 min and 300 $\mu$L of 50% (w/v) TCA were added. Protein was precipitated on ice over night and centrifuged at 13,200 rpm and 4 °C for 40 min. The SN was discarded and the pellet was washed twice with 500 $\mu$L of ice-cold $dH_2O$. The pellet was resuspended in 30 $\mu$L of SDS-loading dye, incubated at 65 °C for 3 min, briefly centrifuged at 13,200 rpm and loaded onto an SDS-polycrylamide gel for Coomassie Blue staining or Western Blot analysis.

To precipitat the culture SN, 400 $\mu$L of cell culture were centrifuged at 5,000 rpm for 5 min. The SN was transferred to new 1.5 mL reaction tubes. After incubation on ice for 10 min, 100 $\mu$L of 50% TCA were added. Further steps were performed as described in the Riezman cell disruption protocol. The pellet was resuspended in 20 $\mu$L of SDS-loading dye.

### 2.3.3 MeOH-Chloroform precipitation

Since TCA-precipitation may be ineffective for precipitation of proteins from the culture SN, precipitation with MeOH-chloroform ($CHCl_3$)was assessed as an alternative.

Therefore, 400 $\mu$L of cell culture were harvested by centrifugation and the SN was transferred into new 2.0 mL reaction tubes. Then, 480 $\mu$L of MeOH, 160 $\mu$L of $CHCl_3$ and 640 $\mu$L of $ddH_2O$ were added and vortexed briefly. After centrifugation at 13,200 rpm for 5 min, precipitated protein

was found in the interphase. The upper layer containing MeOH/d$H_2O$ mixture was carefully removed and an additional 300 $\mu$L of MeOH was added. Tubes were again vortexed and centrifuged at 13,200 rpm and 4 °C for 30 min. The entire SNs were removed and the pellet was dried at 65 °C for 5 min. Afterwards, the dried pellet was resuspended in 30 $\mu$L of SDS-loading dye and loaded onto an SDS-polyacrylamide gel for Coomassie Blue staining or Western Blot analysis.

### 2.3.4 Preparation of concentrated SN containing recombinantly expressed protein

After the cultivation of *P. pastoris* CBS7435 [pPpT4_$\alpha$_S_*Nha*-KHS_$His_{10}$] and *P. pastoris* CBS7435 wild type (WT), 400 mL of cell cultures were harvested by centrifugation with an Anvanti ™ centrifuge using JA 8.1 rotor at 5,000 rpm and 4 °C for 30 min. The SN was sterile filtered with 0.2 $\mu$m filters and transferred into Amicon® Ultra-15 centrifugal filter devices with a molecular weight cutoff of 30 kDa. SNs were concentrated by centrifugation at 4,000 rpm for 15 min.

## 2.4 Purification of recombinant protein

Due to the native signal sequence as well as the $\alpha$-mating factor sequence on the expression vector, secretion of recombinantly expressed protein into the media was established. Purification attempts directly from the culture SN were successful. For purification of recombinant protein from culture SN, gravity-flow purification system as well as the Äkta prime purifier system were tested and compared. In Table 2.1 the used buffer systems and compositions are listed. All purification procedures were either performed at 4°C or in the cold room.

TABLE 2.1: Buffers and compositions used for protein purification

| **Buffer** | **Composition** |
|---|---|
| Binding Buffer | 50 mM $NaH_2PO_4$, pH 7.0, 300 mM NaCl, 10 mM imidazole |
| Washing Buffer | 50 mM $NaH_2PO_4$, pH 7.0, 300 mM NaCl, 50 mM imidazole |
| Elution Buffer | 50 mM $NaH_2PO_4$, pH 7.0, 300 mM NaCl, 250 mM imidazole |
| Desalting Buffer | 50 mM citrate, pH 6.0 |

### 2.4.1 Gravity-flow purification

Purification was performed with self-packed Ni- Sepharose®, columns (GE Healthcare-USA). After equilibration with 5 column volumes (CV) of Binding Buffer, 50 mL of filtered SN were loaded. The column was washed with 5 CV of Binding Buffer and 5 CV of Washing Buffer, which was prepared by diluting the Elution Buffer 1:5 with Binding Buffer. Then, 5 CV of Elution Buffer were applied and the elution fractions were collected in pre-cooled reaction tubes. Elution fractions were pooled, concentrated and desalted using a PD-10 desalting column. After elution, the column was re-equilibrated with 5 CV of Binding Buffer and stored in 20% ethanol (EtOH).

After every purification, the column was regenerated to assure optimal purification conditions. Therefore, residual $Ni^{2+}$ was washed off with 5 CV of 20 mM potassium phosphate, pH 7.4, containing 500 mM NaCL and 50 mM EDTA. Excessive EDTA was removed with 5 CV of Binding Buffer. After washing with $ddH_2O$, beads were recharged with 0.5 CV of 0.1 M $NiSO_4$. Then, the column was washed with 5 CV of $ddH_2O$ and equilibrated with 5 CV of Binding Buffer before storing in 20% ethanol at 4°C.

### 2.4.2 Purification with Äkta purifier system

Even though the gravity-flow protocol used showed good results, for a larger scale purification gravity-flow procedure was not suitable. For all biochemical analyses the gravity-flow purification was performed. However in order to evaluate the amount of recombinantly expressed *Nha*-KHS, after bioreactor cultivation of *P. pastoris* CBS7435 [pPpT4_$\alpha$_S_*Nha*- KHS_$His_{10}$] the Äkta prime system was applied for the purification of *Nha*-KHS from 300 mL of concentrated culture SN. Therefore, a ready-to-use HisTrap™ FF crude column (GE Healthcare, USA) with a CV of 10 mL and a binding capacity of approx. 400 mg was regenerated with the same protocol used for self-packed columns in gravity-flow purification. After regeneration and equilibration of the column with Binding Buffer, 50 mL of filtered and concentrated culture SN was applied at a flow rate of 3 mL $min^{-1}$. The column was washed with 5 CV of Binding Buffer at a flow rate of 3 mL $min^{-1}$. A second washing step was conducted with 20% Elution Buffer and 80% Binding Buffer for 7 CV. Afterwards, the protein was eluted with 15 CV of Elution Buffer at flow rate of 2 mL $min^{-1}$. To monitor the purification process on-line, the absorbance at 280 nm was observed. The elution fractions were collected, pooled, concentrated to 7 mL as described above with an Amicon® Ultra-15 centrifugal filter devices and immediately desalted.

### 2.4.3 Desalting of purified protein

For buffer exchange and removal of high imidazole concentrations after purification, proteins were desalted using either a PD-10 column as for the gravity-flow purification or a HiPrep 26/10 Desalting column. Columns were equilibrated with 50 mM citrate, pH 6.0. Then, concentrated $His_{10}$-tag purified enzyme was loaded. Fractions were eluted with a flow rate of 1 mL $min^{-1}$ and monitored on-line at $A_{280}$.

### 2.4.4 Gel filtration

In order to account for the formation of different oligomers and to further purify the protein, a size-exclusion chromatography step was conducted after gravity-flow purification. Therefore, a HiLoad 16/600 Superdex 200 column combnation with Äkta prime system was used. The column had a diameter of 16 mm and was packed with dextran covalently bound (GE Healthcare, USA). The CV was 120 mL and the separation range of globular proteins was 10-600 kDa. Prior to application of protein to the column, it was equilibrated with Desalting Buffer. Afterwards, the column was loaded with concentrated $His_{10}$-tag purified protein. Then, the protein was carefully eluted with a flow rate of 1 mL $min^{-1}$. Afterwards, the fractions were analyzed via SDS-PAGE and activity assay.

## 2.5 Determination of kievitone hydratase activity

### 2.5.1 Kievitone conversions: Resting cells assays in *E. coli*

Ten as well as 50 $OD_{600}$ units of *E. coli* BL21 Star™ (DE3) [pET26b(+)_*Nha*-KHS_$His_{10}$] and EVC were harvested by centrifugation at 4,000 rpm for 10 min. The SN was discarded. The pellet fraction was resuspended in 98 $\mu$L of 50 mM potassium phosphate, pH 7.0 and transferred into a PYREX® reaction tubes. The reaction was started by adding 2 $\mu$L of kievitone from a 100 mM stock solution in EtOH to a final concentration of 2 mM. Afterwards, the reaction was mixed well and was incubated at 150 rpm and 28°C over night in a 55° angle. Two $\mu$L of substrate and product standards were added to 98 $\mu$L of buffer from 100 mM stock solutions in EtOH, mixed and incubated over night under the conditions mentioned for the resting cells assays. Also, EVCs resuspended in buffer, with and without the addition of substrate were incubated over night as negative controls. After bioconversion, the reaction mix was centrifuged at 13,200 rpm for 10 min, transferred into HPLC-vials and measured via HPLC-UV. Single measurements were conducted due to limited resources of the substrate kievitone.

### 2.5.2 Measurement of enzyme activity with HPLC-UV

The method used was adapted by Stefanie Gabriel [12]. Five $\mu$L of sample were injected into the device. The column (Phenomenex Gemini-NX 5u C18, 250 x 4.6 mm) was eluted with a gradient elution system consisting of 0.1% of formic acid (FA) in water and acetonitrile (ACN). Separation of substrate and product was achieved using a linear gradient from 0 min (5% ACN) to 30 min (98% ACN) at a flow rate of 0.6 mL $min^{-1}$. The column temperature was maintained at 40°C. For detection of the substrate and product, two separate UV/Vis-channels at 220 nm and 291 nm were monitored. Kievitone eluted approximately at 21 min and kievitone-hydrate, due to its increased polarity, at a retention time of 17 min. HPLC-UV analyses were evaluated with the Agilent ChemStation software and quantified using a previously generated calibration curve [12].

## 2.6 Conversion of alternative substrates

### 2.6.1 *In vitro* conversion of alternative substrates using *E. coli* CFE

Two $\mu$L of either XN 100 mM or 8-PN 100 mM, were added to 98 $\mu$L of CFEs for a final substrate concentration of 2 mM. After mixing, the reactions were incubated at at 150 rpm and 28 °C over night. For stopping the reaction, 300 $\mu$L of ACN were added and shaken at 300 rpm for 15 min. Then, after centrifugating at 13,200 rpm to precipitate protein, approximately 80 $\mu$L of SN were pipetted into HPLC vials for HPLC-MS analysis. The substrate standards as well as EVCs without substrate were treated equally. All activity assays were conducted in triplicates.

### 2.6.2 Preparation of resting cells assay in *P. pastoris*

For resting cell assays, the strains *P. pastoris* CBS7435 [pPpB1_S_*Nha*-KHS-$His_{10}$], *P. pastoris* CBS7435 [pPpT4_$\alpha$_S_*Nha*-KHS-$His_{10}$] as well as the wild type strains were cultivated and induced as previously described. Then, 10 and 50 $OD_{600}$ units were harvested by centrifugation at 5,000 rpm for 10 min. The pellets were resuspended in 98 $\mu$L of 50 mM potassium phosphate, pH 7.0, and incubated with 2 $\mu$L of xanthohumol, added from a 100 mM stock in EtOH, at 150 rpm and 28 °C for 15 h.

### 2.6.3 Preparation of *in vitro* activity assays (concentrated SN and purified KHS)

As already mentioned before, culture SN of *P. pastoris* CBS7435 [pPpT4_$\alpha$_S_*Nha*-KHS-$His_{10}$] was concentrated as well as purified with Ni-NTA column. Protein concentrations were determined via Bradford-assay whereas the protein concentration in the purified supernatant was determined via UV-Vis spectroscopy. For each assay 100 $\mu$g of *Nha*-KHS-$His_{10}$ was used for the conversion of either 2 mM XN or 2 mM 8-PN added from a 100 mM stock EtOH. The assays were incubated at 150 rpm and 28 °C for 15 h in a 55° angle.

### 2.6.4 Measurement of enzyme activity with HPLC-MS

Throughout optimization of the activity assay, two instruments were used for determination of substrate conversion. Results including peak area values $[mAU * s]$ on the y-axis were measured with a HPLC-MS in the Biocatalysis building, whereas results stated in mM were obtained via a HPLC-MS system located in the Chemistry department. The enzyme activity results, given in peak area values were measured on an Agilent (1200 series system) equipped with a mass spectra detector (MS), variable wavelength detector (VWD) and an automatic injector (Agilent). The gradient as well as elutents for analysis were the same as in the previously described HPLC-UV method (see chapter of enzyme activity with HPLC-UV). The flow rate was set at 1.0 mL $min^{-1}$. A phonemenex HPLC column (RP-18e (5$\mu$m), 250 x 4.6 mm) was used and the column thermostat was set at 40 °C. Substrates and products were identified by characteristic fragmentation patterns recorded at *m/z* 339.4 for 8-PN, *m/z* 356.4 as well as *m/z* 358.4 for OH-8-PN, wherease XN was detected at *m/z* 355.4 and OH-XN at *m/z* 371.4 and *m/z* 373.4 . For detection of 8-PN and OH-8-PN, the wavelength was set at 290 nm, whereas for XN and OH-XN, the wavelength was set at 371 nm.

For evaluation of biochemical characterization experiments of *Nha*-KHS, an Agilent 1200 HPLC system with MS and VWD detection was applied using an adapted and shortened gradient elution system compared to the method previously described. The elution system consisted of 0.1% FA in water (A) and 0.1% FA in ACN (B). The gradient was set as follows: 0 min, (40% B); 7 min, (98% B); 8 min, (5% B) at flow rate 0.7 mL $min^{-1}$. A Poroshell HPLC column, (RP-18e 5 $\mu$m, 180 x 4.6 mm) was used and the thermostat was set at 30 °C. XN was detected at *m/z* 355.4 and 371 nm and OH-XN at *m/z* 373.4 as well as 371 nm. For quantification of XN and OH-XN, a linear calibration curve with the following equation was establish with at an $R^2$ value of 0.98 with 0.065-0.750 mM purified compounds:

$$y = 655890x + 35044 \tag{2.2}$$

## 2.7 Extraction of XN from hops extract capsules

The extraction and purification of XN from hops extract was meticulously performed by Gernot Strohmeier. XN was extracted from capsules containing hops extract purchased from Allcura, Germany. A total of 606.97 g of extract was applied for extraction in three consecutive batches. To 200 g of powder, 500 mL of MeOH and 1 mL of FA were added and the mixture was heated to 60 °C for 30 min. After that, the insoluble solid was filtered off with a Büchner funnel and was washed four times with each 75 mL each of hot MeOH until the filtrate became virtually colorless. The solvent was removed under reduced pressure and the residue was stored at 4 °C in the presence of nitrogen until continuing the work-up. The combined yield of extracts was 158.4 g. TLC analysis of the crude material: Rf(cyclohexane/ethyl acetate 1:1): 0.03-0.16 (most of contamination); 0.39 (xanthohumol); 0.79 and 0.85 (unknown compounds). For further identification of purity of the extract a dilution of 1:100 was measured via HPLC-UV 2.1 with the same gradient and elutents mentioned for xanthohumol activity assays. The wavelength used was 210 nm.

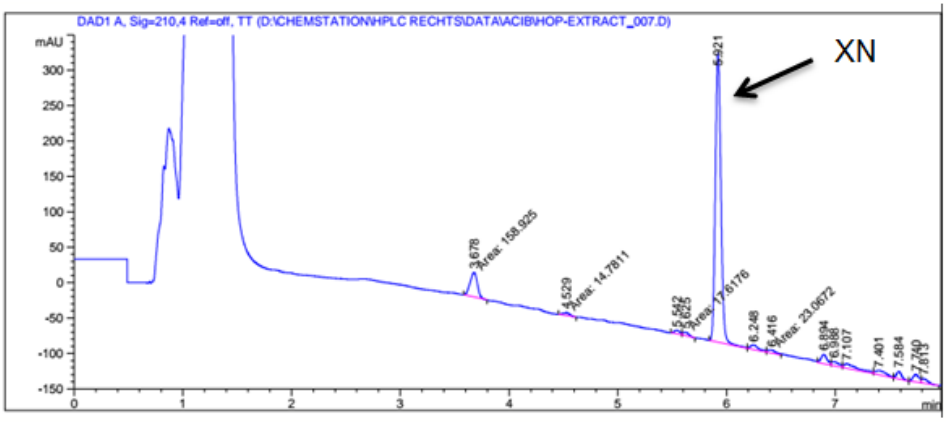


FIGURE 2.1: HPLC-UV signal $[mAU]$ of 210 nm, showing all components of the dissolved hops extract to identify further purification steps. Xanthohumol showed a retention time of $\sim 5.9min$.

To remove the polar contaminants, consecutive solid-phase extractions were conducted. The crude residue was treated with 400 mL of hot cyclohexane/ethyl acetate 3:1 and the mixture filtered through a 4 cm plug of approximately 50 g silica gel in a glass frit. Elution with cyclohexane/ethyl acetate 3:1 was continued until all XN was recovered. After removal of the volatiles under reduced pressure, 102.923 g of crude product was obtained. Then, 300 mL of hot acetone and 200 g silica gel were added and the solvent was removed to obtain the silica gel deposited crude material. This

mass was placed on a flash chromatography column filled with 250 g silica gel pretreated with cyclohexane/ethyl acetate 4:1. Elution was started with cyclohexane/ethyl acetate 4:1 (1 L) and then continued with cyclohexane/ethyl acetate 3:1. All fractions containing XN were combined and evaporated to dryness, leaving 32.985 g of crude product. This material was subjected to flash chromatography purification on 120 g silica gel using cyclohexane/ethyl acetate mixtures starting from 6:1 to 1:1 for elution. After removal of all volatiles from the fractions containing XN, 23.225 g of crude product was obtained. This product was found sufficiently pure to continue with a recrystallization from ethyl acetate/cyclohexane (approximately 45 mL). Following a second recrystallization from 20 mL of ethyl acetate and 50 mL of cyclohexane, 4.23 g pure XN was obtained ($\geq$ 99% purity; rp-HPLC at 210 nm). The mother liquors were combined and purified by flash chromatography on 200 g silica gel using dichloromethane/acetone 50:1 for elution. After pooling the product-containing fractions and removal of the volatiles under reduced pressure, 6.175 g of fairly pure XN was obtained. Then the material was recrystallized from 25 mL of ethyl acetate + 50 mL cyclohexane leading to 4.938g of pure XN ($\geq$ 99% purity; rp-HPLC at 210 nm). The overall yield of pure XN was 9.168g.

## 2.8 Confirmation of the product XN-OH

After successful detection of putative product peaks in HPLC chromatograms, further work mainly focused on XN, since in all assays the highest conversions among all alternative substrates were obtained. To unambiguously confirm the addition of the hydroxy-group to the substrate, Dr. Hansjoerg Weber of the Organic Chemistry department at Graz Univeristy of Technology was asked to perform an NMR-analysis of the isolated putative product.

Therefore, large scale conversions of XN with a total of 5 mg of substrate were conducted. One-hundred $\mu$L of purified *Nha*- KHS-$His_{10}$ (1 mg $mL^{-1}$) were incubated with 19 $\mu$L of 100 mM XN, disslved in EtOH, and 880 $\mu$L of 50 mM citrate, pH 6.0. The conversion was prepared seven times in parallel. The bioconversions were incubated at 150 rpm and 35 °C for 16 h in a 55° angle. Also, a *P. pastoris* wild type strain was incubated with and without substrate. After the addition of 3 mL of ACN, the samples were mixed well and centrifuged at 4,000 rpm for 15 min. Afterwards, the product was extracted, dried by Gernot Strohmeier and stored at -20 °C until it was dissolved in 4 mL of $CD_3OD$ and was sent to NMR analysis. $^{1}$H- and $^{13}$C-NMR experiments were performed on a Varian Inova-500 spectrometer (at 500 MHz and 125 MHz, respectively). Signals were reported in ppm ($\delta$)

using solvent as an internal standard. The sample was then extracted and solidified.

## 2.9 Optimization of assay conditions for XN

For the optimization of the activity assay various conditions and adaptations were performed. Unless otherwise stated, all assays were performed in triplicates and in a reaction volume of 100 $\mu$L, with 10 $\mu$L of purified *Nha*-KHS, 88 $\mu$L of citrate, pH 6.0, and 2 $\mu$L of substrate from a 25 mM stock in EtOH for a final XN concentration of 0.5 mM. After incubation, protein was precipitated with 300 $\mu$L of ACN and assays were centrifuged at 13,200 rpm for 5 min. Then, they were filled into HPLC vials and measured with HPLC-MS.

For optimization of pH conditions, 50 mM citrate, pH 4.0-6.0, 50 mM potassium phosphate, pH 7.0-8.0, as well as 50 mM Tris, pH 9.0, were used. Activity assays were incubated at 150 rpm and 28 °C at a 55° angle for 15 h. For detection optimization of the reaction temperature, conversions were performed from 15 °C to 40 °C, in 5 °C steps. Assays were incubated for 10 min. To optimize incubation times, a time course was performed, starting from 5 min to 48 h at 150 rpm and 28 °C. The assay was performed in 50 mM potassium phosphate, pH 7.0. Due to observed variations in sample area peaks, the same conversion was measured with HPLC-MS instantaneously after conversion as well as after a storage at 4 °C °C for 11 h. The conversion was conducted at 35 °C for 15 min.

Since literature describes a stabilizing effect of FA on flavonoids has been reported [20], addition of FA to the reaction mix after conversion was tested. Also, the effect of MeOH as a protein precipitating agent was compared to the method used previously. Therefore, assays were incubated with 10 $\mu$L of purified *Nha*-KHS [0.5 mg $mL^{-1}$] at 35 °C for 2 min. Afterwards, samples were precipitated with 300 $\mu$L of 100% ACN, 300 $\mu$L of ACN and 4 $\mu$L of FA or 300 $\mu$L of MeOH and 4 $\mu$L of FA. All samples were mixed well, centrifuged at 13,200 rpm for 5 min and measured either directly via HPLC-MS or after storage at RT for 11 h.

To optimize the mass balance, an additional dilution step was applied to samples with high substrate and/or product concentrations. Therefore, activity assays with XN concentrations of 0.5 mM -10.0 mM were incubated with 10 $\mu$L of *Nha*-KHS 0.5 mg $mL^{-1}$ at 35 °C for 3 h. After addition of 300 $\mu$L of MeOH and 1% of FA, conversions including XN 10 mM were additionally diluted 1:10 with MeOH and also measured with HPLC-MS.

In order to test for residual activity of purified *Nha*-KHS after storage under different conditions, the purified enzyme was either frozen at -20 °C,

stored at 4 °C or freeze dried via a Christ lyophilisor. All samples were stored for 60 h and then used for bioconversions with 0.05 mg of enzyme, incubated at 35 °C for 2 min, precipitated with 300 $\mu$L of MeOH and 1% of FA, mixed, centrifuged and measured via HPLC-MS.

To detect effects of organic solvents on the reaction, activity assays with 0.5, 1.0, 5.0, 10.0 and 30.0% of different organic solvents were selected. Therefore, EtOH, DMSO, dodecane, n-hexane and chloroform, all obtained from Roth GmbH, were chosen to be added to the conversion reactions. The reactions were incubated at 35 °C for either 2 min or 3 h. Afterwards, 300 $\mu$L of MeOH and 1% of FA were added to the samples, mixed, centrifuged and measured via HPLC-MS.

## 2.10 Biochemical analyses

### 2.10.1 Kinetics of *Nha*-KHS-His$_{10}$

To determine kinetic parameters of *Nha*-KHS-His$_{10}$ for XN conversion assays with 0.05 mg mL$^{-1}$ of enzyme were conducted. The substrate concentrations increased from 0.125 mM to 3.0 mM. The assays were incubated at 150 rpm and 35 °C of a 55° angle for 2 min. Afterwards, protein was precipitated with 300 $\mu$L of MeOH and 1% of FA, mixed, centrifuged and measured via HPLC-MS as diescribed bove. All samples were measured in triplicates. After determination of specific activity, data were ploted with SigmaPlot®.

In order to confirm the linear range of activity in low concentrations of substrate 0.125 mM-0.325 mM, activity assays were conducted adapting the incubation time from 30 sec to 2 min. All other parameters of the assays were mentioned above.

### 2.10.2 Influences of N-glycosylation on *Nha*-KHS-His$_{10}$ activity

*P. pastoris* CBS7435 [pPpT4_$\alpha$_S_ *Nha*-KHS-His$_{10}$] was cultivated and induced as described above. *Nha*-KHS-His$_{10}$ was purified from the culture SN and the concentration was determined via UV-Vis spectroscopy. Fifty $\mu$L of *Nha*-KHS-His$_{10}$, 11.28 mg mL$^{-1}$, were mixed with 0.5 $\mu$L of Endo$H_f$ and 5.5 $\mu$L of G5 buffer (10x) and incubated for 0.5 -2.5 h at 37 °C. Also, respective negative controls containing deglycosylation enzyme mix with only buffer, *Nha*-KHS-His$_{10}$ with buffer and buffer only, were incubated at 37 °C for 2.5 h. For sample analysis, an SDS-PAGE with Coomassie Blue staining as well as Western Blot analysis were conducted. For expression analyses, 2.5 $\mu$g of *Nha*-KHS-His$_{10}$ were loaded onto the gel. In order to test for differences in stability and activity of (de-)glycosylated *Nha*-KHS-His$_{10}$, thermo stability

analyses via Thermofluor® assays with 20 $\mu$g of *Nha*-KHS-$His_{10}$ and *in vitro* activity assays with 100 $\mu$g of *Nha*-KHS-$His_{10}$ were conducted.

For comparison of thermostability, 1 $\mu$L of either glycosylated *Nha*-KHS-$His_{10}$ or deglycosylated *Nha*- KHS, both 20 mg $mL^{-1}$, were added to 2 $\mu$L of SYPRO® Orange (1:500 dilution) and 22 $\mu$L of respective 50 mM buffer system ranging from pH 4.0 to 9.0. The samples were measured in triplicates with a CFX Connect Real-Time PCR system (BioRad). Samples were preheated to 25 °C before raising the temperature to 95 °C, at 1 °C $min^{-1}$ ramps.

### 2.10.3 Confirmation of $T_m$ and refolding attempt with nanoDSF

*P. pastoris* CBS7435 [pPpT4_$\alpha$_S_ *Nha*-KHS-$His_{10}$] was cultivated and induced as mentioned above. Enzyme was purified and protein concentration was determined via UV-Vis spectroscopy. Then, *Nha*-KHS-$His_{10}$ was diluted to a final concentration of 1 mg $mL^{-1}$ and was rebuffered with either 50 mM citrate, potassium phosphate or Tris, pH 4.0-9.0. Ten $\mu$L of the enzyme were sucked up by a glas capillary and were analyzed via the Prometheus NT.48 (NanoTemper Technologies). All measurements were reproduced in duplicates. The temperature increase was 1 °C $min^{-1}$ starting at 20 °C to 95 °C. For the refolding experiment the same samples were used. Temperature was increased from 20 °C to 65 °C, held for 1 min at 65 °C and decrease the temperature decreased again from 65 °C to 20 °C. The gradient was 5 °C $min^{-1}$.

## 2.11 Generation of *P. pastoris* CBS7435 [pPpT4_$\alpha$_S_*Nha*-KHS-$His_{10}$] multicopy strains (DWP and flask cultivation)

### 2.11.1 Transformation of electrocompetent *P. pastoris* cells

For the creation of multicopy strains, 10 $\mu$g of vector [pPpT4_$\alpha$_S] (30 $\mu$L) were linearized with 2 $\mu$L of *Pst*I, 4 $\mu$L of 10x Orange Buffer and 4 $\mu$L of $ddH_2O$. The reaction mix was incubated at 37°C over night. The linearized plasmid was loaded onto a 1% preparative agarose gel, the correct band was identified by size, cut out of the gel and purified as described previously.

Meanwhile, a single colony of *P. pastoris* CBS7435 was used for inoculation of an ONC in 5 mL of YPD medium, grown at 150 rpm and 28°C for 15 h. The main culture was inoculated with 0.1 $OD_{600}$ units, grown to 0.8-1.0 $OD_{600}$ and centrifuged with a table top centrifuge at 1,600 rpm for 5 min.

The cell pellet was resuspended in 9 mL of BEDS solution and 1 mL of 1 M DTT and was incubated at 100 rpm and 30°C for 5 min. Afterwards, the cell suspension was centrifuged at 1,600 rpm for 2 min and resuspended in 1 mL BEDS solution too. Then, 80 $\mu$L aliquotes of electrocompetent cells were prepared.

The aliquotes were mixed with 10 ng of linearized plasmid, transferred to pre-chilled electroporation cuvettes and incubated on ice for 5 min. Cells were transformed by electroporation (program Pic; electric pulse of 4-5 msec at 2.5 kV) using a MicroPulser electroporator. Immediately after transformation, 500 $\mu$L of ice cold 1 M sorbitol and 500 $\mu$L of YPD were added . For regeneration of the cells, they were incubated at 300 rpm and 28°C for 2 h. Afterwards, aliquots were plated on YPD- Zeocin$^{100}$ and incubated at 28°C for 48 h.

### 2.11.2 Cultivation of multicopy strains in DWPs

In order to evaluate the expression levels of *Nha*-KHS-His$_{10}$ multicopy strains, positive clones were pinned onto YPD- zeocin plates with elevated Zeocin concentration from 100 mg L$^{-1}$ to 2 g L$^{-1}$ for higher selection pressure. Afterwards, a pinhead-size amount of cell material of selected clones was used to inoculate the preculture in a 96-DWP with 500 $\mu$L of BMGY. The plate was incubated at 320 rpm 28 °C and 50% humidity for 12-16 h. Afterwards, the main culture was prepared by inoculation of 350 $\mu$L of BMGY in a new 96-DWP with 0.2 OD$_{600}$ units of preculture and incubated under the same conditions for 24 h. Also, OD$_{600}$ measurements were performed every 12 h to monitor cell growth. Then, 350 $\mu$L of BMMY with 1% methanol were added and the plate was incubated further. Every 12 h, 10 $\mu$L of MeOH were added for induction. After 48 h, the final OD$_{600}$ was measured and 6 OD$_{600}$ units were harvested for Riezman cell disruption. Then, the DWP was centrifuged at 4,000 rpm from 15 min and 400 $\mu$L culture SN were aliquoted for TCA-precipitation and 400 $\mu$L of culture SN for activity analysis. Additionally, selected multicopy strains were cultivated in baffled shake flasks. The pellet was disrupted and protein in the culture SN samples was precipitated using MeOH/$CH_3Cl$. Both fractions were analyzed via SDS-PAGE, Western Blot and activity assay with 2 mM XN. Reactions were performed for 2 min at 35 °C, 150 rpm.

## 2.12 DASGIP® Bioreactor Cultivation of *P. pastoris Nha*-KHS

### 2.12.1 High cell density cultivation

Bioreactor cultivation protocol, media, such as basal salt medium (BSM) [14], and buffers were adapted from Tolner *et al* [48]. After set-up of the DASGIP ® bioreactor cultivation system,the pre-cultures of *P. pastoris* CBS7435 [pPpT4_$\alpha$_S_*Nha*-KHS-$His_{10}$] as well as the wild type strain were incubated at 150 rpm and 28 °C for 48 h. The main cultures were inoculated with 1 $OD_{600}$ unit in 60 mL BMGY and were grown to an $OD_{600}$ of 15. Then, 50 mL of the main cultures were transferred into 550 mL of BSM in bioreactors and incubated at 28 °C, pH 6.0, agitation 500-1,200 rpm, dissolved oxygen (DO) level 100%. Temperature, pH and DO levels were kept constant during fermentation. pH was regulated with 25% ammonia and DO levels were kept above 20% by adapting the stirrer speed at a constant air flow. After 15 h of batch-cultivation glucose was added (see Table 2.2). The glucose fed-batch was continued for 17 h until an $OD_{600}$ of 100 OD was reached.

TABLE 2.2: Glucose-Feed

| **time [h]** | **Glucose [mL $h^{-1}$]** |
|---|---|
| 0.0 | 1.78 |
| 1.0 | 2.11 |
| 2 | 2.58 |
| 3 | 3.15 |
| 4 | 3.54 |
| 5 | 4.70 |
| 6 | 5.74 |
| 7 | 7.00 |
| 8 | 8.56 |
| 9-17 | 10.15 |

The MeOH-induction phase was carried out for 123 h with a flow rate of 5 mL $h^{-1}$. Samples were taken every 6 h, sample t0 was taken before induction. After 123 h of induction the cell cultures were harvested and analyzed as described in the following section.

### 2.12.2 Sample analyses

All protein concentration determinations were conducted by Bradford-assay as described previously. Once every 24 h, culture SN was precipitated using TCA-precipitation and was loaded onto a NuPAGE® SDS-PAGE.

### $OD_{600}$ measurement

Five $\mu$L of well mixed cell culture were diluted with 1,995 $\mu$L of BSM, well mixed and measured with an Eppendorf photometer. All samples were measured in triplicates.

### CDW-measurement

Once every 24 h the cell dry weight (CDW) of the cultures was determined. Therefore, 1 mL of well-mixed cell culture was transfered into a pre-weighed reaction tube. Samples were centrifuged at 13,200 rpm for 5 min. The SN was transferred to another reaction tube and used for further analyses whereas the cell pellet was dried at 100 °C over night and weighed. At the end of cultivation the cell cultures were harvested by centrifuging twice at 5,000 rpm and 4 °C for 1 h and were dried in pre-weighed 50 mL Greiner tubes at 100 °C for 72 h. Then, CDW was determined.

### Activity assay

Every 24 h, activity analyses of expressed protein were performed. Hence, 3 $\mu$L of culture SN of the strains were incubated with 2 mM XN and 95 $\mu$L of BSM, pH 6.0, at 150 rpm and 35 °C for 2 min. The reaction was stopped by adding 300 $\mu$L of MeOH and 1% of FA, mixed well, centrifuged at 13,200 rpm for 5 min and SNs were aliquoted for HPLC-MS. Activity of the wild type strain was measured after 123 h of bioreactor cultivation as negative control.

### Purification of *Nha*-KHS

After 123 h of bioreactor cultivation, about 2.4 L of supernatant containing *Nha*-KHS-$His_{10}$ was harvested at 4 °C and sterile filtered using a vacuum pump and a 0.2 $\mu$m filter. Every step was performed either on ice or at 4 °C. After filtration, SN was stepwise concentrated with cross flow (Pall Corporation) in order to keep the protein on ice as long as possible. After loading of the culture SN, the concentrated protein fraction was washed with 4.8 L of 50 mM citrate, pH 6.0, and was eluted with 300 mL of the same buffer. After concentrating the culture SN, 50 mL of the concentrated supernatant were purified using a 5 mL HisTrapFF column and desalted as previously described. The protein concentration was determined via UV-Vis spectroscopy.

# Chapter 3

# Results

## 3.1 Expression of *Nha*-KHS-$His_{10}$ in *E. coli* and *P. pastoris*

For cloning, *khs* genes used in the project, listed in Table 3.1 and Appendix Table A.9, were supplied by DSM Innovative Synthesis BV (Geleen, the Netherlands). The *E. coli* sequence-optimzed genes were further codon-harmonized for the expression in *P. pastoris* by Anita Emmerstorfer-Augustin (from DNA 2.0).

TABLE 3.1: Kievitone hydratase genes. The gene sequences in the respective GenBank entries were sequence-harmonized for expression in *P. pastoris* and *E.coli*.

| **Gene** | **Organism** | **Gene length [bp]** | **Protein size [kDa]** | **Accession number of protein sequence** |
|---|---|---|---|---|
| *Ate*-KHS-$His_{10}$ | *Aspergillus terreus* | 1152 | 41.2 | XP_001217367.1 |
| *Fso*-KHS-$His_{10}$ | *Fusarium solani* | 1104 | 40.3 | AAA87627 |
| *Nha*-KHS-$His_{10}$ | *Nectria haematococca* | 1098 | 39.9 | XP_003041184.1 |

The harmonized genes for *E. coli* were amplified via PCR to include two restriction sites *Hind*III and *Nde*I and a C-terminal His*10*-tag for in frame cloning into the expression vector and immunodetection, respectively. The two restriction sites in the sequences were further used for ligation with the *E. coli* expression vector pET26b(+) (see FIGURE 3.1). All cloning procedures had been performed previously by Stefanie Gabriel [12] or otherwise indicated. Expression of *Nha*-KHS-$His_{10}$ was initiated by induction of T7 promotor with IPTG. Selection pressure for transformed *E. coli* strains was applied by the addition of Kanamycin.

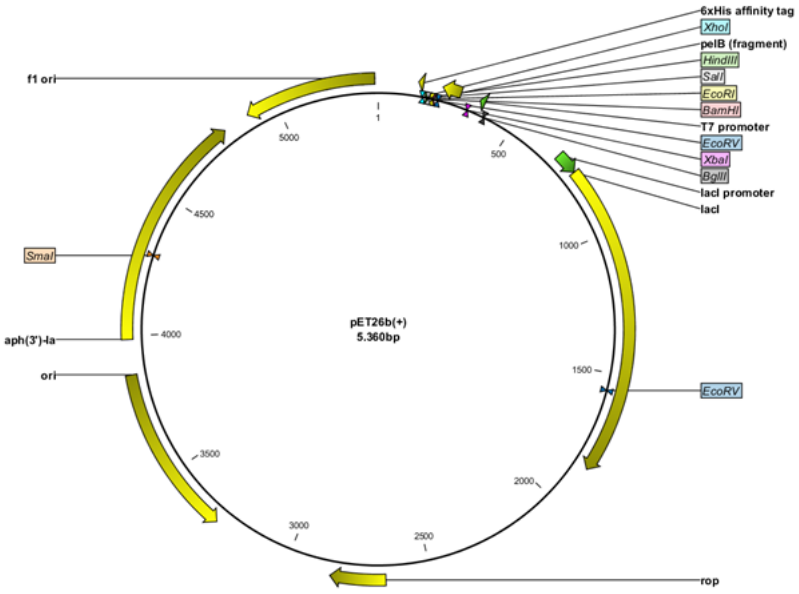


FIGURE 3.1: Expression vector pET26b(+) by Novagen [23], used for expression of *Nha*-KHS in host organism *E. coli*.

The codon-harmonized gene sequences for *P. pastoris* were cloned into *E. coli- P. pastoris* shuttle vectors pPpB1_S and pPpT4_$\alpha$_S (FIGURE 3.2) by Anita Emmerstorfer-Augustin. Therefore, the genes were amplified via PCR, adding the restriction sites for *Nde*I and *Not*I or *Xho*I and *Not*I (see Appendix Table A.13). Cultivation and expression of the C-terminally $His_{10}$-tagged *Nha*-KHS-$His_{10}$ in *P. pastoris* was conducted as mentioned in Materials and Methods. The *P. pastoris* strains of *Nha*-KHS-$His_{10}$ containing the disguised or masked signal sequences to silence secretion (nosig-variants) as well as the variants with a masked signal sequence (FLAG-variants) were cloned into the shuttle vector pPpB1_S using *Not*I and *Eco*RI also by Anita Emmerstorfer-Augustin.

Due to the high secretion levels of *Nha*-KHS-$His_{10}$ expressed in *P. pastoris* [pPpT4_ $\alpha$_S], this strain was used for all analyses with purified KHS as well as concentrated supernatant. The shuttle vector $pPpB1\_S$ was used for expression of *Nha*-KHS-His-$_{10}$ variants with either masked signal sequences (FLAG-tag) or no N-terminal signal sequence (nosig) in order to test for the feasibility of intracellular expression of *Nha*-KHS-$His_{10}$.

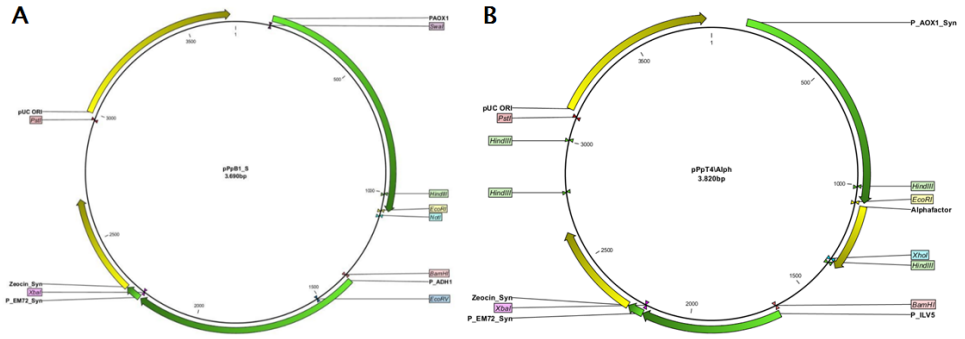


FIGURE 3.2: Expression vectors pPpB1_S and pPpT4 $\alpha$_S used for expression of *Nha*-KHS in host organism *P. pastoris* [19].

After expression and cell harvest, sterile filtration of the culture SN as well as Ni-NTA column purification and desalting, the *Nha*-KHS-His$_{10}$ concentrations were determined by UV-Vis spectrophotometry. Therefore, spectral scans from 250 to 1,000 nm (FIGURE 3.3) were performed and $A_{280}$, was used for the calculations of the protein concentration (see Equation 2.1). The molar extinction coeficient $\varepsilon_{280}$ of 83,310 $M^{-1}$ $cm^{-1}$ was computed by the ProtPram, a tool offered on the ExPASy web portal [30]. As seen in the UV-Vis absorption spectra no other peaks are indicated, especially in the wavelength range of between 300- and 500 nm. No conserved cofactor binding domains was identified after sequence analysis of the enzyme, which was also confirmed by the UV-/Vis spectrum.

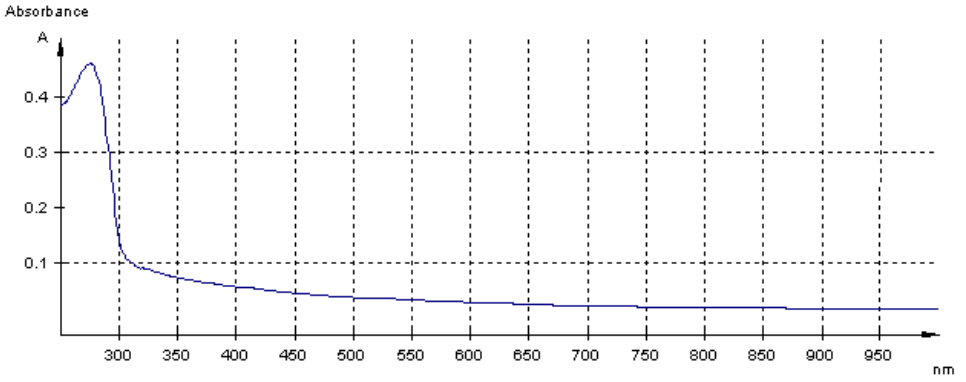


FIGURE 3.3: UV-Vis spectra from 250 to 1000 nm of concentrated *Nha*-KHS, purified with Ni-NTA column.

After protein quantification, gel filtration of *Nha*-KHS-His$_{10}$ purified via Ni-NTA column was performed (FIGURE 3.4 **(A)**). One clear peak with a maximum 1650 mAU eluted at approximately 77 mL, indicating a monomeric conformation in solution. Elution fractions C5 to D2 were, further, analyzed via SDS-PAGE (FIGURE 3.4 **(B)**). Detection of only one hand further confirmed the presence of the monomer in solution. In order to analyze the activity of the enzyme, *in vitro* activity assays were performed.

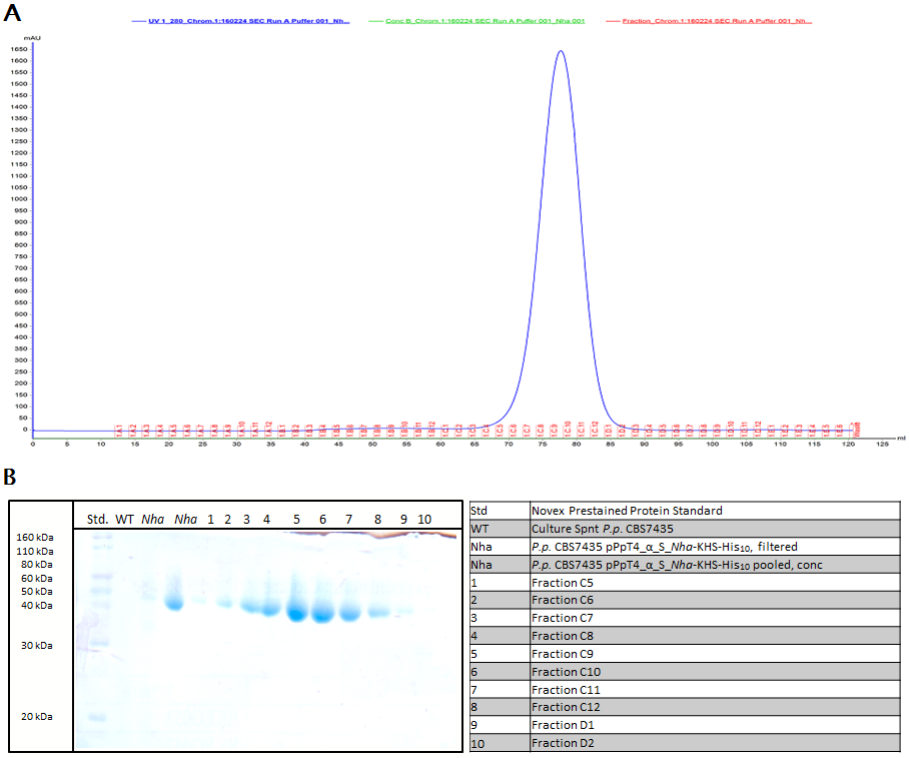


FIGURE 3.4: Gel filtration of *Nha*-KHS-His$_{10}$. **(A)** Chromatogram of gel filtration of *Nha*-KHS-HIs$_{10}$ (deglycosylated 39.9 kDa), previously purified with Ni-NTA column. Blue line: Absorbance at 280 nm. **(B)** SDS-PAGE analysis followed by Coomassie Blue staining of gel filtration fractions C5-D2.

For the activity assay, 0.31 mg mL$^{-1}$ of His-tag purified and 0.28 mg mL$^{-1}$ of gel-filtered *Nha*-KHS were measured in triplicates (FIGURE 3.5).

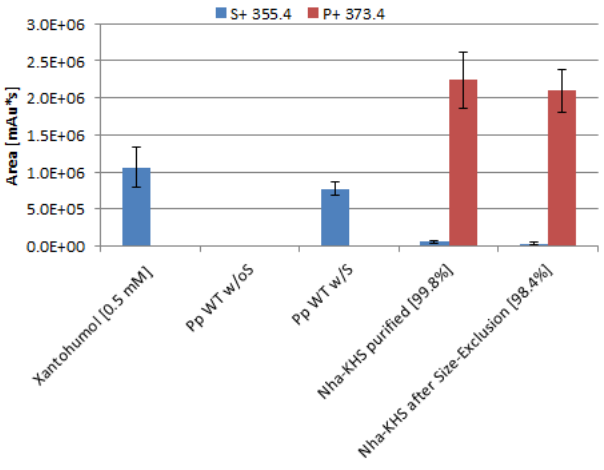


FIGURE 3.5: *In vitro* activity of His$_{10}$-tag purified and gelfiltrated *Nha*-KHS-His$_{10}$. Area values $[mAU \cdot s]$ obtained from HPLC-MS measurement. The 0.5 mM substrate standard, Ni-NTA column purified *Nha*-KHS-His$_{10}$, 0.31 mg mL$^{-1}$, 0.28 mg mL$^{-1}$ gel-filtered *Nha*-KHS-His$_{10}$ were used for XN conversion. The culture SN was used for the activity assays of *P. pastoris* wild type CBS7435 with and without substrate. Measurements conducted in triplicates.

The enzyme activity in both samples was highly similar (FIGURE 3.5).

Most probably due to the higher concentration of applied His-tag purified enzyme, the area value of XN-hydrate was slightly higher. However, the conversion rates of 99.8% and 98.4% were within standard deviations. Therefore, the conversion rate of both samples can be identified as equal. The wild type control incubated with either buffer or substrate showed no conversion. Also a 0.5 mM substrate standard was incubated and measured via HPLC-MS. Due to lack of assay optimization, the area values of the substrate varied. XN is very insoluble in aqueous solution, which made it difficult to stabilize the mass balance. After identifying the positive ionized product as more reliable for detection, the positive-ionized SIM mode at m/z 373.4 was chosen for evaluating product conversions.

## 3.2 Kievitone conversions: Resting cells assays in *E. coli*

In previous work, it was shown that activity assays performed with *E. coli* CFEs showed detectable amounts of kievitone-hydrate [12]. However, establishing a reliable resting cells conversion would save time and expenses, and was therefore tested for feasibility. After cultivation, induction and harvest of 10 and 50 $OD_{600}$ units of *E. coli* BL21 Star$^{TM}$ (DE3) expressing *Nha*-KHS-$His_{10}$, kievitone was added for conversion. Due to limited access to the substrate, only single biological measurements were conducted for all samples (FIGURE 3.6).

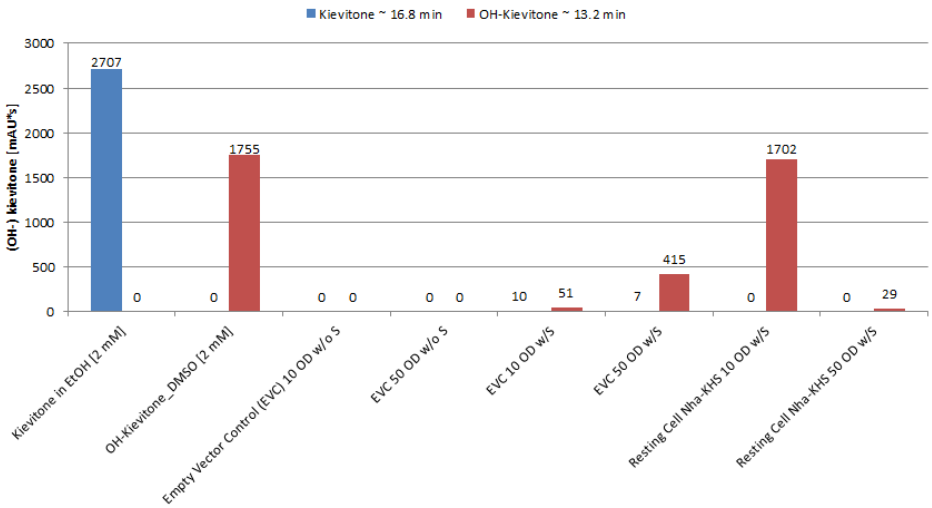


FIGURE 3.6: Conversion of kievitone with *E. coli* resting cells. Area values $[mAU \cdot s]$ obtained from HPLC-UV measurement at 220 nm. The 2 mM substrate standard eluted at $\sim$ 16.8 min, whereas the 2 mM product eluted at $\sim$ 13.2 min and EVC were also included in the graph. The resting cells conversion was performed with 10 and 50 OD units of strains *E. coli* BL21 Star$^{TM}$ (DE3) [pET26b(+)_*Nha*-KHS_$His_{10}$] and EVC.

For comparison substrate standard, dissolved in EtOH, as well as product standard, dissolved in DMSO, were treated as other samples and measured via HPLC-UV. Kievitone was eluted after $\sim$ 16.8 min of retention time, whereas kievitone-hydrate was eluted after $\sim$ 13.2 min ($\sim$ 3.6 min difference in retention time, data not shown). Polar substances elute earlier than non-polar ones and therefore, the product was always detected before the substrate. Due to the different solvent of the standards as well as unstable conditions, the area values generally varied notably (FIGURE 3.6). The highest conversion was identified upon using 10 $OD_{600}$ units of *E.coli* expressing *Nha*-KHS-$His_{10}$. 50 $OD_{600}$ units also showed some activity, however significantly less than in 10 $OD_{600}$ units. Evidently irritating was the product signal in the EVC strains (10 and 50 $OD_{600}$ units). Moreover, substrate was not detectable in any sample after incubation over night, even though comparison with the substrate standard did not suggest complete conversion. Therefore, no valid mass balance could be retrieved. Due to the inconclusive results, the experiment was performed twice with identical overall results.

## 3.3 Examination of alternative substrates (8-PN and XN)

The limited access to kievitone did not allow for in detail characterization of KHSs on the basis of converting the natural substrate. Moreover, the results retrieved so far could only be obtained as single measurements. Therefore, access to alternative substrate was required for full biochemical characterization of the enzyme. In previous work, the sterol, cholesta-5,7,24-trien-3beta-ol (FIGURE 4.8), had been tested for conversion and proven to be inactive [12]. However, since the compound is much bulkier, less flexible and less polar than kievitone, the substrate was likely unable to enter the enzyme cavity or bind to the active site for addition of water to the prenylated carbon-carbon double bond. The two flavonoid-substrates 8-PN and XN (FIGURE 4.1), must be closely related to kievitone than the sterol, were tested for conversion with *Nha*-KHSs. Enzyme activity assays were performed in triplicates *in vivo* and *in vitro* two different organisms, *E. coli* and *P. pastoris*, to detect conversion of 8-PN and XN. Product conversions were roughly calculated in percentages, by assume the substrate and product peak of a sample as 100%. Further the product peak was set in realtions to the 100%. However, it is no absolute calculation and should only give an approximate evaluation of the product peak.

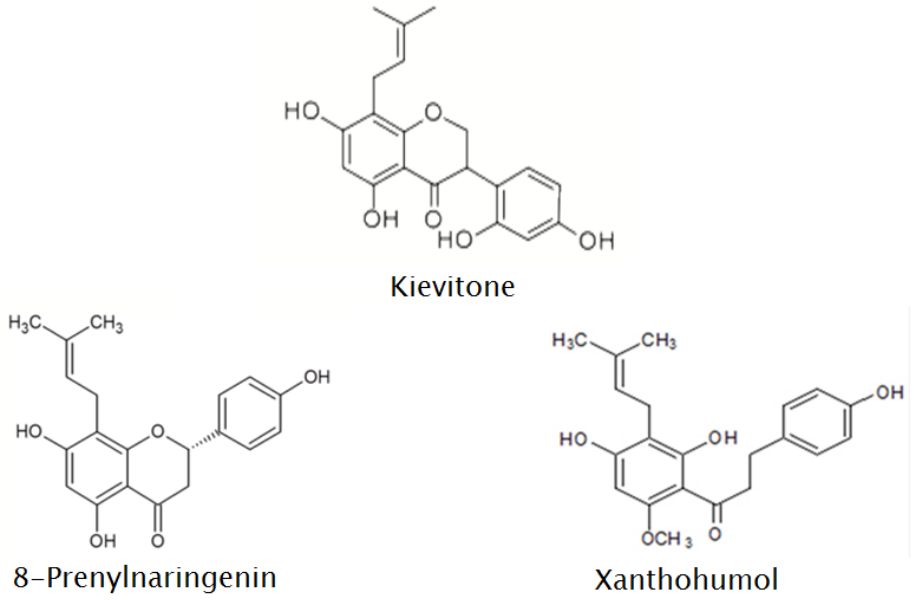


FIGURE 3.7: Chemical structures of the original substrate kievitone and the alternative substrates 8-prenylnaringenin and xanthohumol.

### 3.3.1 8-prenylnaringenin (8-PN)

After dissolving the solid 8-PN in EtOH, expression of *Nha*-KHS-$His_{10}$ in *P. pastoris*, activity assays with concentrated culture SN containing *Nha*-KHS-$His_{10}$ were conducted as described in Materials and Methods. The samples were measured with HPLC-MS (FIGURE 3.8). The SCAN mode from *m/z* 200-700 was applied for analyzing all masses within the range. The three SIM channels of the MS were set to detect the negatively ionized substrate (*m/z* 339.4) as well as the positively and negatively ionized product (*m/z* 356.4 or 358.4).

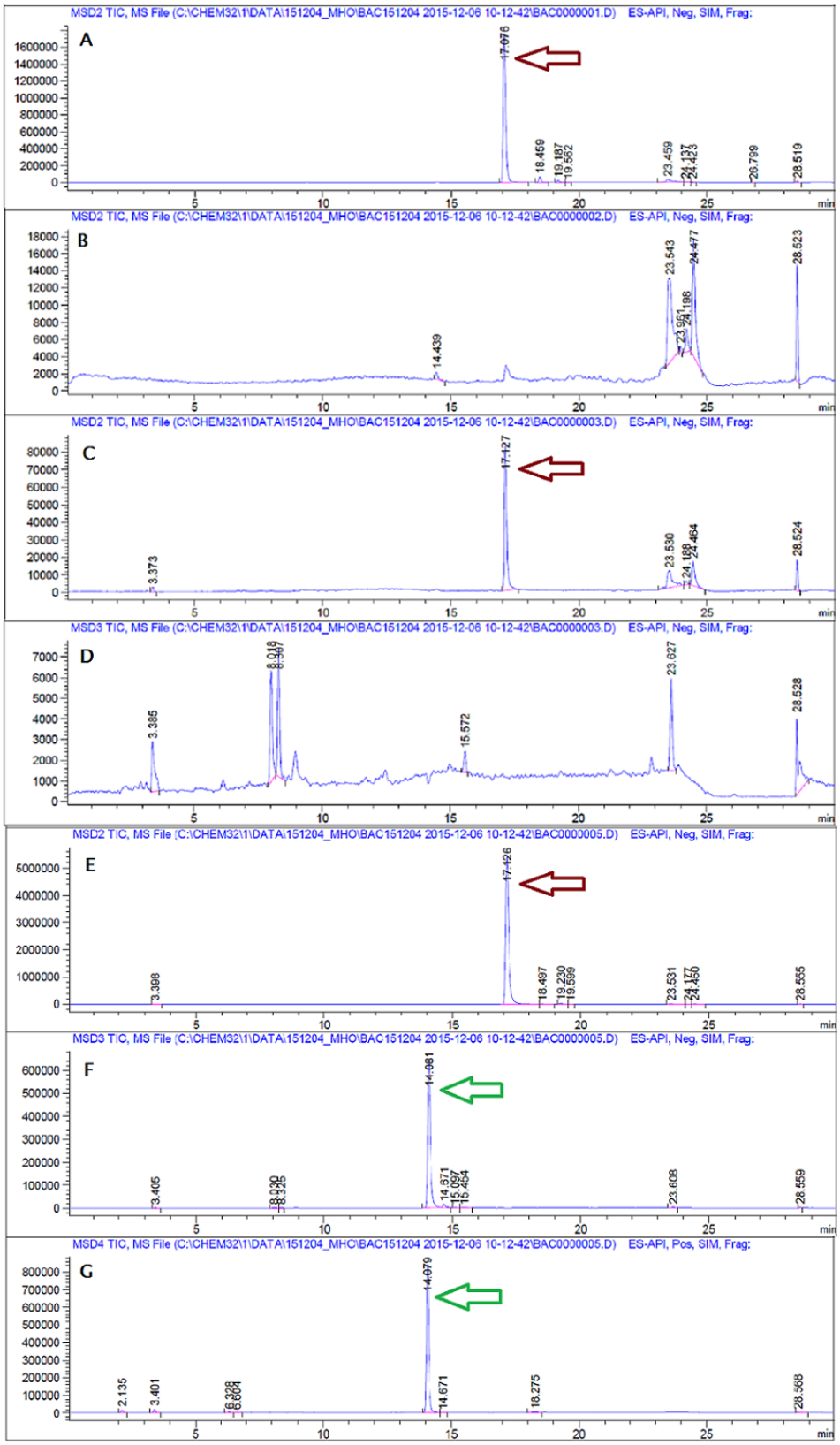


FIGURE 3.8: HPLC-MS chromatograms of 8-prenylnaringenin (8-PN) conversions to 8-(3-hydroxy-3-methyl-butyl)naringenin (8-PN-OH) with concentrated culture SNs after expression of *Nha*-KHS in *P. pastoris* in the different SIM modes.**A** SIM mode negative ionized substrate (*m/z* 339.4)of substrate standard at a retention time of $\sim$ 17.1 min. **B** SIM mode negative ionized substrate (*m/z* 339.4) of the biological standard without substrate, no peak.**C** SIM mode negative ionized substrate (*m/z* 339.4) of the biological standard with substrate. **D** SIM mode negative ionized product of the biological standard with substrate (*m/z* 356.4), no peak. **E** SIM mode negative ionized substrate (*m/z* 339.4) of concentrated culture SN containing *Nha*-KHS detecting the product at a retention time of $\sim$ 17.1 min. **F** SIM mode negative ionized product (*m/z* 356.4) of concentrated cultured SN containing *Nha*-KHS detecting the product at the retention time of $\sim$ 14.1 min. **G** SIM mode positive ionized product (*m/z* 358.4) of conc. SN containing product at the retention time of $\sim$ 14.1 min. Red Arrow: 8-prenylnaringenin. Green Arrow: 8-(3-hydroxy-3-methyl-buthyl)naringenin.

Substrate as well as product were positively identified ( FIGURE 3.8). In FIGURE 3.8 **(A-B)** the chemical as well as biological standards with and without addition of substrate, respectively, are displayed in the negative ionized substrate channel (*m/z* 339.4). The chemical standard sample is substrate in buffer, whereas the biological standards are EVC with and without substrate. Both controls were treated as the other samples to prove that the conversion was caused by the expressed enzyme. 8-PN was detected at a retention time of $\sim$ 17.1 min for the chemical standard, whereas the wild type control without substrate showed no distinct peak in substrate as well as in product mode. The wild type control with substrate showed a distinct peak at the retention time $\sim$ 17.1 min and no peak in the product modes (FIGURE 3.8 **(C-D)**). In FIGURE 3.8 **(E-G)** the chromatograms of the biocatalysis samples with concentrated *Nha*-KHS can be inspected. A substrate peak at $\sim$ 17.1 min as well as negative and positive ionized product peaks at $\sim$ 14.1 min could be identified. Due to the correct mass of the peaks as well as the similar retention time difference of $\sim$ 3.0 min compared to kievitone and kievitone-hydrate, the product was consequently indentified as 8-(3-hydroxy-3-methyl-butyl)naringenin (8-PN-OH).

For further analyses of *Nha*-KHS with 8-PN, CFE-assays with *E. coli* strain expressing *Nha*-KHS-$His_{10}$ as well as assays with concentrated *P. pastoris* culture SN and purified *Nha*-KHS-$His_{10}$ and resting cells assays with *P. pastoris* were performed (FIGURE3.9 and FIGURE 3.10).

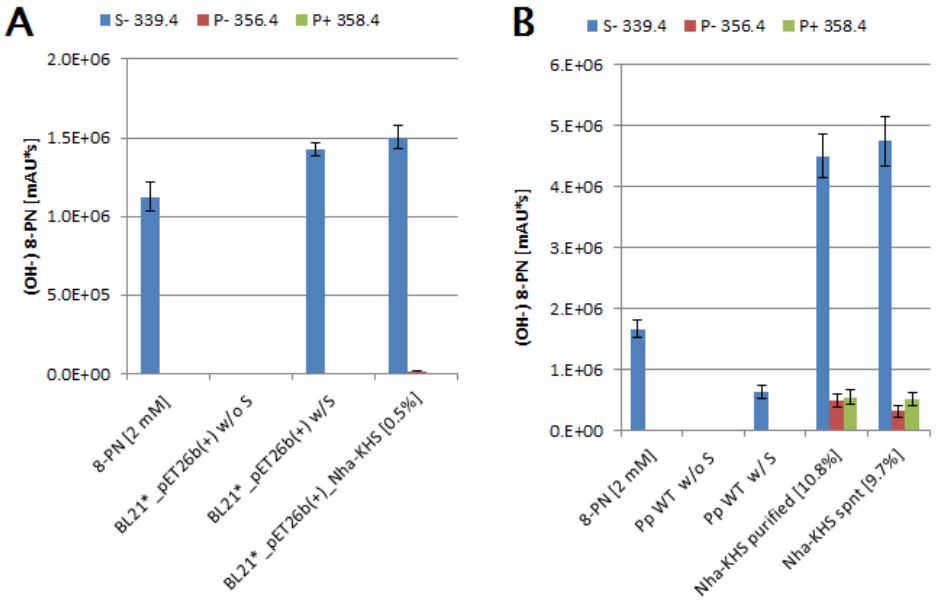


FIGURE 3.9: Activity analyses with 8-PN, CFE-assays with *E. coli* strain expressing *Nha*-KHS-$His_{10}$ (**A**) and concentrated *P. pastoris* culture SN and purified *Nha*-KHS-$His_{10}$ (**B**). Area values $[mAU \cdot s]$ of SIM modes of negatively ionized substrate (*m/z* 339.4), negatively ionized product (*m/z* 356.4) and positively ionized product (*m/z* 358.4) obtained with HPLC-MS, which were coupled to activity assays with 2 mM of 8-PN. The conversion was performed with CFE of *E. coli* BL21 Star$^{TM}$ (DE3)[pET26b(+)_*Nha*-KHS-$His_{10}$] (**A**) and 1 mg $ml^{-1}$ of concentrated culture SN (**B**) and purified *Nha*-KHS-$His_{10}$, from *P. pastoris* CBS7435 [pPpT4_$\alpha$_S_*Nha*-KHS-$His_{10}$]. Substrate standard, EVC and wild type with and without substrate were included as controls.

In FIGURE 3.9 **(A)**, the CFE- assay detected only a slight signal of the product in the negatively ionized product SIM mode (*m/z* 356.4). In comparison to the substrate area value the product area accounted for 0.5% of the substrate peak. The positively ionized product signal had a diminutive signal, was not visible on the scale of the graph. However, 2 mM of chemical standard as well as EVC showed no putative product peaks. In comparison to the CFE- activity assay, conversion with the concentrated culture SN as well as purified *Nha*-KHS-$His_{10}$ assays (FIGURE 3.9 **(B)**) showed a product formation of $\sim$ 10%. Positively as well as negatively ionized SIM mode of the product displayed similar area values. However, a dramatic decrease of substrate area values were detected in both *P. pastoris* strains overexpressing *Nha*-KHS-$His_{10}$ intra- and extracellularly.

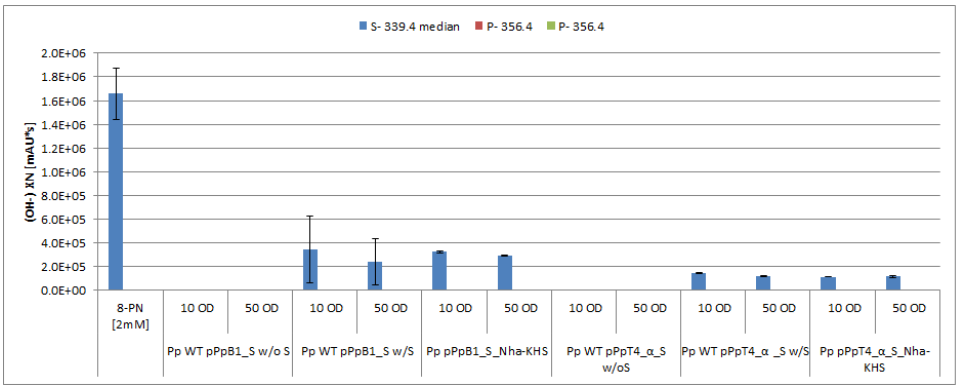


FIGURE 3.10: Conversion of 8-PN with resting cells of *P. pastoris* expressing *Nha*-KHS using either pPpB1_S or pPpT4_$\alpha$_S vector system. Area values $[mAU \cdot s]$ of SIM modes of negatively ionized substrate (*m/z* 339.4), negatively ionized product (*m/z* 356.4) and positively ionized product (*m/z* 358.4) obtained with HPLC-MS coupled to activity assays. Ten and 50 $OD_{600}$ units of cells were used for the assay. Two mM of substrate standard, EVC and wild type strain with and without substrate were included as controls.

No conversion or product peak was observed in the resting cells assays with 8-PN (FIGURE 3.10). Due to overall similar results of all resting cells assays, no significant differences in using 10 or 50 $OD_{600}$ units of cells could be seen. The area values identified for the wild type controls expressing *Nha*-KHS-$His_{10}$ decreased greatly in each assay. Strains containing vector [pPpT4_$\alpha$_S] displayed a greater loss of substrate. The chemical standards of the activity assays with purified protein correlated well with the area value of the resting cells assay in *P. pastoris* (FIGURE 3.10). The area values determined for the 2 mM substrate and CFE or *P. pastoris* culture SN-purified protein assays varied considerably.

### 3.3.2 Xanthohumol (XN)

After dissolving the solid XN in EtOH as well as expression and purification of *Nha*-KHS-$His_{10}$ from *P. pastoris* culture SN, activity assays with the concentrated SN as well as purified enzyme were performed as described

in Materials and Methods. Samples were measured with HPLC-MS (FIGURE 3.11). The SCAN mode from *m/z* 200-700 was applied for analyzing all masses within the range. The three SIM channels of the MS were set to detect the positively ionized substrate (*m/z* 355.4) as well as the positively and negatively ionized product (*m/z* 373.4 or 371.4).

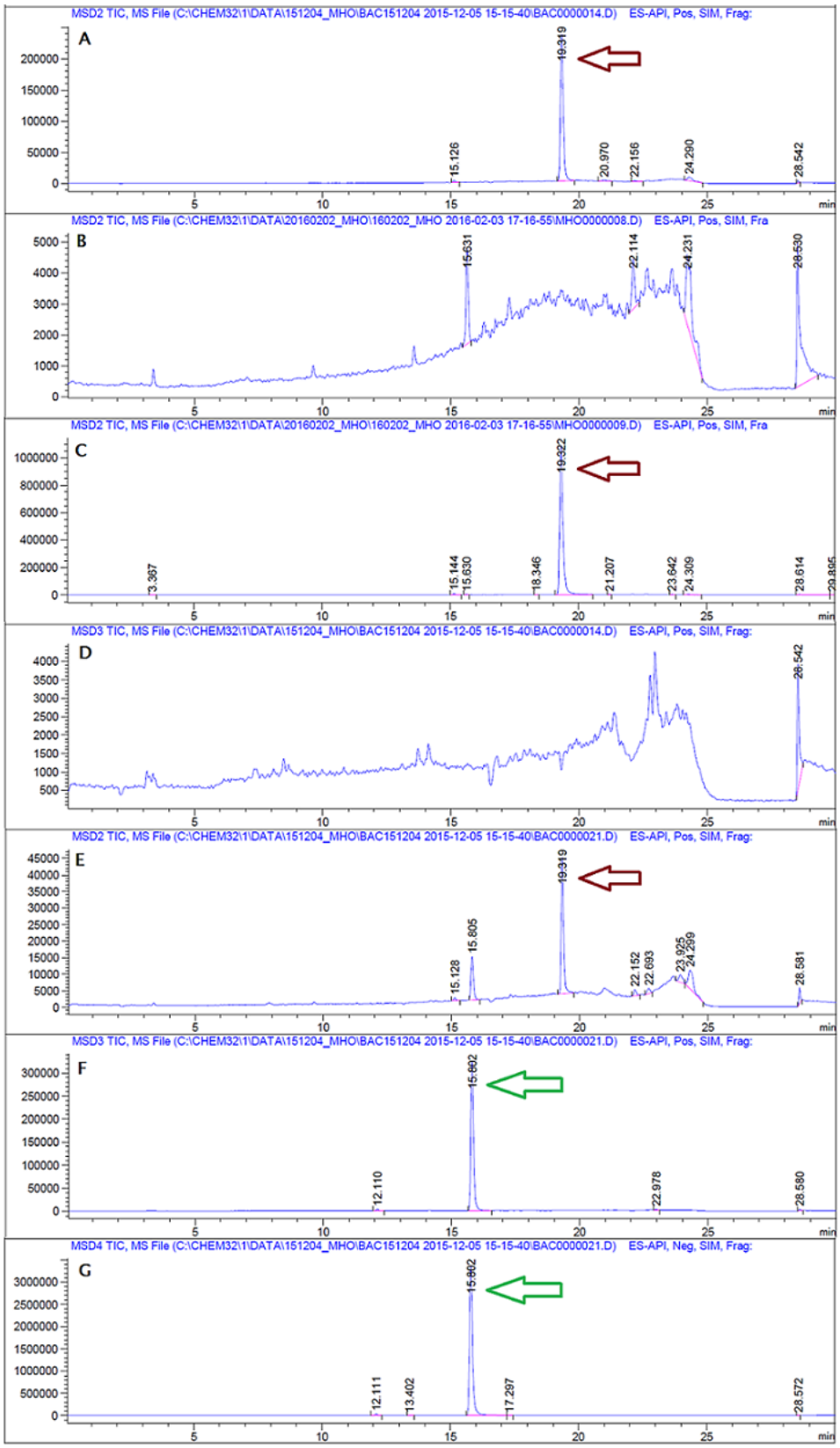


FIGURE 3.11: HPLC-MS chromatograms of xanthohumol (XN) conversions to xanthohumol-hydrate (XN-OH) in the different SIM modes.**A** SIM mode positively ionized substrate (*m/z* 355.4)of substrate standard at a retention time of $\sim$ 19.3 min. **B** SIM mode positively ionized substrate (*m/z* 355.4) of the biological standard without substrate, no peak.**C** SIM mode positively substrate (*m/z* 355.4) of the biological standard with substrate. **D** SIM mode positively product (*m/z* 373.4), no peak was detected in the SN of *P. pastoris* wild type strain without substrate. **E** SIM mode positively ionized substrate (*m/z* 355.4) of concentrated *P. pastoris* culture SN containing *Nha*-KHS-$His_{10}$ at the retention time of $\sim$ 19.3 min. **F** SIM mode positively ionized product (*m/z* 373.4) of concentrated *P. pastoris* culture SN detecting product at the retention time $\sim$ 15.8 min. **G** SIM mode negatively ionized product (*m/z* 371.4) of concentrated culture SN containing *Nha*-KHS-$His_{10}$ detecting negatively ionized product at the retention time of $\sim$ 15.8 min. Red Arrow: xanthohumol. Green Arrow: xanthohumol-hydrate.

Substrate as well as product were positively identified, see FIGURE 3.11. In FIGURE 3.11 **(A-B)** the chemical as well as biological standards are displayed in the positive ionized substrate SIM mode (*m/z* 355.4). XN was detected at retention time of $\sim$ 19.3 min, whereas the wild type control without substrate showed no distinct peak in substrate as well as in product modes. However, the wild type control with substrate showed a distinct peak at the retention time $\sim$ 19.3 min and no peak in the product modes (FIGURE 3.11 **(C-D)**). In FIGURE 3.11 **(E-G)** the chromatograms of the biocatalysis samples with concentrated 1 mg ml$^{-1}$ *Nha*-KHS can be inspected. A substrate peak at $\sim$ 19.3 min as well as negative and positive ionized product peaks at $\sim$ 15.8 min could be identified. Due to the correct mass of the peaks as well as the similar retention time difference of $\sim$ 3.5 min compared to kievitone and kievitone-hydrate, it was identified as xanthohumol-hydrate (OH-XN).

For further analysis of *Nha*-KHS-His$_{10}$ with the alternative substrate XN, CFE-activity assays with the *E. coli* strain expressing *Nha*-KHS-His$_{10}$ as well as assays using concentrated *P. pastoris* culture SN, *P. pastoris* and *E. coli* were performed (FIGURE 3.12, FIGURE 3.13 and FIGURE 3.14).

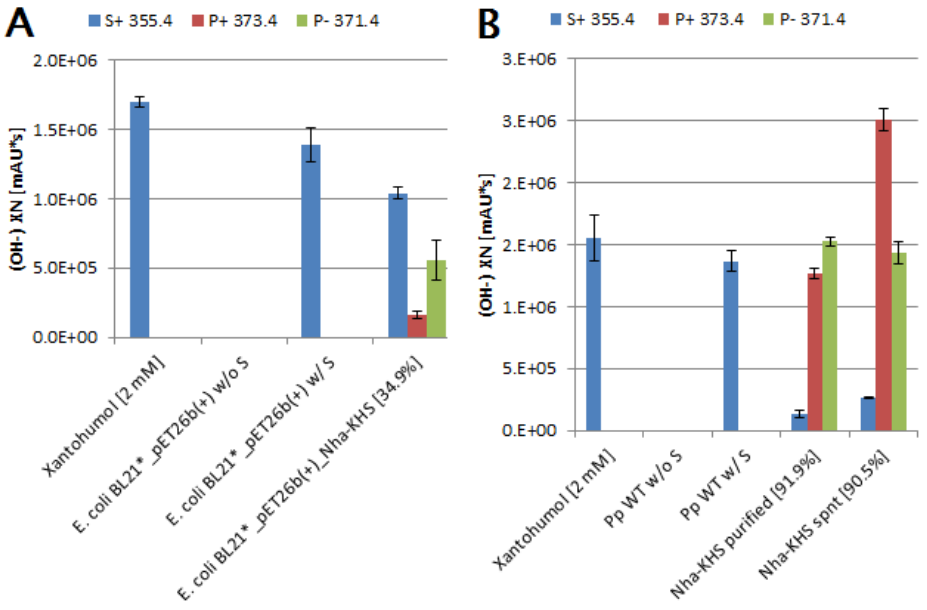


FIGURE 3.12: Activity assays conducted with *E.coli* (**A**) as well as with concentrated *P. pastoris* culture SN and purified protein (**B**). Area values $[mAU \cdot s]$ of SIM modes of positively ionized substrate (*m/z*355.4), positively ionized product (*m/z*373.4) and negatively ionized product (*m/z*371.4) obtained with HPLC-MS measurements, coupled to activity assays with the alternative substrate XN. The conversion was performed with CFE of the strains *E. coli* BL21 Star$^{TM}$ (DE3)_pET26b(+)_*Nha*-KHS-His$_{10}$ and *P. pastoris* CBS7435 pPpT4_$\alpha$_S_*Nha*-KHS-His$_{10}$ culture SN, 1 mg mL$^{-1}$. Two mM substrate standard, EVC and a *P. pastoris* wild type strain with and without substrate were included as controls.

In FIGURE 3.12 **(A)**, negatively ionized product (*m/z* 371.4) as well as positively ionized product (*m/z* 373.4) was detected in the CFE. In comparison to the substrate area value, the product area accounted for 34.9% of the

substrate area peak. The 2 mM chemical standard as well as EVC showed no product peak. In comparison to the activity assay with *E. coli* CFE, conversions with the concentrated culture SN as well as purified *Nha*-KHS-$His_{10}$ (FIGURE 3.12 **(B)**) showed a product conversion of $\sim$ 90% based on the consumed substrate. The peak of the positively ionized product peak of the concentrated culture SN was seen as an outlier. The negatively ionized SIM mode of the product showed similar results compared to the positively ionized product peak as seen in the resting cells assay (FIGURE 3.13 and FIGURE 3.14). The wild type strain compared to the chemical standard of XN conversion assays showed slight loss of substrate.

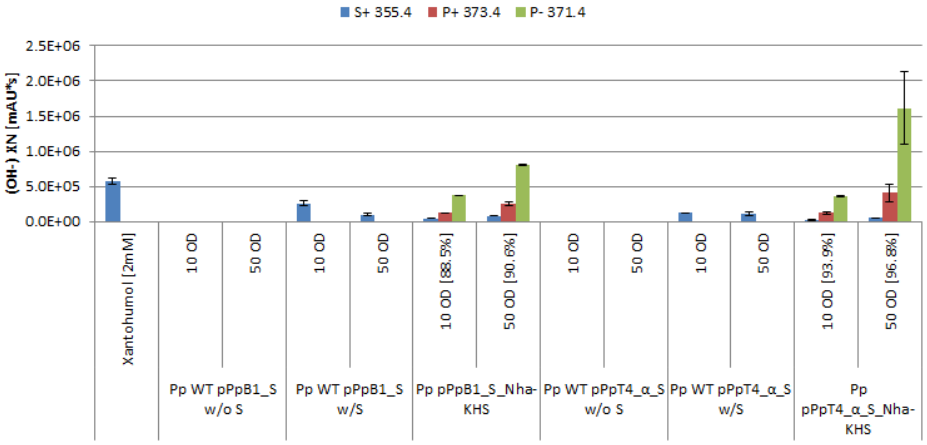


FIGURE 3.13: *P. pastoris* resting cells conversion with XN. Peak area values $[mAU \cdot s]$ of SIM modes of positively ionized substrate (*m/z* 355.4), positively ionized product (*m/z* 373.4) and negatively ionized product (*m/z* 371.4) obtained with HPLC-MS measurements, which were coupled to resting cells assays with the alternative substrate of 2 mM XN. The conversions were performed with the strains *P. pastoris* CBS7435 [pPpB1_S_*Nha*-KHS$His_{10}$], *P. pastoris* CBS7435 [pPpT4_$\alpha$_S_*Nha*-KHS$His_{10}$] as well as the wild type strain (10 and 50 $OD_{600}$ units). Triplicates were performed.

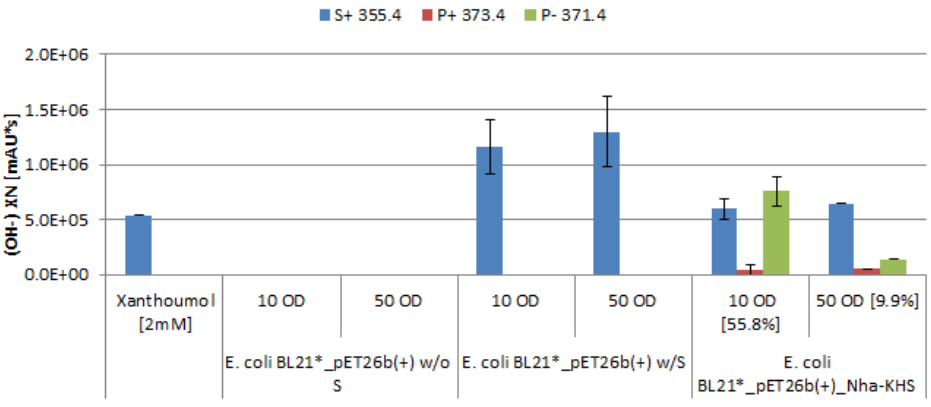


FIGURE 3.14: *E. coli* resting cells conversion with XN. Peak area values $[mAU \cdot s]$ of SIM modes of positively ionized substrate (*m/z* 355.4), positively ionized product (*m/z* 373.4) and negatively ionized product (*m/z* 371.4) obtained with HPLC-MS measurements, coupled to activity assays with the alternative substrate 2 mM XN. The resting cells conversions were performed with the strains *E. coli* BL21 Star$^{TM}$ (DE3) [pET26b(+)_*Nha*-KHS$His_{10}$] as well as with the EVC (10 and 50 $OD_{600}$ units). Triplicates were performed.

Resting cells assays, in *P. pastoris* (FIGURE 3.13) as well as *E. coli* (FIGURE 3.14), resulted in conversion of XN to OH-XN. Remarkably, in the resting cells assays in *P. pastoris* more than 80% of the substrate was converted to OH-XN and also assays performed with *E. coli* resting cells $\sim 50\%$ conversion was achieved in the 10 $OD_{600}$ unit samples. So far, the results indicated no negative influences of low or high cell densities for conversion of XN by *P. pastoris* resting cells. The conversion rates correlated with the $OD_{600}$ units used. However, a strong decrease of conversion was observed in the 50 $OD_{600}$ unit samples of the strain with intergrated [pPpT4_$\alpha$_S] construct. *E. coli* resting cells assay with high cell density conversions displayed decreased conversion rates. Controls showed no product formation, however highly decreased substrate peak area values of the wild type controls with substrate.

## 3.4 Confirmation of the xanthohumol-hydrate (OH-XN)

In order to unambiguously verify formation of the hydrated product from XN, an NMR analysis was performed. Therefore, a large scale conversion of XN to OH-XN was conducted. Five mg of xanthohumol were converted to 3 mg of OH-XN (60% recovery) over night. The extraction of the product was performed by Gernot Strohmeier. After dissolving the product ($\geq$ 95% purity, tested by HPLC-UV) in $CD_3OD$, $^1H$ and $^{13}C$ NMR analysis was conducted by Hansjörg Weber, from the Organic Chemistry at Graz University of Technology. The chromatogram of the $^{13}C$ NMR is shown in FIGURE 3.15 **(B)**. The chromatograms were interpreted with the software SpinWorks. In order to predict the structure of the compound, the peaks (numbered 1-18, according to the numbered carbon atoms of the chemical structure in **(A)**) were identified in chemical groups, and then, the structure was drawn. OH-XN was positively confirmed as the sole reaction product from incubation of *Nha*-KHS-$His_{10}$ with XN.

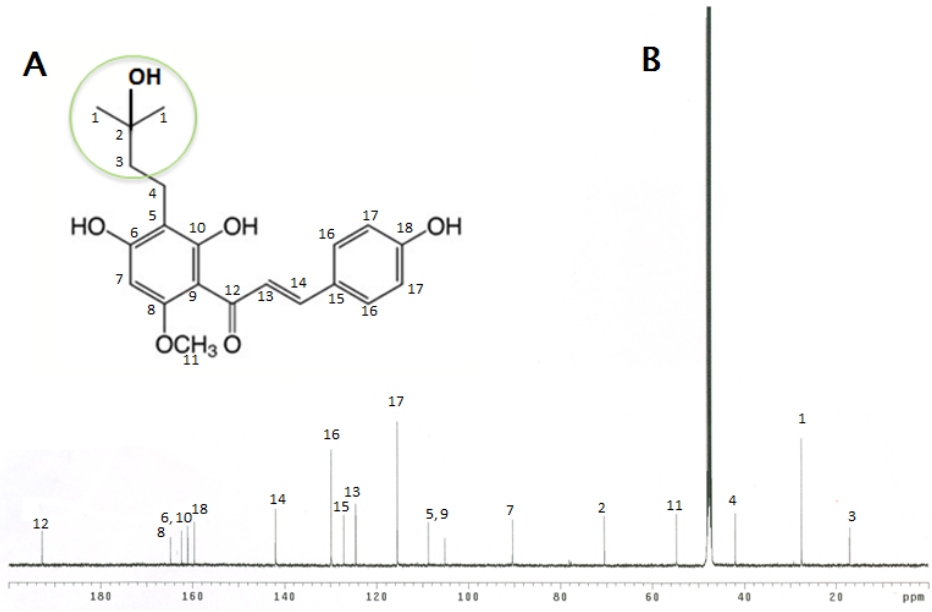


FIGURE 3.15: **A** Structure of the compound analyzed by $^{13}$C-NMR. **B** Chromatogram of the extracted and purified product of XN bioconversion with purified *Nha*-KHS-His$_{10}$ after $^{13}$C-NMR analysis.

For HPLC-UV, the UV absorption maxima of substrate and product compound were determined. Therefore, respective HPLC-UV spectra from 200-500 nm were obtained (FIGURE 3.16).

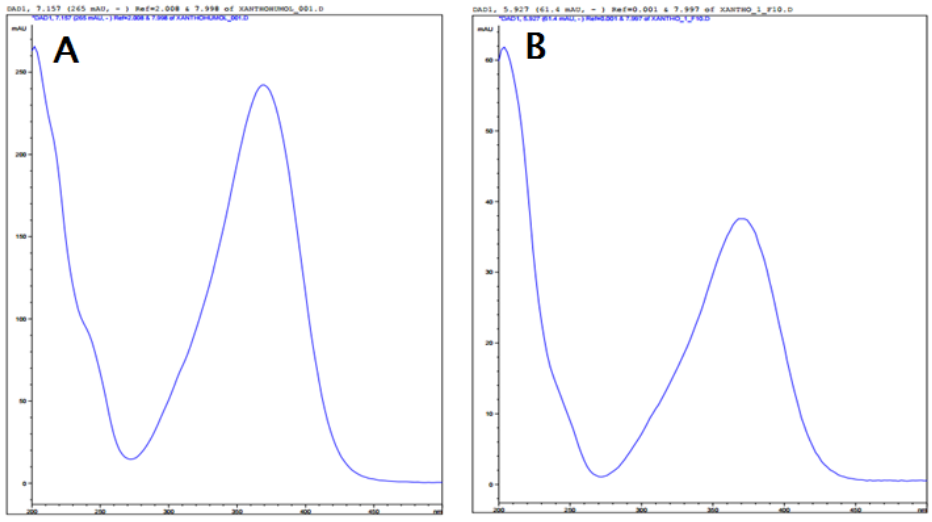


FIGURE 3.16: Area values $[mAU]$ per wavelength [nm] of HPLC-UV measurement for analyzing the absorption maxima of **A** XN and **B** OH-XN.

The absorption peak at 210 nm was caused by impurities. XN was known to have an absorption maximum of 371 nm [36], which was confirmed in **(A)** by the peak at 371 nm. As seen in **(B)**, also the absorption maximum of 371 nm was detected. Due to the significantly smaller height of the peak (40 mAU compared to 250 mAU for XN), it was concluded that the sample was of significantly lower concentration compared to XN. Due

to determination of the absorption maximum of OH-XN, further activity assays could be quantified with HPLC-UV at 371 nm.

## 3.5 Optimization of assay conditions for XN

In order to obtain kinetic parameters, the optimal assay conditions were determined. Also, due to the limited access to the native substrate, no thorough optimizations of *Nha*-KHS-$His_{10}$ assays had been performed previously. All optimization trials were performed with 0.5 mM of XN, except for evaluation of the effect of different storage conditions on the purified enzyme as well as influences of different organic solvents on the reaction. For those assays, the substrate concentration was 1 mM.

Firstly, the effect of different pH values, varying from pH 4.0-9.0, was tested using several buffer systems (FIGURE 3.17 (**A**). In FIGURE 3.17 (**B**) the optimal reaction temperature was determined by incubating the reactions at temperatures ranging from 15-40 °C.

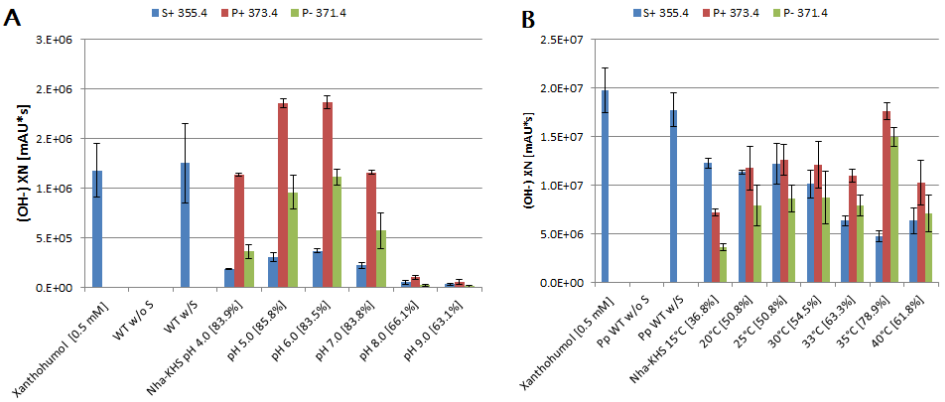


FIGURE 3.17: pH (*A*) and temperature (*B*) optimization of activity assays with XN. Peak area values $[mAU \cdot s]$ of SIM modes of positively ionized substrate (*m/z* 355.4), positively ionized product (*m/z* 373.4) and negatively ionized product (*m/z* 371.4) obtained with HPLC-MS measurements, coupled to activity assays with the model substrate XN. **(A)** Assay reactions were performed under different pH conditions (pH 4.0-9.0). **(B)** The incubation temperature of the bioconversions was varied from 15-40 °C. 0.5 mM of substrate and 1 mg $mL^{-1}$ of enzyme was used. Biological triplicates were measured.

The results suggested that the optimal pH for the *Nha*-KHS-$His_{10}$ reaction was between pH 5.0 and pH 6.0. At pH values higher than pH 7.0, problems with detection of enzyme activity, as well as substrate and product occurred. Conditions of pH 4.0 and 7.0 showed only half of activity as well as substrate compared to the optimal conditions. Conversion rates of the product were detected by about 83%, except of pH 8.0 and 9.0. Conversion rates were summed up by adding substrate as well as product area values of each sample (100%) and compared to the product peak. For that reason, the conversion rate for pH 4.0 and 7.0 are highly similar to the optimal pH conditions. Less substrate as well as product was detected, therefore,

the ratio of conversion equaled the one of optimal conditions. Therefore, the mass balance is not ideal. The percentages of product peak should only guide and should not be taken as absolute.

As identified in conversion rates of the product as well as positive ionized product area value, the optimal temperature of *Nha*-KHS-$His_{10}$ was observed at 35 °C. By performing an additional activity experiment above 45 °C, the activity tendency could be further confirmed. Furthermore, all samples revealed an increase in area value $[mAU \cdot s]$ by 9 fold. The higher sensitivity of measurements was caused by the Christmas cleaning of the HPLC-MS (Biokatalysis) and was proceeded until measurements were obtained from HPLS-MS (Chemistry).

After storage of samples at 4 °C for 11 h due to delays of analytics, substrate decrease was detected (FIGURE 3.18 **(A)**). Product peak area values $[mAU \cdot s]$ seemed not affected. However, the decreases in substrate resulted in variable substrate peak area values and occasionally in high standard deviations. According to Guido *et al.* [42], an addition of 1% of FA improved the stability of their samples. Also different solvents were tested to increase reproducibility, decrease standard deviations and improve the quality of XN and OH-XN detected. To confirm the stabilizing effect of FA on XN, 1% of FA was added to either ACN or MeOH after the protein precipitation and stored at RT for 11 h (FIGURE 3.18 **(B)**).

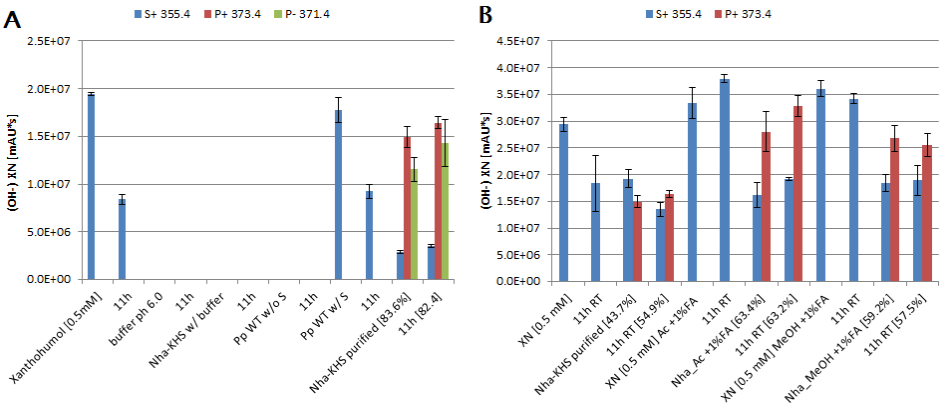


FIGURE 3.18: Activity assays conducted on the same day, but measured directly or after 11 h of storage at 4 °C (*A*) and (*B*) optimization of activity assays with 1% of FA after 11 h of storage. Peak area values $[mAU \cdot s]$ of SIM modes of positively ionized substrate (*m/z* 355.4), positively ionized product (*m/z* 373.4) and negatively ionized product (*m/z* 371.4) obtained with HPLC-MS measurements, which were coupled to activity assays with the model substrate XN. 0.5 mM of substrate and 0.5 mg $mL^{-1}$ (*A*) and 1 mg $mL^{-1}$ (*B*) of purified *Nha*-KHS-$His_{10}$ were used for the assays. Biological triplicates were performed.

Assays optimized with 1% of FA (FIGURE 3.18 **(B)**) and compared with assays stored at 4 °C for 11 h (FIGURE 3.18 **(A)**) revealed that the peak area values of substrate and product were reproducible. Samples including 1% of FA showed almost no variation in XN peak area values before and after

storage. Furthermore, the comparison of the results from both activity assays revealed higher peak area values of samples with 1 % FA for XN as well as OH-XN. Substrate and product values increased by 100% after addition of 1% FA. Different solvents (MeOH or ACN) used for protein precipitation after the hydration reaction occurred did not affect the detection of substrate and product notably.

A time course experiment was performed. Conversion times starting with 10 min to 48 h were tested (FIGURE 3.19 **(A)**). Further, analytics of prenylated flavonoids were highly concentration dependent. Difficulties for detection of substrate and product concentrations, higher than 2 mM, were identified. An additional dilution step with MeOH before HPLC-MS analysis was found to increase feasibility of concentration determinations (FIGURE 3.19 **(B)**).

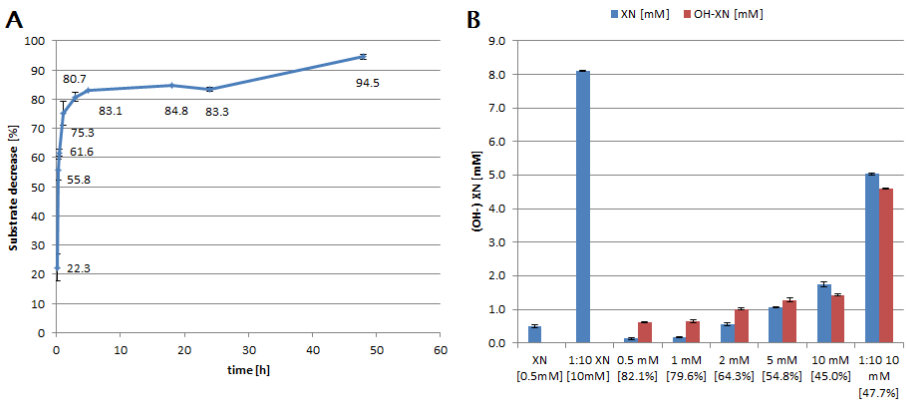


FIGURE 3.19: **(A)** Activity assays showing substrate decrease [%] over time. 0.5 mM of XN were applied. **(B)** The influences of an additional dilution step after the bioconversion was tested to increased proficiency of HPLC-MS analytics. 0.5 mg $mL^{-1}$ of purified *Nha*-KHS-$His_{10}$ used was. (OH-)XN concentrations were obtained via HPLC-MS measurements, which were coupled to activity assays with the model substrate XN. Biological triplicates were performed.

After 15 min, 55.8% of substrate was already converted (FIGURE 3.19 **(A)**). Near-complete conversion of about 80+% was achieved after 3-5 h. After 24 h without the addition of FA, degradation or insolubility of the substrate was initiated. Samples incubated longer than 24 h showed high percentages of substrate decrease. However, no more product was detected. Therefore, the accuracy in detection of substrate and product decreased after 24 h of incubation. Before the additional dilution step, up to 2 mM of XN and OH-XN were positively identified (FIGURE 3.19 **(B)**). However, after the additional dilution step of a 10 mM sample, 5 mM of substrate as well as 4.5 mM of product were effectively recovered. By increasing either the enzyme concentration or the incubation time, the 81% conversion rate could be established for higher substrate concentrations.

For further characterization of *Nha*-KHS-His$_{10}$, storage possibilities of the purified enzyme were tested for remaining activity. Hence, activity assays with protein samples of freeze-dried, frozen and refrigerated enzyme were conducted after a storage of 72 h.

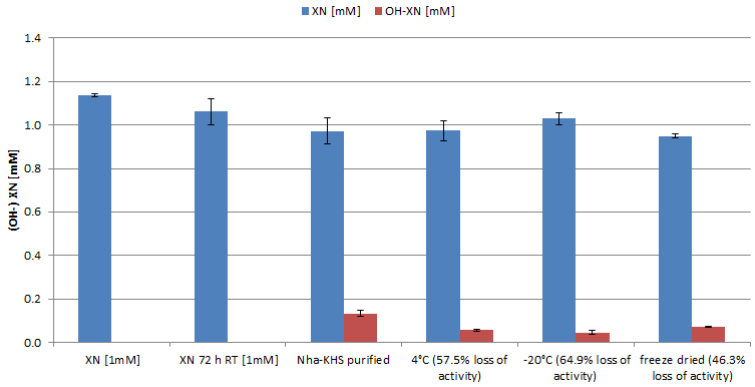


FIGURE 3.20: Activity analyses of purified *Nha*-KHS-His$_{10}$, which was either frozen, refrigerated or freeze dried for storage for 72 h. One mM of XN and 0.05 mg mL$^{-1}$ of enzyme was used. (OH-)XN concentrations $[mM]$ were obtained with HPLC-MS analysis, which was coupled to activity assays with the model substrate XN.

Figure 3.20 clearly indicated a decrease of activity of all stored *Nha*-KHS-His$_{10}$ assessed by a 2 min incubation of XN. The freeze-dried hydratase showed the lowest decrease of activity (46%) and storage at -20 °C revealed a 65% decrease of activity. The activity of the purified *Nha*-KHS-His$_{10}$ measured immediately after conversion was assumed to be 100%. Substrate peak area values were reproducible after an storage of 72 h at RT. Therefore, it can be concluded that the decrease in activity was subject to decrease in activity of the enzyme and not to detection failure.

To determine the influences of organic solvents on the activity of *Nha*-KHS-His$_{10}$, several hydrophobic and hydrophilic organic solvents were tested. Different concentrations ranging from 0.5 to 30% (v/v) of the solvents were added to the activity reaction mix. In order to identify influences of organic solvent in the short and long time scale, incubation times of the activity assays were performed for 2 min (FIGURE 3.21 **(A)**) and 3 h (**(B)**). Polar (EtOH, DMSO and chloroform) as well as nonpolar organic solvents (hexane and dodecane) were applied.

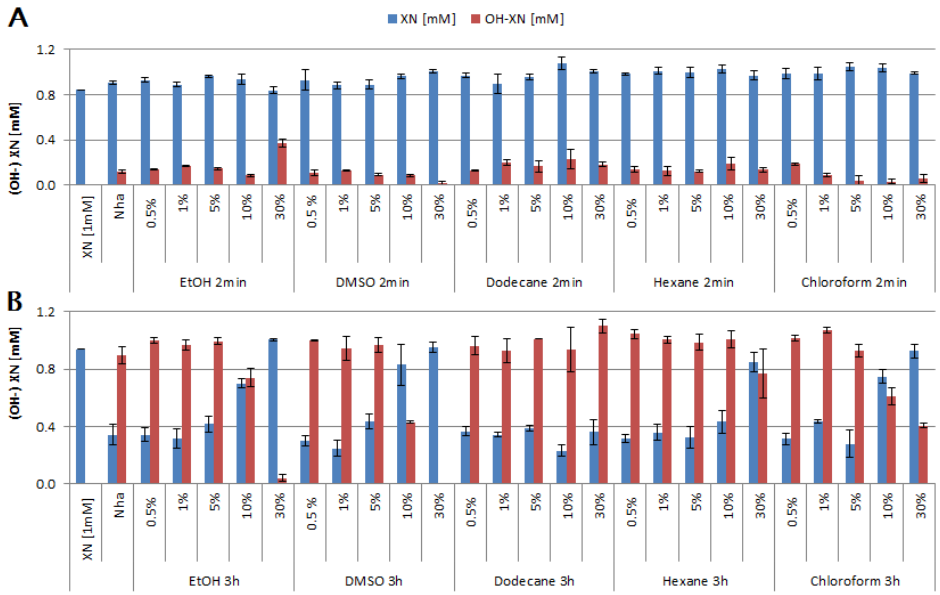


FIGURE 3.21: Influences of EtOH, DMSO, dodecane, n-hexane and chloroform as organic solvents on the activity assays of *Nha*-KHS-$His_{10}$. Concentrations ranging from 0.5% to 30% were incubated for either 2 min (**A**) or 3 h (**B**). One mM of XN and 0.05 mg $mL^{-1}$ of enzyme was used. (OH-)XN concentrations in mM were obtained via HPLC-MS measurements, coupled to activity assays with the model substrate XN. Biological triplicates were performed.

Analysis of 2 min conversions revealed a positive effect of addition of 30% (v/v) of EtOH to the reaction mixture. However, the effect was apparently reversed over an incubation time of 3 h. In general, EtOH seemed to have little to no effect on the activity of *Nha*-KHS-$His_{10}$ upon an addition of less than 30% (v/v) of EtOH for 2 min incubation. However, over a duration of 3 h EtOH concentrations above 5 % (v/v) seemed to inhibit the reaction. Inhibitory effects were also identified by addition of $\geq$ 5% (v/v) of DMSO and chloroform over 3 h. Further, adding $\geq$ 10% (v/v) of DMSO inhibited the reaction already after 2 min of incubation time. Analysis of activity of *Nha*-KHS-$His_{10}$ after addition of nonpolar solvents such as dodecane and hexane showed no distinctive influence. Incubation with the solvents for 2 min or 3 h revealed no changes in activity. Only 30% (v/v) of hexane revealed a negative effect on the conversion.

## 3.6 Kinetics of *Nha*-KHS

After optimization of the activity assay, kinetic parameters of purified *Nha*-KHS-$His_{10}$ were determined in 2 min activity assays with the alternative substrate XN. All measurements were conducted in triplicates. Substrate concentrations varying from 0.125 mM to 3 mM were incubated with 0.05 mg $ml^{-1}$ of purified *Nha*-KHS-$His_{10}$. Specific activities, measured in $\mu$mol $min^{-1}$ $mg^{-1}$, were plotted over substrate concentrations in mM. Nonlinear fitting was performed in SigmaPlot® (FIGURE 3.22).

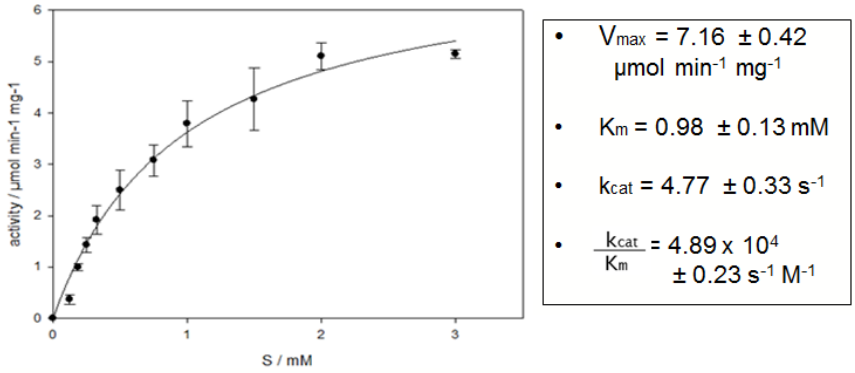


FIGURE 3.22: Plot of the initial velocity against the substrate concentration for *Nha*-KHS-$His_{10}$ catalyzed XN conversion. Activity assays with substrate concentrations from 0.125 to 3.0 mM were coupled to HPLC-MS measurements. Biological triplicates were performed. The used enzyme concentration was 0.05 mg $mL^{-1}$. Non-linear curve fitting was performed with SigmaPlot.

Fitting of values onto an hyperbola resulted in a $V_{max}$ of 7.16 $\pm$ 0.42 $\mu$mol $min^{-1}$ $mg^{-1}$ and $K_m$ of 0.98 $\pm$ 0.13 mM. Furthermore, the turnover number $k_{cat}$ = 4.77 $\pm$0.33 $s^{-1}$ was used to further calculate:

$$\frac{k_{cat}}{K_m} = 4.89 \times 10^4 \pm 0.23 s^{-1} M^{-1} \tag{3.1}$$

In order to confirm substrate saturation even at low XN concentrations, activity assays with 0.125 to 0.325 mM were performed with conversion times of 30 s to 2 min (FIGURE 3.23).

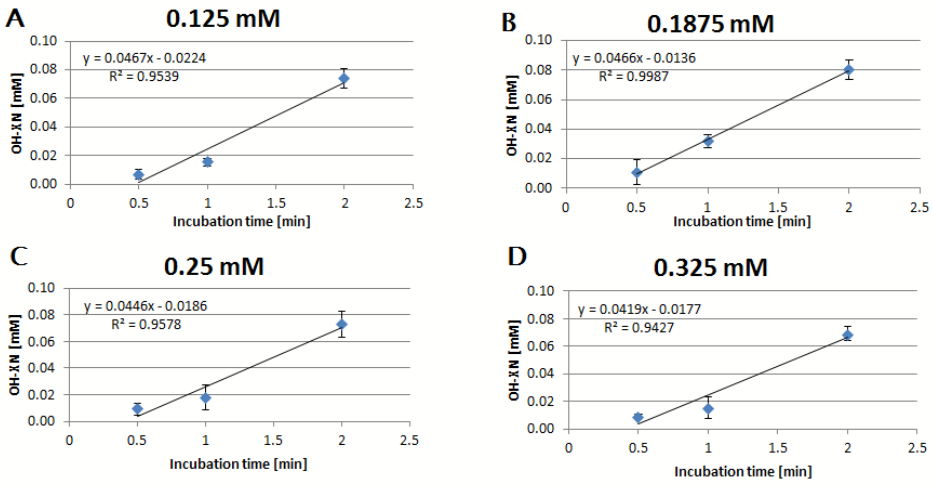


FIGURE 3.23: Activity assays with 0.125- 0.325 mM of XN (**A-D**), 0.05 mg $mL^{-1}$ of purified *Nha*-KHS-$His_{10}$ and incubation times from 30 s to 2 min *in vitro* were coupled with HPLC-MS measurements. Biological triplicates were performed.

Diagrams displaying the conversions of 0.125-0.325 mM substrate with 0.05 mg $mL^{-1}$ of purified enzyme presented a clear linear relationship of all concentrations over time. $R^2$-values were >95%. Therefore, substrate saturation for all tested concentrations in previously determined kinetic parameters was confirmed.

## 3.7 Expression and activity analysis of *Nha*-KHS variants in *P. pastoris*

### 3.7.1 Expression analyses of muteins in native signal sequences, nosig- and FLAG-variants, and glycosylation variants

Since previously, no protein expression for strains expressing proteins with mutated (nosig) and masked (FLAG) signal sequences, and single mutation variants of three N-glycosylation sites was observed, expression and activity analyses were repeated. Therefore, expression, Riezman cell disruption for pellet samples as well as MeOH/$CHCl_3$ and TCA- precipitation of culture SN samples were conducted and used for Western Blot analysis (FIGURE 3.24 and FIGURE3.25).

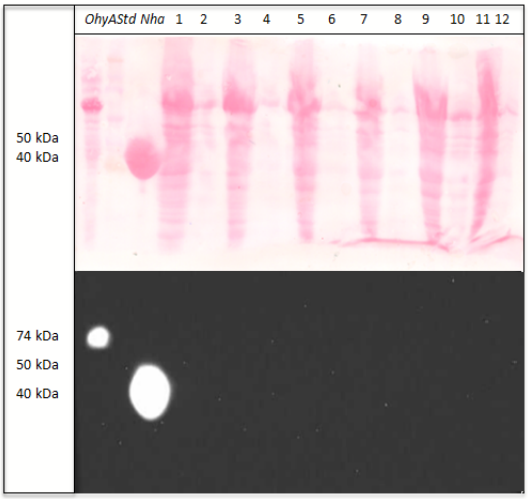


| | |
|---|---|
| *OhyA* | Positive control [74 kDa] |
| Std | Novex Protein Ladder |
| *Nha* | Positive control [deglycosylated 39.9 kDa] |
| 1 | *Pp Δhis 4*_nosig 1_*Nha*-KHS-$His_{10}$ pellet |
| 2 | *Pp Δhis 4*_nosig 1_*Nha*-KHS-$His_{10}$ culture SN |
| 3 | *Pp Δhis 4*_nosig 2_*Nha*-KHS-$His_{10}$ pellet |
| 4 | *Pp Δhis 4*_nosig 1_*Nha*-KHS-$His_{10}$ culture SN |
| 5 | *Pp Δhis 4*_nosig 3_*Nha*-KHS-$His_{10}$ pellet |
| 6 | *Pp Δhis 4*_nosig 1_*Nha*-KHS-$His_{10}$ culture SN |
| 7 | *Pp Δhis 4*_FLAG1_*Nha*-KHS-$His_{10}$ pellet |
| 8 | *Pp Δhis 4*_Flag1_*Nha*-KHS-$His_{10}$ culture SN |
| 9 | *Pp Δhis 4*_FLAG2_*Nha*-KHS-$His_{10}$ pellet |
| 10 | *Pp Δhis 4*_FLAG2_*Nha*-KHS-$His_{10}$ culture SN |
| 11 | *Pp Δhis 4*_FLAG3_*Nha*-KHS-$His_{10}$ pellet |
| 12 | *Pp Δhis 4*_FLAG3_*Nha*-KHS-$His_{10}$ culture SN |

FIGURE 3.24: Western Blot analysis of 3 clones of *P. pastoris* CBS7435 Δ$his4$_nosig _ *Nha*-KHS-$His_{10}$ and *P. pastoris* CBS7435 Δ$his4$ _ FLAG _*Nha*-KHS-$His_{10}$ (deglycosylated 39.9 kDa). Strains were grown under standard cultivation conditions, harvested and disrupted using the Riezman cell disruption protocol. The samples were loaded onto an SDS-PAGE for Western Blot analysis.

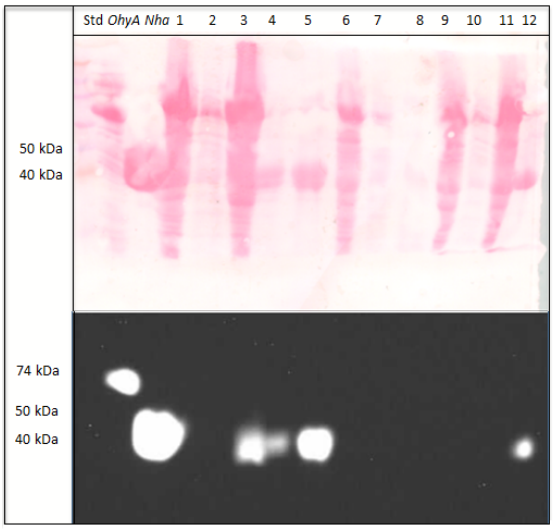


| | |
|---|---|
| Std | Novex Protein Ladder |
| *OhyA* | Positive control [74 kDa] |
| *Nha* | Positive control |
| 1 | *Pp Δhis 4* (WT) pellet |
| 2 | *Pp Δhis 4* (WT) culture SN |
| 3 | *Pp pPpB1_S_Nha*-KHS-$His_{10}$ pellet |
| 4 | *Pp pPpB1_S_Nha*-KHS-$His_{10}$ culture SN (TCA) |
| 5 | *Pp pPpB1_S_Nha*-KHS-$His_{10}$ culture SN (MeOH/Chloroform) |
| 6 | N112A pellet |
| 7 | N112A culture SN (TCA) |
| 8 | N112A culture SN (MeOH/Chloroform) |
| 9 | N132A pellet |
| 10 | N132A culture SN |
| 11 | N219A pellet |
| 12 | N219A culture SN |

FIGURE 3.25: Western Blot analysis of *P. pastoris* CBS7435 $\Delta his4$ glycosylation variants of pPpB1_S_ *Nha*-KHS-$His_{10}$ (N112A, N132A, N219A) (nonglycosylated 39.9 kDa). Strains were grown under standard cultivation conditions, harvested and disrupted using Riezman cell disruption protocol. Then, samples were loaded onto an SDS-PAGE for Western Blot analysis.

On both immunoblotting images, the positive control *Nha*-KHS-$His_{10}$ with a calculated size of 39.9 kDa for the deglycosylated enzyme and positive control with the size of 74 kDa were visible. However, none of the nosig- as well as FLAG-variants (FIGURE 3.24) showed a Western Blot signal. Sample analyses were conducted twice for verification of the obtained results. In FIGURE 3.25, lane 3-5 showed the positive control pellet (lane 3) and the culture SN fractions after either TCA (lane 4) or MeOH/$CHCl_3$ (lane 5) precipitation. The *P. pastoris* construct with the intracellular expression cassette showed strong signals in the pellet and culture SN fractions. However, the MeOH/$CHCl_3$ precipitation sample revealed the strongest signal of all detected KHSs. The glycosylation variant N219A, also showed a signal at the expected size. Therefore, the potentially deglycosylated mutant N219A was successfully expressed and detected via Western Blot. Interestingly, no signal for the N219A variant was obtained in the pellet fraction.

### 3.7.2 Activity analysis of nosig-, FLAG- and glycosylation variants of *Nha*-KHS-$His_{10}$

For verification of the Western Blot results in FIGURE 3.24 and FIGURE 3.25, activity assays with the pellet and culture SN fractions of 50 $OD_{600}$ of all nosig-, FLAG- and gycosylation variants of *P. pastoris* pPpB1_S_*Nha*-KHS-$His_{10}$ were conducted with 0.5 mM of XN.

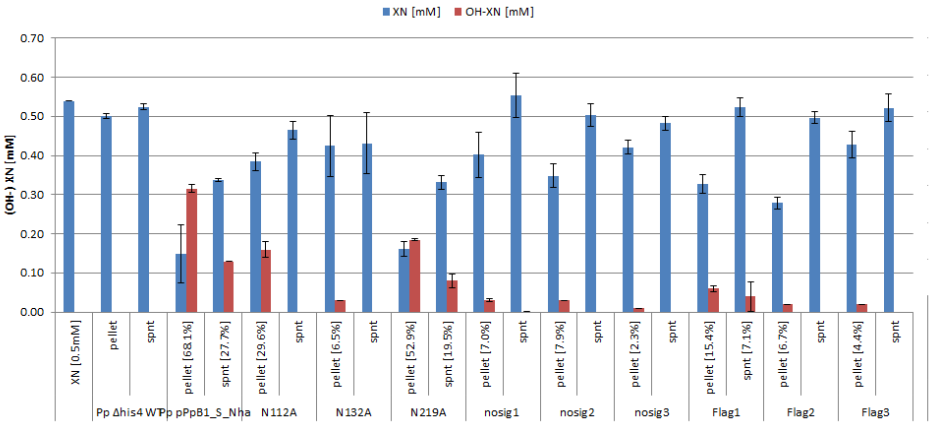


FIGURE 3.26: Activity analysis of glycosylation variants of *Nha*-KHS-$His_{10}$ (N112A, N132A, N219A), nosig variants as well as FLAG variants after expression in *P. pastoris*. XN(-OH) concentrations in mM were obtained with HPLC-MS, coupled to activity assays. 0.5 mM of substrate, as well as of 50 $OD_{600}$ units were used for conversion with pellet fractions and concentrated culture SN.

All glycosylation variants showed activity in the pellet fraction. However, only for variant N219A activity was also detected in the culture SN (FIGURE 3.26). Furthermore, activity was observed for nosig variants as well as variants with a masked signal peptide. All variants lacking the signal sequence as well as masked variants showed ∼5% of activity in the cell pellet fractions compared to the pellet fraction of the intracellularly expressed *Nha*-KHS-$His_{10}$. Additionally, FLAG variant 1 (FLAG1) also displayed substrate conversion in the culture SN fraction. To summarize, all variants converted XN to XN-OH, even though Western Blot analyses did not detect a signal for each variant.

## 3.8 Enzymatic deglycosylation of *Nha*-KHS

Initially, *Nha*-KHS variants lacking predicted N-glycosylation sites were generated for 3D structure determination. However, since the respective variants could not be expressed in *P. pastoris* to sufficient protein yield, *Nha*-KHS was enzymatically deglycosylated with Endo$H_f$ to determine the effects of N-glycosylation on *Nha*-KHS stability and activity. Therefore, *Nha*-KHS-$His_{10}$ was incubated from 30 min to 2.5 h with Endo$H_f$ and 2.5 $\mu$g of deglycosylated enzyme was loaded onto an SDS-PAGE (FIGURE 3.27 **(A)**). Further, deglycosylated samples were used for Western Blot analysis and PonceauS staining (FIGURE 3.27 **(B)**).

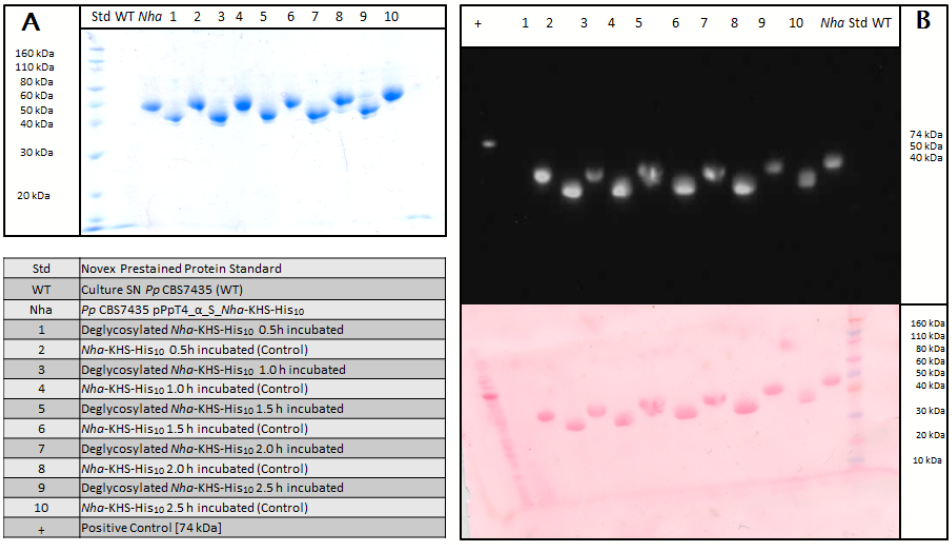


| | |
|---|---|
| Std | Novex Prestained Protein Standard |
| WT | Culture SN *Pp* CBS7435 (WT) |
| Nha | *Pp* CBS7435 pPpT4_α_S_*Nha*-KHS-$His_{10}$ |
| 1 | Deglycosylated *Nha*-KHS-$His_{10}$ 0.5h incubated |
| 2 | *Nha*-KHS-$His_{10}$ 0.5h incubated (Control) |
| 3 | Deglycosylated *Nha*-KHS-$His_{10}$ 1.0 h incubated |
| 4 | *Nha*-KHS-$His_{10}$ 1.0 h incubated (Control) |
| 5 | Deglycosylated *Nha*-KHS-$His_{10}$ 1.5 h incubated |
| 6 | *Nha*-KHS-$His_{10}$ 1.5 h incubated (Control) |
| 7 | Deglycosylated *Nha*-KHS-$His_{10}$ 2.0 h incubated |
| 8 | *Nha*-KHS-$His_{10}$ 2.0 h incubated (Control) |
| 9 | Deglycosylated *Nha*-KHS-$His_{10}$ 2.5 h incubated |
| 10 | *Nha*-KHS-$His_{10}$ 2.5 h incubated (Control) |
| + | Positive Control [74 kDa] |

FIGURE 3.27: (**A**) SDS-PAGE and (**B**) Western Blot analysis of enzymatically deglycosylated *Nha*-KHS-$His_{10}$ expressed in *P. pastoris*. The expected size of nonglycosylated *Nha*-KHS-$His_{10}$ was 39.9 kDa. Samples were incubated at 37 °C for 0.5-2.5 h and 2.5 $\mu$g of enzyme was loaded.

No effect of different incubation times on the deglycosylatin of *Nha*-KHS-$His_{10}$ was observed. All samples from 30 min to 2.5 h incubation time with Endo$H_f$ showed the same deglycosylation efficiency. Nonglycosylated *Nha*-KHS-$His_{10}$ showed an apparent protein size of 39.9 kDa on the SDS-PAGE, whereas the glycosylated protein showed a slightly larger apparent size (FIGURE 3.27 **(A)**). Glycosylated samples showed also a slightly smaller second band. Western Blot analysis confirmed the identity of the second band to be *Nha*-KHS-$His_{10}$ (FIGURE 3.27 **(B)**). Due to the low amount of Endo$H_f$ used, only a very faint band was detected at ~70 kDa. Analysis of the Western Blot showed slightly stronger signals for the deglycosylated samples.

Thermo stability assays (FIGURE 3.28 **(B)**) and activity assays (FIGURE 3.28 **(A)**) were conducted to compare the influences of N-glycosylation on enzyme activity and stability. Due to the similar N-deglycosylation patterns of samples deglycosylated for 0.5-2.5 h, only samples incubated for 0.5 and 2.5 h with Endo$H_f$ were tested. All controls were also tested for activity. *Nha*-KHS-$His_{10}$ incubated with dH2O instead of Endo$H_f$, buffer only and buffer and Endo$H_f$ mixture were treated as the deglycosylated samples. The purified *Nha*-KHS-$His_{10}$ was directly used for the activity assay. For thermo stability determination, the protein was incubated in different buffer systems ranging from pH 4.0 to 9.0 and analyzed via the thermofluor® assays (FIGURE 3.28 **(B)**). Twenty $\mu$g of protein was labeled with SYPRO® Orange and analyzed with real time PCR by BioRad. Measurements were performed in triplicates.

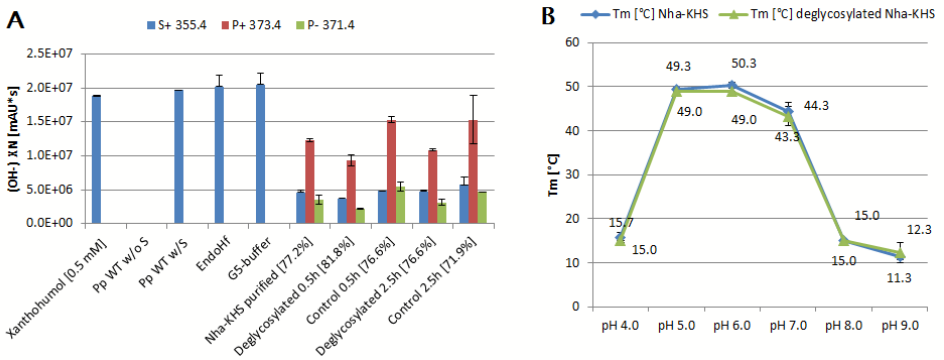


FIGURE 3.28: (**A**) Activity assays with deglycosylated *Nha*-KHS-$His_{10}$ coupled to HPLC-MS measurements, conducted with 0.5 mM of substrate and 1 mg $mL^{-1}$ of enzyme. (**B**) Thermofluor® assays of purified (de-)glycosylated*Nha*-KHS-$His_{10}$ in different buffer systems (deglycosylated size 39.9 kDa). Samples were deglycosylated with Endo$H_f$ enzyme mix at 37 °C for 0.5-2.5 h.

After the performance of activity assays with 0.5 mM of substrate, a decrease in activity of deglycosylated samples was determined. All samples showed an decrease of substrate by at least 75%. XN-OH peak area values $[mAU \cdot s]$ revealed a decrease in area values of 30% of deglycosylated samples compared to the controls and purified *Nha*-KHS-$His_{10}$. Therefore, about equal substrate decrease was detected in all samples, but deglycosylated samples showed decreased concentrations of product. Due to the lack of hydratase activity detected in the enzyme mix and buffer, influences on enzyme activity caused by Endo$H_f$ enzyme reaction components were excluded. Also equal amounts of substrate in all chemical and biological standards were obtained. Therefore, it can be concluded that the Endo$H_f$ enzyme reaction components did not have any effect on the peak area values obtained. Therefore, the deglycosylated enzyme was less active than the glycosylated *Nha*-KHS-$His_{10}$.

The thermo stability shift assays revealed that samples ranging between pH 5.0 and 6.0 had a $T_m$ up to 50 °C. No notable difference in thermo stability between N-glycosylated and deglycosylated samples was identified. However, samples of pH 4.0, 8.0 and 9.0 showed a highly decreased $T_m$, which led to the conclusion that the protein was less stable under these conditions.

## 3.9 Confirmation of $T_m$ with nanoDSF

Since the determination of $T_m$ with the thermofluor® method used a fluorescent dye, a lable-free analysis was performed additionally in order to compare both results. Therefore, the melting temperatures of *Nha*-KHS-$His_{10}$ in buffer system ranging from pH 4.0 to pH 9.0 were determined with real time PCR measuring the first derivatives of fluorescent tryptophanes at

350 nm. Measurements were performed in triplicates and a protein concentration of 1 mg $mL^{-1}$ was used (FIGURE 3.29).

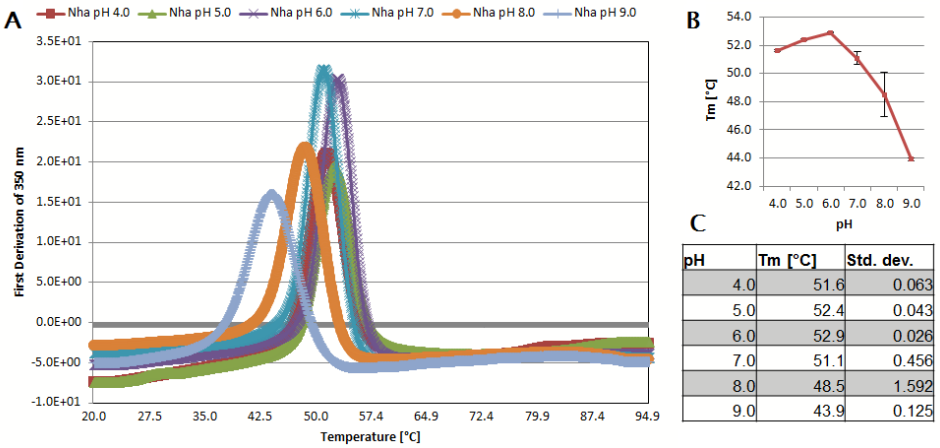


| pH | Tm [°C] | Std. dev. |
|---|---|---|
| 4.0 | 51.6 | 0.063 |
| 5.0 | 52.4 | 0.043 |
| 6.0 | 52.9 | 0.026 |
| 7.0 | 51.1 | 0.456 |
| 8.0 | 48.5 | 1.592 |
| 9.0 | 43.9 | 0.125 |

FIGURE 3.29: Thermostability analyses of 1 mg $mL^{-1}$ of purified *Nha*-KHS-$His_{10}$ measured by Prometheus NT.48 by NanoTemper. Biological triplicates were performed. (**A**) Melting scan of the first derivative of fluorescence of tryptophanes at 350 nm (25-95 °C, 1 °C $min^{-1}$ temperature increase). Colored lines correspond to melting temperatures under different pH conditions, pH 4.0 to pH 9.0 (**B-C**).

FIGURE 3.29 (**A**) indicated clearly that most fluorescence was displayed at pH 6.0 and 7.0., indicating that pH 6.0 and 7.0 offered optimal structural realignment for detecting most aggregated tryptophanes. However, structurally pH 5.0-6.0 showed the most stable conformation. At $\sim$ 53 °C (FIGURE 3.29 **(B)**), the protein was stable and started to unfold with increased temperature (1°C increase $min^{-1}$). Wider peaks detected more aggregates, which corresponds to higher unfolding under these pH conditions. Under the tested conditions, *Nha*-KHS-$His_{10}$ is thermally most stable at acidic pH values. Above pH 7.0, $T_m$ decreased significantly.

For further stability tests, a refolding experiment of the tertiary structure of *Nha*-KHS was performed. Through increasing temperature the structure will undergo conformational changes until it will finally unfold. By increasing the temperature over the melting temperature and decreasing it, the tertiary structure should be retained. One mg $mL^{-1}$ of purified *Nha*-KHS-$His_{10}$ was tested with the increase of temperature of 5 °C $min^{-1}$ up to 65 °C, held for 1 min and decreased by 5 °C $min^{-1}$ to a final temperature of 20 °C (FIGURE 3.30).

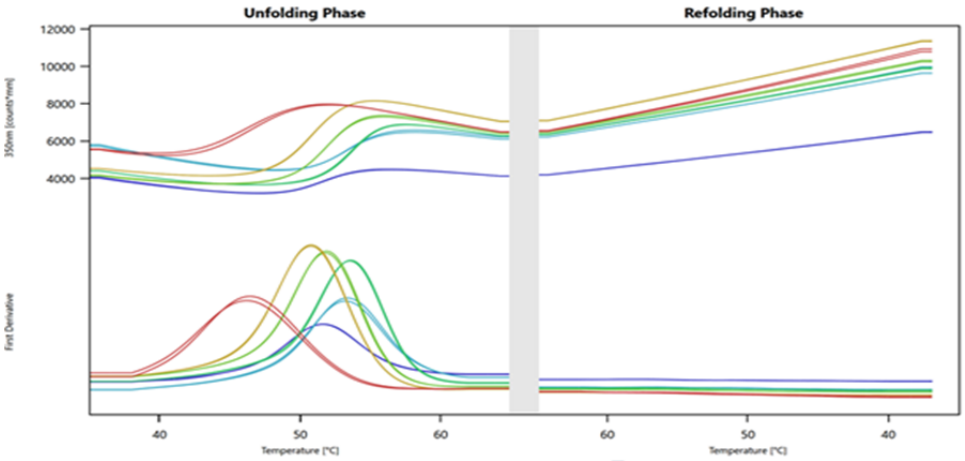


FIGURE 3.30: Thermo stability analyses of 1 mg $mL^{-1}$ of purified *Nha*-KHS-$His_{10}$ measured by Prometheus NT.48 by NanoTemper. Melting scans of fluorescence at 350 nm, measured in $counts \cdot min$, as well as the first derivative of fluorescence of tryptophanes at 350 nm are displayed. The measurements had a folding (25-65 °C, 5 °C $min^{-1}$ temperature increase), refolding phase (65-25 °C, 5 °C $min^{-1}$ temperature decrease) and a holding phase at 65 °C for 1 min.

The unfolding phase confirmed the previously obtained $T_m$ of *Nha*-KHS-$His_{10}$ at 53.5 °C. However, after holding and during the refolding phase no peaks in fluorescence for successful refolding were obtained.

## 3.10 Multicopy strains (DWP and flask cultivation)

In order to potentially increase the level of expressed and secreted protein in *P. pastoris*, multicopy strains were generated by transforming 5 $mu$g of linearized pPpT4_$\alpha$_S_*Nha*-KHS-$His_{10}$ into electrocompetent *P. pastoris* CBS7435 cells. Afterwards, single colonies were chosen after selection by antibiotic pressure and expressed in DWP and 50 mL flask cultivations. Growth curves were measured over the 72 h growth phases (FIGURE 3.31). SDS-PAGE, Western Blot (FIGURE 3.32 as well as activity assays (FIGURE 3.33) were conducted for analysis of the expression level and activity. Protein concentrations were determined via Bradford assays (TABLE 3.2.

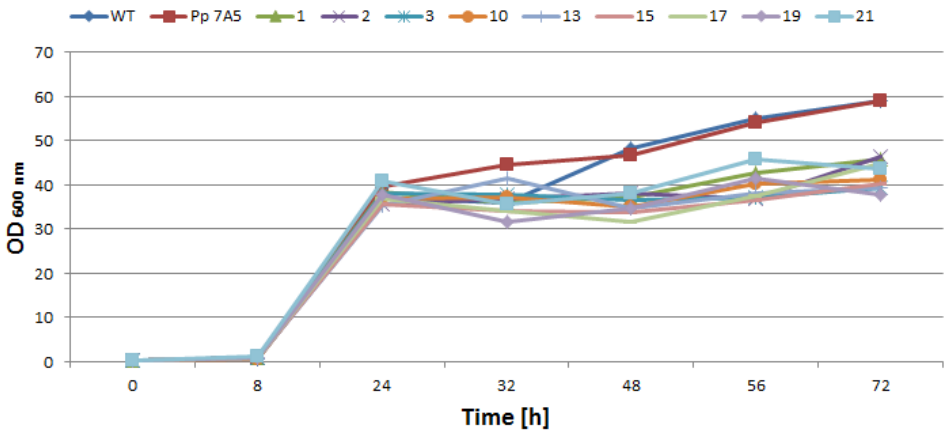


FIGURE 3.31: $OD_{600}$ measurements of *P. pastoris* CBS7435 [pPpT4 _$\alpha$_S_ *Nha*-KHS-$His_{10}$] multicopy strains 1-21 cultivated under standard conditions in 300 mL baffled flasks.

Colonies, numbered 1-21, were compared to the strain *Pp* 7A5 (*P. pastoris* CBS7435 [pPpT4 _$\alpha$_S_ *Nha*-KHS-$His_{10}$]) previously used in characterization, expression, purification and activity studies of *Nha*-KHS-$His_{10}$. Previously, strains had shown different growth and expression behaviors (data not shown). Therefore, cultivations in DWP as well as flasks were conducted and compared. Due to the similar growth patterns observed, FIGURE 3.31 represented both growth curves, in flasks as well as 96-DWPs. Clearly indicated, wild type strain as well as the original strain grew during 72 h i.e. glucose for 24 h, and on MeOH for 48 h to an $OD_{600}$ of 59 whereas multicopy strains 1-21 reached an $OD_{600}$ of 46 units only. Interestingly, a higher total protein concentration was obtained in DWP cultivation compared to flask cultivations of the SN of multicopy strains as well as the wild type strain (TABLE 3.2). The highest protein concentration of 0.262 mg $mL^{-1}$ was identified for the original strain. Strains 1 and 19 showed the highest protein concentrations of 0.100 mg $mL^{-1}$ compared to all other multicopy strains.

TABLE 3.2: Protein concentrations of multicopy strains of DWP as well as flask cultivation.

| **Sample** | **DWP [mg $mL^{-1}$]** | **flask [mg $mL^{-1}$]** |
|---|---|---|
| WT | 0.059 | 0.046 |
| *Pp*7A5 | 0.147 | 0.262 |
| 1 | 0.046 | 0.103 |
| 2 | 0.056 | 0.048 |
| 3 | 0.090 | 0.025 |
| 10 | 0.065 | 0.029 |
| 13 | 0.062 | 0.037 |
| 15 | 0.076 | 0.092 |
| 17 | 0.066 | 0.079 |
| 19 | 0.065 | 0.099 |

| | | |
|---|---|---|
| 21 | 0.060 | 0.071 |

Protein secretion levels were analyzed via TCA precipitation of 400 $\mu$L culture SN over night and loaded for Western Blot analysis (FIGURE 3.32 **(A)**).

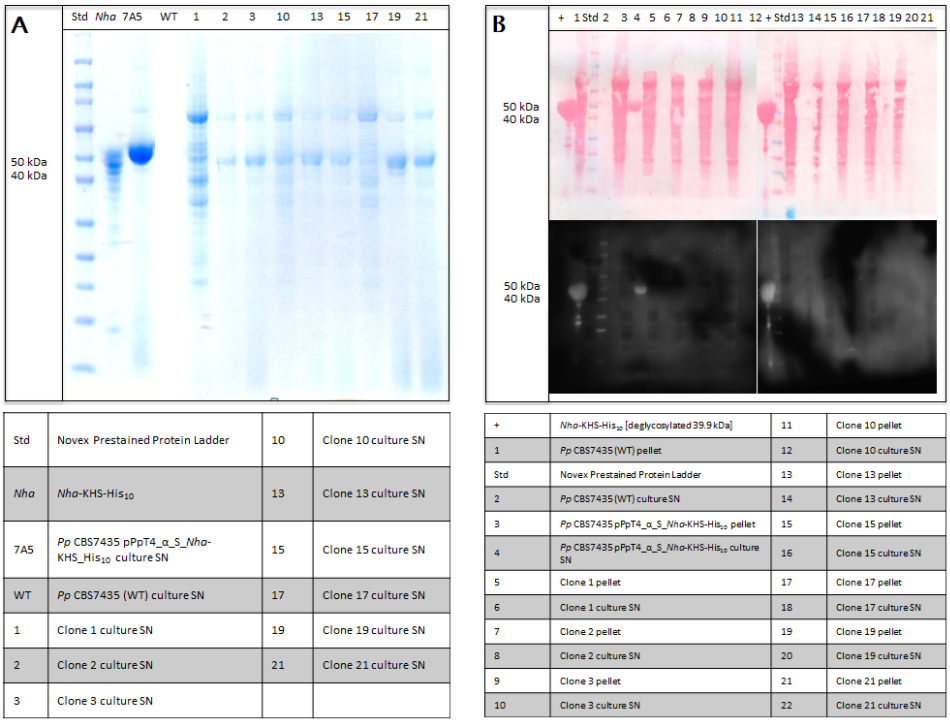


| | | | |
|---|---|---|---|
| Std | Novex Prestained Protein Ladder | 10 | Clone 10 culture SN |
| *Nha* | *Nha*-KHS-$His_{10}$ | 13 | Clone 13 culture SN |
| 7A5 | *Pp* CBS7435 pPpT4_α_S_*Nha*-KHS_$His_{10}$ culture SN | 15 | Clone 15 culture SN |
| WT | *Pp* CBS7435 (WT) culture SN | 17 | Clone 17 culture SN |
| 1 | Clone 1 culture SN | 19 | Clone 19 culture SN |
| 2 | Clone 2 culture SN | 21 | Clone 21 culture SN |
| 3 | Clone 3 culture SN | | |

| | | | |
|---|---|---|---|
| + | *Nha*-KHS-$His_{10}$ [deglycosylated 39.9 kDa] | 11 | Clone 10 pellet |
| 1 | *Pp* CBS7435 (WT) pellet | 12 | Clone 10 culture SN |
| Std | Novex Prestained Protein Ladder | 13 | Clone 13 pellet |
| 2 | *Pp* CBS7435 (WT) culture SN | 14 | Clone 13 culture SN |
| 3 | *Pp* CBS7435 pPpT4_α_S_*Nha*-KHS-$His_{10}$ pellet | 15 | Clone 15 pellet |
| 4 | *Pp* CBS7435 pPpT4_α_S_*Nha*-KHS-$His_{10}$ culture SN | 16 | Clone 15 culture SN |
| 5 | Clone 1 pellet | 17 | Clone 17 pellet |
| 6 | Clone 1 culture SN | 18 | Clone 17 culture SN |
| 7 | Clone 2 pellet | 19 | Clone 19 pellet |
| 8 | Clone 2 culture SN | 20 | Clone 19 culture SN |
| 9 | Clone 3 pellet | 21 | Clone 21 pellet |
| 10 | Clone 3 culture SN | 22 | Clone 21 culture SN |

FIGURE 3.32: SDS-PAGE (**A**) and Western Blot analysis (**B**) of *P. pastoris* CBS7435 [pPpT4 _α_S_ *Nha*-KHS-$His_{10}$] multicopy strains 1-21. After cultivation and protein expression under standard conditions, culture SN samples were precipitated with TCA overnight and pellet samples were disrupted with the Riezman protocol prior to SDS-PAGE and Western Blot.

The best expression and secretion levels were identified in the original strain. Due to similarity of results between DWP and flask cultivation, FIGURE 3.32 represents both cultivation results. The protein samples of clone 1 showed various undefined smaller bands upon SDS-PAGE (FIGURE 3.32 **(A)**) in comparison with *Nha*-KHS-$His_{10}$ and a strong band for the alcohol oxidase 1 (AOX1) protein at 74 kDA [27]. Also colony 17 revealed a similar pattern, however, with lower total protein concentrations. The positive control, *Nha*-KHS-$His_{10}$, was purified 3 weeks prior to loading and was most likely partially degraded. The degradation pattern, however, did not match the lower bands of clones 1 and 17. All multicopy strains showed a rather strongly expressed AOX1p band compared to *Pp* 7A5. Clone 19 also showed a higher total protein concentration and a rather strong *Nha*-KHS-$His_{10}$ signal. Western Blot analysis confirmed the result seen on the SDS-PAGE (FIGURE 3.32 **(B)**). Only the degraded positive control as well

as *Nha*-KHS-His$_{10}$ expressed in the original strain was detectable by Western Blot. The amounts of expressed KHSs of the multicopy strains were too low for detecting signals.

As already seen in other experiments, activity analysis often resulted in detection of enzyme activity even though no protein could be detected by Western Blot analysis. Therefore, an activity assay (FIGURE 3.33) was performed by using 98 $\mu$L of culture SN for conversion of 2 mM XN.

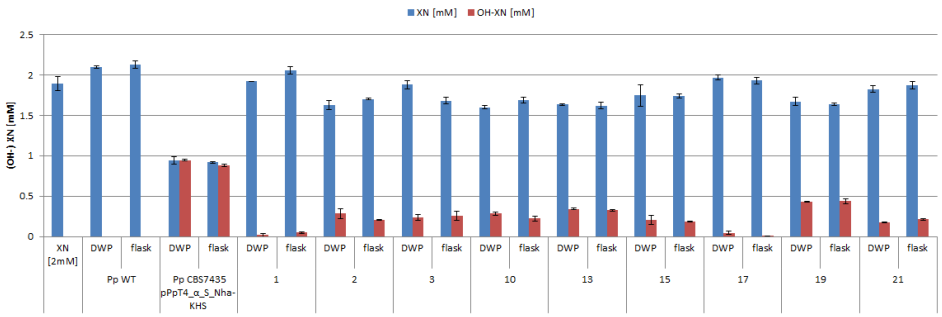


FIGURE 3.33: Activity analysis coupled to HPLC-MS of *P. pastoris* CBS7435 [pPpT4_$\alpha$ _S_*Nha*-KHS-His$_{10}$] culture SNs of multicopy strains 1-21. Two mM of substrate were used. Strains were cultivated in DWPs and baffled flasks. Activity measurements were performed with 98 $\mu$L of culture SN of *Nha*-KHS-His$_{10}$ multicopy strains.

After 2 min of incubation time, more than 50% of the substrate was converted to XN-OH by *Pp* 7A5, whereas the second-best converter, clone 19, showed a conversion of 30% (FIGURE 3.33). Comparing DWP and flask cultivation, no noticeable differences were observed. Mass balances of substrate and product equaled the applied substrate concentrations.

## 3.11 DASGIP® Bioreactor Cultivation of *Nha*-KHS

After attempts to generate a higher yield variant than *P. pastoris* CBS7435 [pPpT4_$\alpha$_S_*Nha*-KHS-His$_{10}$] failed, it was concluded that protein expression of *Pp* 7A5 should be upscaled in a bioreactor. The upscaling should give insight in the feasibility of large scale production in an industrial setting. Therefore, a DASGIP® bench-top high cell density fed-batch cultivation (HCDC) over an induction periode of 123 h was conducted. Before the induction phase with 5 mL h$^{-1}$ of MeOH, a cultivation up to 15 OD$_{600}$ as well as a glucose fed-batch bioreactor cultivation to an OD$_{600}$ of 100 were conducted to generate high cell density. The cultivation design was based on the protocol by Tolner *et al.* [48]. For analysis of cell growth, as well as protein expression and activity analyses, samples were taken every 6 h and further characterized as described.

### 3.11.1 Growth analyses

Every 6 h over the time course of 123 h, samples were taken for analyses of cell growth and viability. One mL of cell culture was obtained from the batch and weighed after drying. Furthermore, dilutions of cells were measured photometrically at 600 nm to obtain the optical density of the culture. Two growth curves, cell dry weight (CDW) in mg $mL^{-1}$ (**(A)**) as well as $OD_{600}$ measurements (**(B)**) over time [h] were recorded.

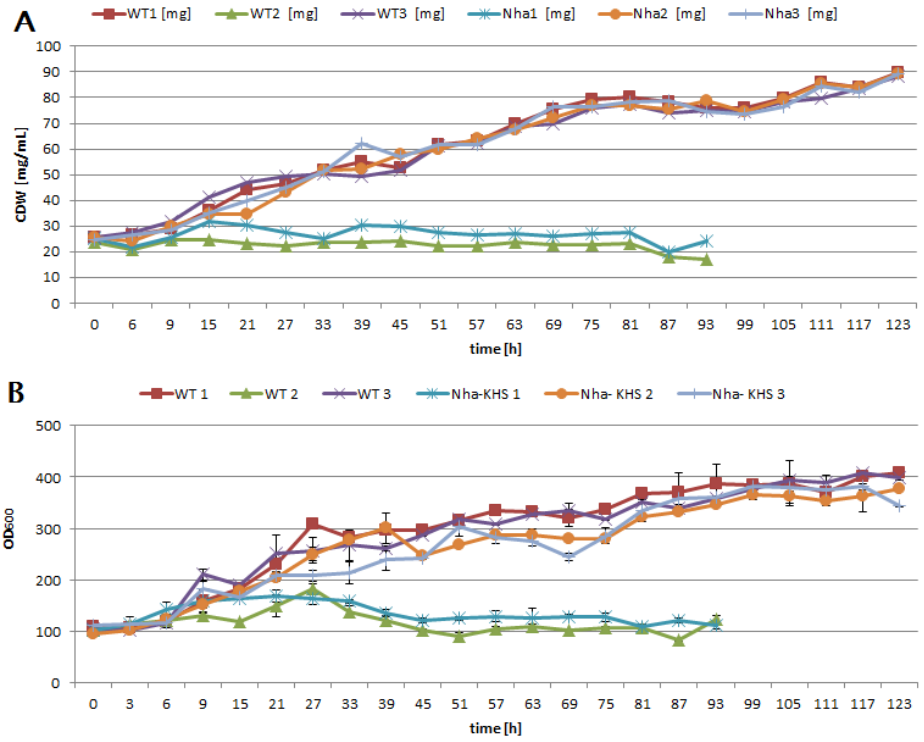


FIGURE 3.34: Growth analysis of *P. pastoris* CBS7435 [pPpT4_$\alpha$_S_*Nha*-KHS-$His_{10}$] and WT strains (1-3) of a DASGIP® fed-batch bioreactor cultivation over 123 h of MeOH induction. (**A**) Single measurements of cell dry weight (CDW) in mg $mL^{-1}$ over time [h]. (**B**) $OD_{600}$ measurements over time [h], measured in triplicates.

Both curves indicated highly similar growth behaviors during the induction phase over 123 h (FIGURE 3.34). Standard deviations of $OD_{600}$ measurements showed a few variations in the results. However, trends indicated a increasing biomass until 123 h in both representations. Strains wild type (WT) 2 and *Nha*-KHS 1 stopped growing after 9-15 h and continued with equal cell density over the next 80 h until shut off of the two bioreactors. Final sample analyses resulted in 90 mg $mL^{-1}$ of CDW and an $OD_{600}$ of roughly 400. Correlation between CDW and $OD_{600}$ revealed a $R^2$ value of $\geq$0.93, most probably caused by the inconsistent $OD_{600}$ measurements. Growth of WT srtains compared to strains recombinantly expressing *Nha*-KHS-$His_{10}$ indicated highly similar behaviors.

For further analysis of growth, specific growth rates [$\mu$] were calculated

during MeOH-feed (3.3). Calculation revealed in all four batches of WT and *P. pastoris* secreting *Nha*-KHS-$His_{10}$ a growth rate of 0.0092 ±0.0001 $h^{-1}$, which indicated highly similar growth behavior. Due to positive correlation between specific growth rate and protein expression, a steady increase in cell mass was beneficial for continuously increased protein secretion.

TABLE 3.3: Specific growth rates of *P. pastoris* CBS7435 [pPpT4_α_S_ *Nha*-KHS-$His_{10}$] during induction phase

| **Sample** | **$\mu$ induction phase [$h^{-1}$]** |
|---|---|
| *P. pastoris* CBS7435 (1) | 0.0093 |
| *P. pastoris* CBS7435 (3) | 0.0091 |
| *P. pastoris* expresssing *Nha*-KHS-$His_{10}$ (2) | 0.0091 |
| *P. pastoris* expressing *Nha*-KHS-$His_{10}$ (3) | 0.0092 |

### 3.11.2 Protein analyses

For monitoring protein concentrations in mg $mL^{-1}$ in the batches, Bradford-assays of culture SN samples were performed in triplicates every 6 h. Figure 3.35 presents the increased total protein concentration of all 6 cultivated batches.

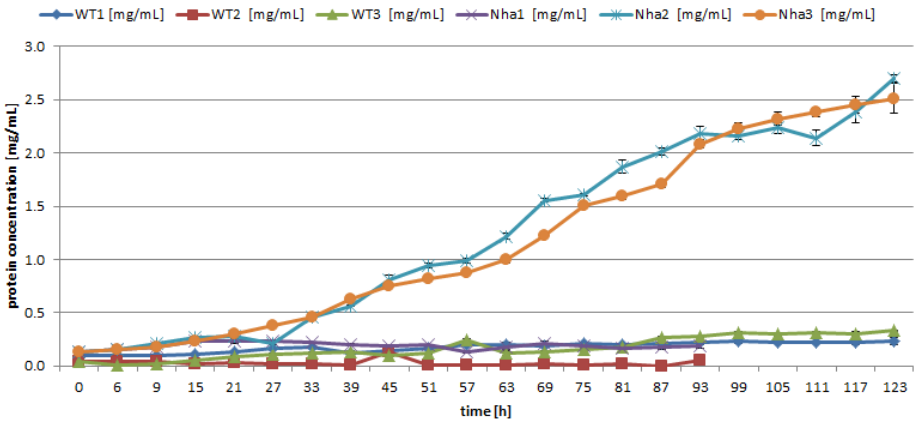


FIGURE 3.35: Total protein concentration in mg $mL^{-1}$ of culture SN over induction time [h] of *P. pastoris* CBS7435 [pPpT4_α_S_*Nha*-KHS-$His_{10}$] and WT strains (1-3) cultivated via DASGIP® fed-batch fermentation. Concentrations were determined via Bradford-assays.

WT strains showed minimal protein concentrations in culture SN, detected from the supplemented feed, whereas *P. pastoris* strains expressing *Nha*-KHS-$His_{10}$ showed a final protein concentration of 2.61 mg $mL^{-1}$. As expected, *Nha*-KHS strain 1 and WT strain 2 did not reveal an increase in protein concentration due to growth deficiency and lack of protein expression.

For more detailed protein analyses, protein samples in culture SN fractions were precipitated with TCA over night and loaded onto an SDS-PAGE (FIGURE 3.36). Samples were analyzed every 24 h.

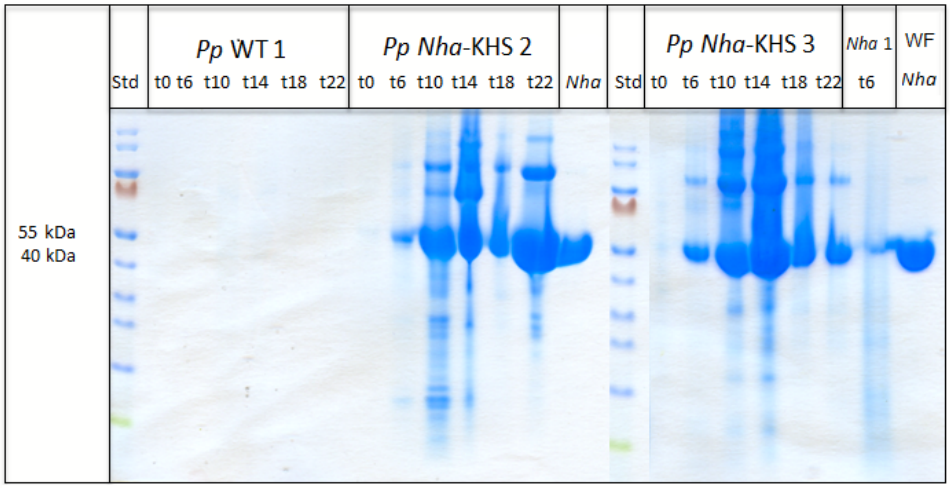


| Sample | t0 | t6 | t10 | t14 | t18 | t22 |
|---|---|---|---|---|---|---|
| Time [h] | 0 | 27 | 51 | 75 | 99 | 123 |

FIGURE 3.36: SDS-PAGE of culture SN samples of *P. pastoris* WT and *P. pastoris* CBS7435 [pPpT4_$\alpha$_S_*Nha*-KHS-His$_{10}$] strains (1-3) of every 24 h. About twenty $\mu$g of purified *Nha*-KHS-His$_{10}$ and a pooled washing fraction (WF) were loaded. The expected size of the deglycosylated enzyme is 39.9 kDa. Only sample t6, 27 h of induction, was loaded of *Nha*-KHS strain 1. Standard: PageRuler Prestained Protein Ladder ranging from 10 -180 kDa.

Samples of the WT strain showed no bands and no smear (FIGURE 3.36). A very slight band was detected by analyzing samples of *Nha*-KHS-His$_{10}$ before induction. After 27 h, a distinct band at 47 kDa was visible. The increased signal of the band correlated with the increasing protein concentration over time. However, *P. pastoris* strain 3 expressing *Nha*-KHS-His$_{10}$ showed no increased signal of band at time points 99 h and 123 h, which was most likely due to suboptimal bioreactor cultivation conditions. Between 69-75 h of induction, strain 3 expressing *Nha*-KHS-His$_{10}$ presented difficulties to retain 20 % of DO levels and fell underneath. Therefore, its growth and protein expression were limited. After 12 h of catching up, strain 3 recovered and showed similar expression levels as strain 2. However, the stagnation time of strain 3 can also be detected in the activity assessment in FIGURE 3.38 **(B)**.

As seen in Figure 3.36, strain 1 expressing *Nha*-KHS-His$_{10}$ after 27 h of induction was loaded for analysis. A clear band with the correct size of *Nha*-KHS-His$_{10}$ was detected. The concentration of the band seemed to be less than from strains 2 and 3. Furthermore, protein degradation was detected in the smear. Therefore, it was concluded that strain 1 expressing *Nha*-KHS-His$_{10}$ did not regenerate after the pH drop within the first 12 h. Also the pooled elution and washing (WF) fractions of the purification of

the harvested and concentrated culture SN including *Nha*-KHS-$His_{10}$ were loaded. Protein purification was performed, by loading 50 mL of the concentrated culture SN onto a 5 mL HiTrapFF column and following the protocol described in Materials and Methods.

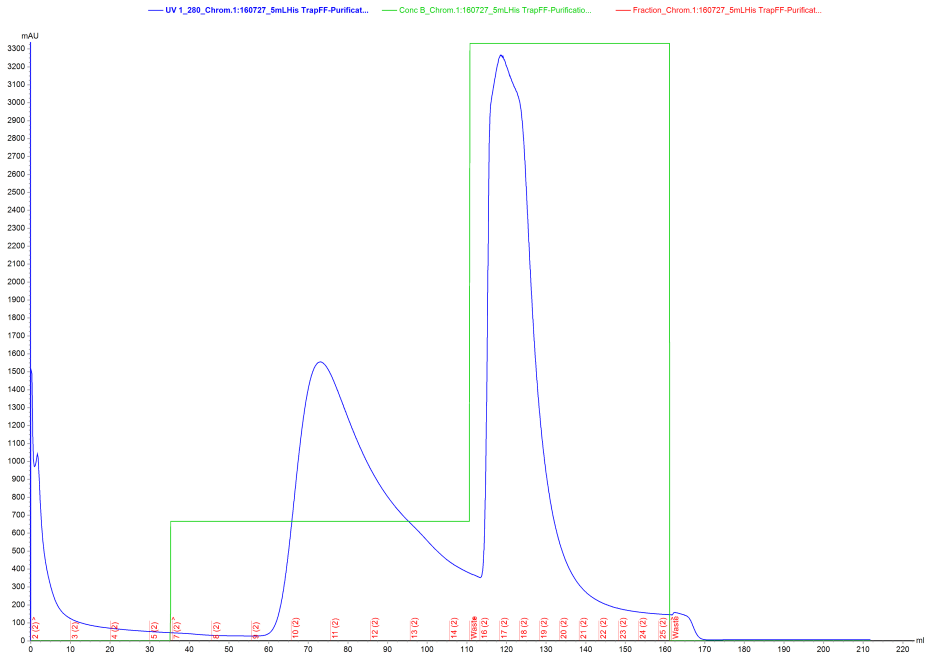


FIGURE 3.37: Chromatogram of *Nha*-KHS purified via *HisTrap* protocol using Äkta prime system. Blue line: Absorbance at 280 nm. Green line: Concentration of Imidazole from 10 mM to 250 mM.

In the washing fraction, a loss of 48% of enzyme was observed. Washing with 50 mM imidazole caused a loss of 1600 mAU whereas 3300 mAU were eluted with 250 mM imidazole (FIGURE 3.37). The *Nha*-KHS-$His_{10}$ band of elution as well as the wash fraction on the SDS-PAGE confirmed the loss due to the similar intensity of both bands. Washing fraction revealed also a faint band at the expected size of AOX1p (74 kDa). Therefore, washing was effective. However, adaptions would be required when doing the next large scale attempt to minimize the loss of enzyme.

After successful partial purification of *Nha*-KHS-$His_{10}$, the protein concentration was determined via UV-Vis spectrophotometry and an over all conclusion of protein concentrations of the downstream processing is summarized in TABLE 3.4.

TABLE 3.4: *Nha*-KHS-His purification

| **Sample** | ***Nha*-KHS protein concentration [mg mL$^{-1}$]** | **Total protein concentration [mg mL$^{-1}$]** |
|---|---|---|
| 2,000 mL SN | 2.61 (Bradford-assay) | 5,220 |
| 300 mL conc. SN | 11.7 (Bradford-assay) | 3,510 |
| 75 mL of purified *Nha*-KHS | 23.4 (UV-Vis spec.) | 1,755 |

An overall protein secretion of 2.6 g L$^{-1}$ into the culture SN was achieved after 123 h of induction. After concentration of the culture SN, 300 mL of SN containing 11.7 g L$^{-1}$ of protein were recovered. After the final steps of purification and desalting, 75 mL of purified *Nha*-KHS-His$_{10}$ with a concentration of 23.4 g L$^{-1}$ were recovered.

### 3.11.3 Enzyme activity

For detection of increasing activity of *Nha*-KHS-His$_{10}$, conversion assays with 98 $\mu$L of culture SN were performed with 2 mM XN for 2 min. Ever 24 h, samples of the induced strains were analyzed as well as time point 0, which have been taken before induction (FIGURE 3.38).

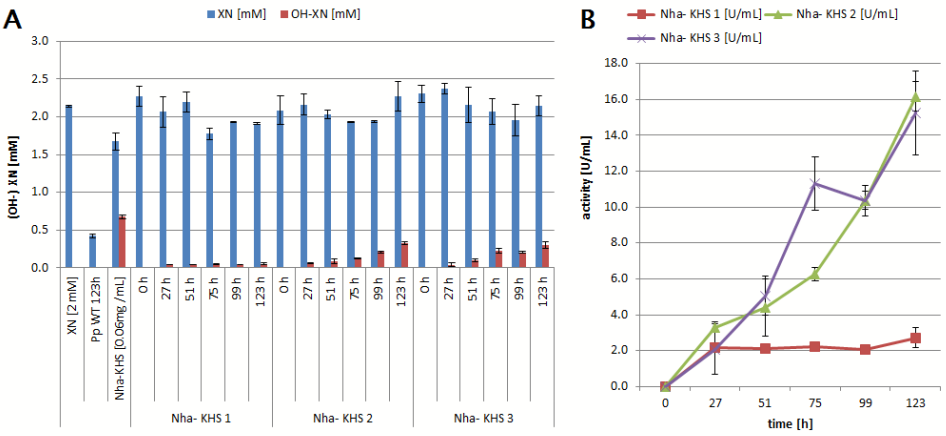


FIGURE 3.38: (**A**) Activity assays conducted with 3 $\mu$L of *P. pastoris* CBS7435 [pPpT4_$\alpha$_S_*Nha*-KHS-His$_{10}$] strains (1-3) cultivated via DASGIP® fed-batch fermentation. Activity assays were coupled to HPLC-MS. Two mM substrate was used. Biological triplicates were performed. (**B**) Volumetric activity was plotted over the induction time.

By following the time course of *Nha*-KHS-His$_{10}$, in strains 2 and 3 a clear increase in product was observed (FIGURE 3.38 **(A)**). Total protein concentration determination revealed a concentration of 2.61 mg mL$^{-1}$ in samples taken before harvest. Protein concentration positively correlated with the increase of XN-OH detected. Purified *Nha*-KHS-His$_{10}$ with a concentration of 0.06 mg mL$^{-1}$ of enzyme yield a conversion of 0.676 mM XN-OH. Culture SN samples, taken at the last time point revealed a conversion of 0.323 mM

XN-OH. Samples taken before induction did not display activity. Therefore, slight bands seen at sample t0 on the SDS-PAGE (FUGURE 3.36), are most likely loading errors. Time course of *Nha*-KHS-$His_{10}$ strain 1 showed an constant conversion of 0.045 mM XN-OH due to its lack of growth after the first 24 h. To emphasize the correlation between volumetric activity over induction time, FIGURE 3.38 **(B)** was included. Strain 2 and 3 showed a final activity of 16.2 U $mL^{-1}$. Strain 3 displayed an stagnation in expression on day 3. However, a recovery was seen on day 5 before harvest. If DO levels of strain 3 would have been kept constant it would probably have had a higher potential regarding activity and expression levels.

# Chapter 4

# Discussion

Due to previously obtained results [12], the most active and best expressed KHS was identified as *Nha*-KHS-$His_{10}$. Therefore, all experiments were conducted with *Nha*-KHS-$His_{10}$ so far. However, sequence analyses of *Fso*-KHS differed from *Nha*-KHS with an unanticipated double methionine (Met) residues in the beginning of the amino acid sequence. Naturally, not many proteins are known, which start their amino acid chain with double Met residues. However, Van Damme *et al.* [47] indicated, that Met-Met residues located at the N-terminus are frequently acetylated by NatF, the putative N-terminal acetyltransferases F. N-acetylation are common co-translational modifications. However, the function of N-terminal acetylation is still rather unknown. Previous investigations point to regulatory roles in function and localization of the protein [34].Therefore, the double Met could decrease expression and activity of *Fso*-KHS. For analyses of the hypothesis, the sequence of *Fso*-KHS will be normalized, cloned into *P. pastoris* and be investigated regarding expression and activity.

For characterization of *Nha*-KHS-$His_{10}$ several studies were performed. Upon investigation of the UV-Vis spectrum of *Nha*-KHS-$His_{10}$, it was concluded that the enzyme is independent of co-factors such as flavin adenine dinucleotide. For cofactor-dependent proteins, peak variations from 350-500 nm of wavelength are typical as described in Engleder *et al.* [22]. Also sequence analysis of the enzyme showed no binding domains for cofactors. The chromatogram as well as the SDS-PAGE analysis of purified samples after a Ni-NTA column and gel filtration (FIGURE 3.4) confirmed the highly efficient protein purification. Gel filtration via Äkta purifier system did not yield in purer protein samples. Therefore, all further purifications were performed with solely Ni-NTA column purification.

## 4.1 Kievitone conversions: Resting cells biocatalysis in *E. coli*

As seen in the resting cells conversion (see FIGURE 3.6) of kievitone to kievitone-hydrate, the highest activity was detected with 10 $OD_{600}$ units

of *E. coli* strain overexpressing *Nha*-KHS-$His_{10}$. However, 10 $OD_{600}$ units showed a significantly higher conversion than 50 $OD_{600}$ units. It was assumed that the high cell density and volume of 50 $OD_{600}$ units interfered with substrate access by the enzyme and therefore, only limited conversion took place. Furthermore, no valid mass balance was obtained. Substrate was absent in all samples measured with HPLC-UV. Due to the high cell density it is possible that kievitone as well as kievitone-hydrate are interacting with the cell surfaces and therefore, were only detectable to a certain extent. In order to forego the unequal mass balance, an extraction step using e.g. ethyl ether for solubility extraction [45] after the conversion could prove helpful.

Moreover, it had been reported that insoluble compounds such as prenylflavonoids require stabilizing agents such as 1% of FA after biocatalysis due to cyclization of the compound in aqueous solutions [42, 10]. The stabilizing agent aids in the retrieval of a balanced substrate and product recovery via HPLC-MS detection. Possible explanations indicate a solvent effect, which is caused by the substrate's and product's miscibility behavior in aqueous solution [20, 10].

## 4.2 Examination of alternative substrates (8-PN and XN)

For further analyses of KHS(s), the acquisition of an alternative substrate beyonf kievitone was of high priority. Therefore, structurally similar compounds were identified (FIGURE 4.1). 8-PN as well as XN, both extracted from the female flower of hops (*Humulus lupulus L.* and used for preserving and flavouring beer, belong to the prenylated flavonoids [42]. The compounds are under investigation for estrogenic effects for e.g. breast enhancements [44] as well as cancer chemopreventive activities [36] and, therefore, could reveal even greater scientific and industrial interest, if proven active.

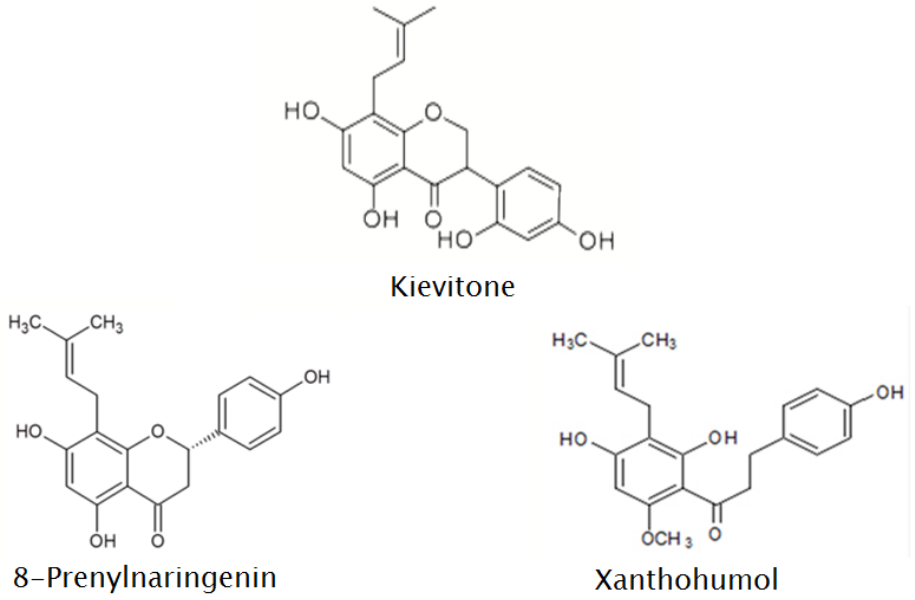


FIGURE 4.1: Chemical structures of the original substrate kievitone and the alternative substrates 8-PN and XN.

CFE-acitivity assays from bacterial expression hosts and concentrated culture SN as well as purified *Nha*-KHS-$His_{10}$ from a fungal expression host showed conversions of 8-PN to the hydrated product 8-(3-hydroxy-3-methyl-butyl)naringenin. Therefore, both expression hosts are suitable for the conversion of 8-PN, even though the CFE of *E. coli* expressing *Nha*-KHS-$His_{10}$ showed only limited amounts of the product. The cause for the smaller conversion compared to fungally expressed *Nha*-KHS could originate in the higher expression levels of proteins in *P. pastoris* [3]. Unfortunately, no samples of the *P. pastoris* resting cells conversions showed no product peak. The substrate peaks indicated a loss of substrate to possibly the cells, which could be ingesting the compounds and metabolize it to unidentified products. An additional extraction step could confirm the hypothesis and also aid in reaching variance of substrate are values.

XN showed substrate conversions up to 90%, which indicated a highly elevated activity and a greater affinity for the enzyme than 8-PN. In the activity assays performed, the hydration of the substrate was identified via NMR. Also the resting cells assay concept was applied successfully and could save time and resources when a high throughput screening assay will be required. Solely the decrease of substrate in wild type controls of *P. pastoris* would require improvement to equalize the mass balance of substrate input and product output.

To conclude, XN as well as 8-PN were successfully converted to the hydrated products. However, the activity and affinity of *Nha*-KHS-$His_{10}$ to XN showed conversion rates up to 90%. Due to the flexibility in the second

open ring, XN may access the active site more easily by forcing the third ring into a conformational change whereas 8-PN is structurally constricted. Due to the more significant conversion rates, it was decided to focus further characterization studies of *Nha*-KHS-$His_{10}$ on XN as model substrate.

## 4.3 Confirmation of the product XN-OH

The NMR analysis of the product after an upscaled conversion assay confirmed the hydration of the substrate. Also confirmation of the absorption maxima of the substrate and product were established at 371 nm. Due to the result it can be assumed that for all flavonoid-compounds the product's absorption maximum equal the absorption maximum of the substrate. The importance of the finding will have an influence on the detection method via HPLC-UV. So far the adapte protocol from DSM was applied [12], in which the detection of the DAD-channels varied for kievitone (290 nm) and kievitone-hydrate (220 nm). Nevertheless, both substances should be evaluated at 290 nm, because neither the prenylated group nor the addition of the hydroxy group should modify the absorption maximum. Both chemical groups do not cause any changes in the absorption maximum, because the chemical groups are no chromophores. Chromophores, e.g. nitroso, thiocarbonyl, azo, azoxy, azoamoido and p-quinonoid, or so called color-bearing groups, are unsaturated groups with the ability of projecting color when oxidized. The substituted hydroxyl-group is identified as auxochrome, which means that it can influence the absorption maximum when combined with a chromophore [26]. Nevertheless, the absence of a suitable chromophore prevents the change in the absorption maximum of the hydrated product.

## 4.4 Optimization of assay conditions for XN

Due to the limited access to kievitone as substrate, no activity assay opimization had been perfromed so far. Therefore, no characterizations of *Nha*-KHS-$His_{10}$ conducted. KHS was reported to be most active at pH 5.5 [46]. However, no confirmation or disapproval had been reported since 1990. For evaluation of optimal assay parameters of purified *Nha*-KHS-$His_{10}$, examinations of several conditions e.g. pH, temperature, conversions over a time course, influences of organic solvents etc. were performed with the model substrate XN.

By analyzing pH conditions, the ratio of converted product [%] of suboptimal conditions varied only slightly from conversion rates of the optimal

pH, at 5.0-6.0. Hence, the assessment of pH optimum by Turbek et al. [46] was confirmed.

Temperature analysis suggested the ideal condition at 35 °C. Up to the present, activity analyses were conducted at 28 °C due to the standard condition of fungal cultivation and expression [12, 46].

As described previously, the fluctuation in detected XN as well as XN-OH was observed on various occasions. To improve the accuracy of the analysis, the addition of 1% of FA for counteracting cyclization of prenylated flavonoids was required [10] and performed. Therefore, incubation studies with and without FA were performed. Furthermore, MeOH used for protein precipitation was examined in comparison to the standard reagent ACN so far. No significant differences in activity using MeOH or ACN were identified. Due to high solubility of XN in MeOH and lower standard deviations obtained, MeOH was used as standard reagent for protein precipitation further on.

## 4.5 Kinetics of *Nha*-KHS

After optimization of the activity assay, procedures were initiated to determine kinetic parameters in 2 min activity assays with the alternative substrate XN. Specific activities [$\mu$mol min$^{-1}$ mg$^{-1}$] were ploted over substrate concentrations in mM aided by SigmaPlot®. Through the fitting of values onto an hyperbola, $V_{max}$ of 7.16 $\pm$ 0.42 $\mu$mol min$^{-1}$ mg$^{-1}$ and $K_m$ of 0.98 $\pm$ 0.13 mM were determined. Through these parameters, the turnover number $k_{cat}$ = 4.77 $\pm$0.33 s$^{-1}$ was calculated. Due to the rather slow turnover number of 5 molecules of XN per second, activity assays with 0.125-0.325 mM substrate were performed. Results presented a clear linear relationship of all concentrations over time. $R^2$-values were >95%. Thereby, strengthening the previously determined kinetic parameters.

## 4.6 Expression and activity analysis of nosig-, FLAG-variants of *P. pastoris*

Based on previous, negative detections of signal sequence and glycosylation variants on the *Nha*-KHS protein level, expression and activity analyses were repeated. No signals for nosig- as well as FLAG-variants were detected via Western Blot analysis. Nosig-variants were muteins which lacked the native signal sequence to abrogate the transport of the protein to the outer cellular space. For disguise of the native signal sequence, a FLAG-tag was added upstream to the localizing signal. Activity assays

performed with cellular lysates indicated unambigiously the presence of *Nha*-KHS-$His_{10}$. A FLAG-tag variant even revealed activity in the SN fraction. Therefore, it can be concluded that the $alpha$-His Western Blot analysis was not sensitive enough to identify the low concentrations of KHS loaded. Enzymatic deglycosylation of *Nha*-KHS-$His_{10}$ prior to activity analyses as well as different C-terminal tags e.g. Spy-tag could enhance signal detection. The method is based on detection similar to Western Blot, however, SpyTag-SpyCatcher system has no need for an antigen-antibody readout. In contrast, it is a covalent bond-forming tag/domain pair for attaching a fluorescence signal to target proteins and is getting optimized for disrupted cells [6].

## 4.7 Influences of N-glycosylation on *Nha*-KHS - Expression of glycosylation variants as well as enzymatic deglycosylation)

Protein glycosylation is known for its involvement in protein stability, secretion as well as activity [35]. To investigate influences of glycosylations on *Nha*-KHS-$His_{10}$, the focus was centered onto N-glycosylation. *Nha*-KHS consensus sequence was predicted to have four N-glycosylation sites [12]. N-glycans are transferred posttranslationally onto asparagine residues [50]. Therefore, $Asp^{112}$ (N112A), $Asp^{122}$ (N122A), $Asp^{144}$ (N144A) and $Asp^{219}$ (N219A) were identified. Previously, site-directed mutagenesis was performed to exchange asparagine for alanine to hinder glycosylation. Transformation into *P. pastoris* was successful for 3 variants, which were further used for expression and activity analysis.

Expression analysis of the glycosylation variants revealed that variant N219A was functionally expressed. Through MeOH-chloroform precipitation of the culture SN, a stronger signal was detected via Western Blot compared to TCA-precipitation. So far the standard protein precipitation was conducted with TCA and incubation time on ice for 2-3 h. By following the MeOH/chloroform precipitation protocol (see Materials and Methods) or TCA incubation over night at 4 °C, signals increased and became equally strong. After activity analysis of the pellet and culture SN fractions of the glycosylation variant N219A, 65% of the conversion rates of *P. pastoris* CBS7435 $\Delta his4$ [pPpB1_ S_ *Nha*-KHS-$His_{10}$] were obtained. A decrease of about 30% of activity was observed upon enzymatic deglycosylation. Therefore, two independent approaches lead to similar result. Other glycosylation variants revealed activity in the intracellular fraction. Variant N122A showed similar conversion results in the pellet fraction as N219A. Therefore, optimization of Western Blot analysis, as mentioned

above, could result in detection of expression levels of variant N112A. The decrease of activity due to the change in N-glycosylation site could emphasize that N-glycosylation plays a significant structural role of the protein in order to be most active. Previous studies observed a decrease in activity and secretion levels by replacement of aspargine with alanine in especially the last possible N-glycosylation site [37]. The lack of detection of expressed *Nha*-KHS-$His_{10}$ variants N112A and N122A could also be caused by a conformational change of the protein. Also stress in the endoplasmic reticulum (ER) caused by the defective protein could have caused the lack of detection [38]. The ER as well as its lumen are known locations of protein glycosylation [1] and therefore, could inhibit secretion of *Nha*-KHS-$His_{10}$, when stress levels are elevated. Further investigations with e.g. marker of ER stress induction would be required to identify the direct cause.

Enzymatical deglycosylation of *Nha*-KHS-$His_{10}$ was chosen to investigate differences in pH and thermo stability of deglycosylated *Nha*-KHS-$His_{10}$. Due to the deglycosylation, more intense as well as sharper signals were obtained when performing Western blot analysis. Activity assays confirmed the decrease in activity by 30%. Stability assessments of glycosylated vs. deglycosylated enzyme showed no variation in either pH or thermo stability. Therefore, *Nha*-KHS-$His_{10}$ was most stable at pH 5.0-6.0 and revealed a melting temperature of 53 °. Conditions at pH 4.0 and 8.0-9.0 were too instable for the detection of the thermofluor assay using SYPRO® Orange as reporter molecule. Also, possible background noises could have overlaid the signals at pH 4.0 and 8.0-9.0 and therefore, have falsified the results obtained. However, deglycosylation had no effect on physical attributes such as pH stability or melting temperature.

## 4.8 Confirmation of $T_m$ and refolding attempt with nanoDSF

Through experiments conducted with Prometheus NT.48 by NanoTemper, melting temperatures observed under different pH conditions via thermofluor® shift assays were confirmed. The optimum $T_m$ was identified at pH 6.0 and 52.9 °C. Intrinsic tryptophan fluorescence lifetime measurements conducted by nanoDSF showed slightly more sensitive results concerning suboptimal conditions. Therefore, pH 9.0 showed the lowest $T_m$ of 43.9 °C whereas the thermo shift assay conducted with the fluorescent dye revealed a $T_m$ of 11.3 °C. Through the unfolding process by increasing the temperature, tryptophan appeares on the surface and gives a distinct fluorescence

signal whereas SYPRO® Orange binds to hydrophobic badges on the protein and on the environment, which interferes with the distinct signal at pH 4.0,8.0-9.0.

For further stability and structural studies, a refolding of the unfolded tertiary structure was attempted. During the unfolding phase, confirmation of $T_m$ was once more obtained. However, after unfolding of the protein and incubation at 65 °C for 1 min no refolding of the protein was observed. The disability of refolding indicated a structural inflexibility of the protein. Beta-sheet proteins have been demonstrated previously to be resisting refolding attempts than $\alpha$-helical proteins. According to Junker and Clark [18], the refolding process of $\beta$-sheets was described as rather slow. Therefore, incubation at too high temperature e.g. 65 °C will result in unfolded protein.

## 4.9 Multicopy strains (DWP and flask cultivation)

By creating clones with multiple functional copies of expression constructs, it was attempted to increase expression levels of *Nha*-KHS-$His_{10}$ compared to the previously used *P. pastoris* strain (*Pp* 7A5). After selection of 9 colonies by increased antibiotic concentrations, growth behavior, total protein concentration, expression and activity levels were investigated.

Analyses revealed higher protein expression levels of the original strain secreting *Nha*-KHS-$His_{10}$ in comparison to the multicopy variants. All together it can be concluded that *Pp* 7A5 showed the highest enzyme activity as well as expression levels in the culture SN.

## 4.10 DASGIP®-bioreactor cultivation of *Nha*-KHS

For monitoring cell viability through cell density during induction phase, two approaches were chosen. The rather fast method of $OD^{600}$ measurements as well as CDW determination. The second approach showed more consistent results compared to the less reliable $OD^{600}$ measurements. However, CDW analyses were obtained 18 h after taking samples, so that no direct monitoring was achieved. Wild type strain as well as *P. pastoris* strain secreting *Nha*-KHS-$His_{10}$ revealed highly similar growth behaviors. Both strains reached a CDW of 90 mg $mL^{-1}$ as well as 400 $OD_{600}$. In previous studies, *P. pastoris* strains reached a CDW of 100 mg $mL^{-1}$ in BSM media under optimized conditions and induction over 120 h [31]. The specific growth rate [$\mu$]of wild type as well as *P. pastoris* strain secreting *Nha*-KHS-$His_{10}$ was 0.0092 $\pm$0.0001 $h^{-1}$. Due to correlation between $\mu$ and protein

expression [43], protein production is reported to benefit from a high specific growth rate.

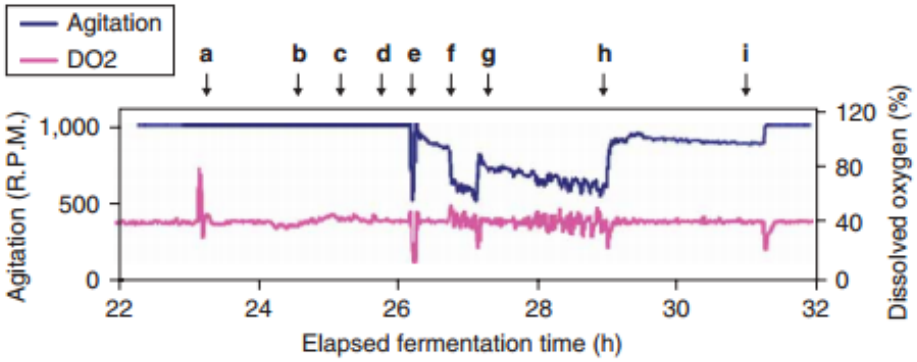


FIGURE 4.2: Trends of an optimal *P. pastoris* fed-batch bioreactor cultivation [48]. Agitation speed[rpm] as well as dissolved oxygen (DO) level [%] over bioreactor cultivation time [h].

Even though reasonable results e.g. expression levels were obtained, further improvements would increase *Nha*-KHS titer and yiel. Due to the pH drop during the first 12 h of MeOH induction as well as limited DO levels, which fall under 20%, bioreactor cultivation procedure can be optimized. Therefore, higher protein concentrations as well as survival of all batches might be obtained. Further, increased volumetric enzyme activity and increased DO levels during the limited induction period when agitation reaches its maximum could be reached by increasing air pressure of 0.10 mPa $\pm$0.50. The approach of supplementing batches with pure oxygen did not turn out as significant as compared to increased levels of air pressure [40].

In order to use *Nha*-KHS in an industrial setting, further upscaling studies will be required. Therefore, 10-100 L as well as 1,000 L scale up studies such as a biomas-stat fed-batch HCDC as described in Liu *et al.* [40] would be appropriate approaches. So far it was demonstrated that the current strain expressing *Nha*-KHS-$His_{10}$ is feasible for upscaling to gain protein concentration of 2.6 g $L^{-1}$. As the next section will reveal, the 3D-structure was resolved and possible optimization procedures for broadening the substrate scope of the enzyme proposed. After extensive characterization of optimized strains, industrial interest in upscaling as well as downstream processes could follow. Through the fed-batch bioreactor cultivation it was shown that *Nha*-KHS-$His_{10}$ would be a good candidate for these approaches.

## 4.11 Structural analysis of *Nha*-KHS

After application of standard protocols for expression and purification via Ni-NTA column of *P. pastoris* derived *Nha*-KHS-$His_{10}$, the structural biology

research group of Karl Gruber at University of Graz continued with crystallization and structural analyses. After optimizations of the crystallization protocol e.g. pH condition or salt content, native protein crystals were obtained (see FIGURE 4.3). First, only plate-shaped crystals were detectable. However, after several weeks also rectangular cuboid-shaped crystals became visible. After X-ray crystallography for first scattering experiments and the final measurements at the synchrotron in Hamburg, the diffraction patterns of the native crystals were obtained.

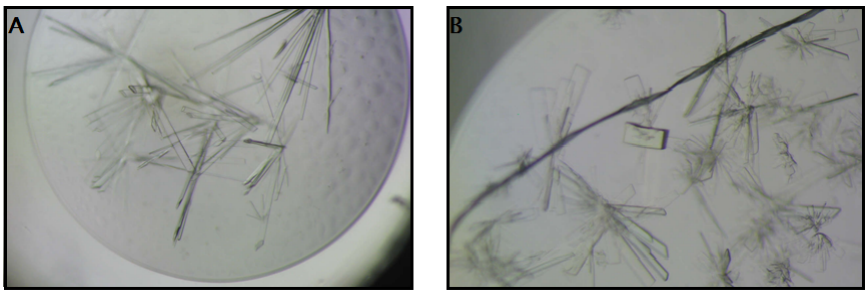


FIGURE 4.3: Two different crystal structures of *Nha*-KHS-$His_{10}$ were observed. (**A**) Plate-shaped crystals. (**B**) Plate- and rectangular cuboid-shaped crystals.

Due to lack of a starting model, heavy metal soaking was conducted after retrieval of the native data set. Heavy metal atoms are electron dense. Their differences in intensity of measured spots can be evaluated and can give indications of phase angles [2]. In order to gain sufficient information of phases, several heavy metal derivatives using gold, tantalum and platinum clusters, were constructed and also measured with the synchrotron to gain high quality electron density maps to create a 3D-model. According to the model, the protein was proposed to be a homodimer, consisting of mainly $\beta$-sheets and loops. The predominating $beta$-sheet structure explained the failure of structural resolvement with molecular replacement, which is known to show limited success under these conditions [16]. In FIGURE 4.4, the predicted 3D-structure as well as side- and top-view can be inspected.

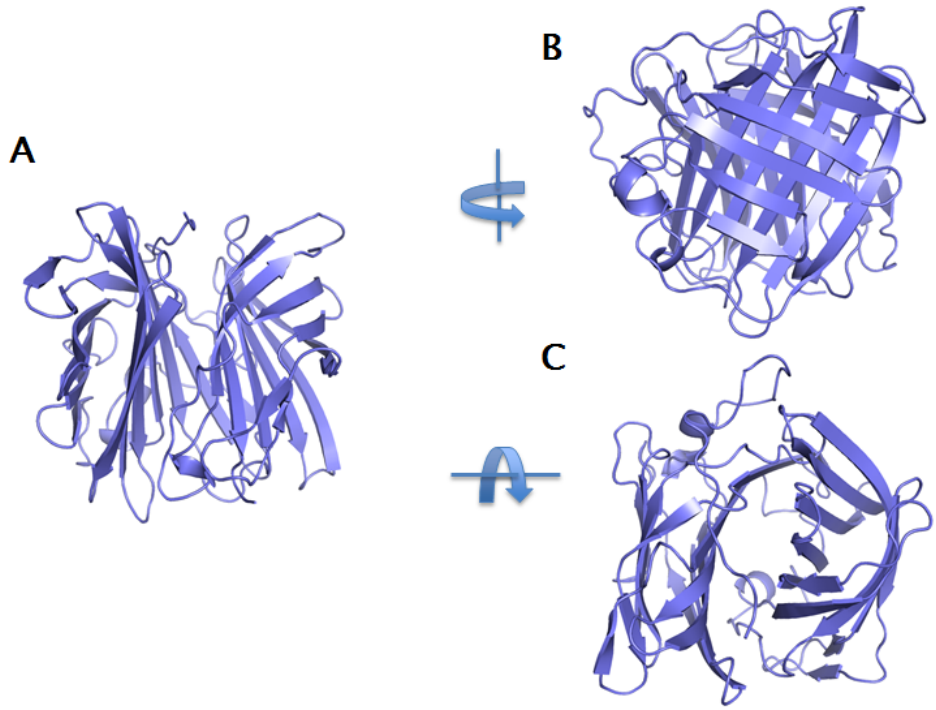


FIGURE 4.4: The predicted 3D-overall structure of the homodimer *Nha*-KHS, shown in different angles, **(B)** side-view and **(C)** top-view.

The crystal structure of *Nha*-KHS was revealed at 1.9 Å resolution (see Table 4.1). The crystallographic groups of native and heavy-atom (HA) forms varied. The native form featured a monoclinic ($P2_1$) and the second displayed an orthorhombic crystal structure ($C222_1$). Both crystal classes were identified with the standard unit cell [29]. The different crystal forms were discovered at different incubation time points, which could be due to the different glycosylation patterns discovered in the electron density map. Hence, native crystals showed glyco-chains surrounding the crystal structure whereas the 2$^{nd}$ form showed only a few glycosylated residues.

TABLE 4.1: Experimental details of the structure determination of *Nha*-KHS.

| **Data set** | **1$^{st}$ crystal form** | **2$^{nd}$ crystal form** |
|---|---|---|
| Crystal form | native | tantalum bromide cluster (HA-dataset) |
| Resolution [Å] | 1.9 | 1.9 |
| Crystallographic group | $P2_1$ | $C222_1$ |
| Unit cell [Å] (a/b/c) | 51.3/128.6/70.3 | 78.0/80.0/137.9 |
| Unit cell [°] ($\alpha/\beta/\gamma$) | 90/102/90 | 90/90/90 |

Furthermore, previously established elution fraction after gel filtration

revealed only a signal, indicated a purified monomer (FIGURE 3.4). However, homodimeric crystallization suggests that the homodimer in the asymmetric unit forms an active homodimer, whereas in solution the protein is found as monomer. As soon as binding of ligand occurs, dimerization could be modulated. To optimze gel filtration for investigating homodimeric appearance, a pH-dependent experiment could be conducted. Dimerization is pH-dependent, therefore, incubations at different pH-conditions before gel filtration analyses could give indications of homodimers [28]. On the other hand, on multiple SDS-PAGEs.

Taking a closer look at the 3D structure, it seems to be extensively overlapping with the 3D structure of puttative AttH (NE1406) originating from *Nitrosomonas europaea*, an obligate chemolithoautotrophic bacteria [4]. The alignment of the 3D structures was performed by the alignment tool HHpred (FIGURE 4.5 **(A)**). *Nha*-KHS is colored grey and putative AttH (NE1406) is colored salmon. The structure of putative AttH was obtained at 2.0 Å resolution. Even though the 3D structures of both proteins seemed structurally similar, BLAST® protein alignment tool predicted only a 27% sequence identity upon alignment of primary amino acid sequences of *Nha*-KHS (see Appendix, FIGURE A.1 **(A)**) and putative AttH (PDB:2inch). Furthermore, putative AttH was suggested to be a carotenoid 1,2-hydratase from *Nitrosomonas europaea* (see Appendix, FIGURE A.1 **(B)**).

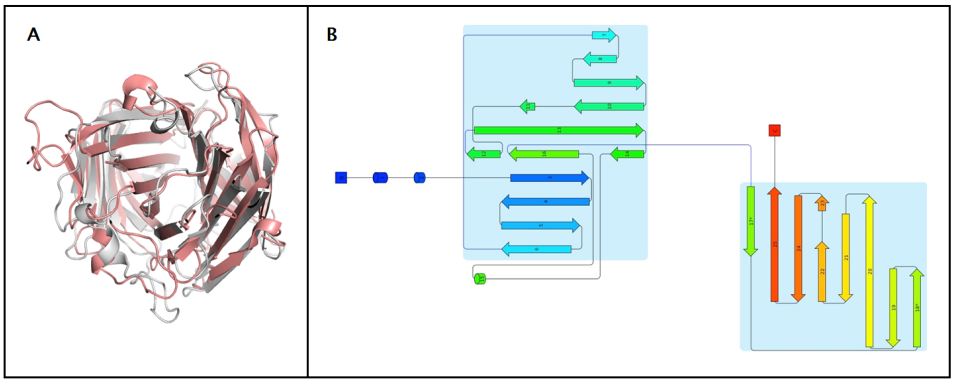


FIGURE 4.5: Identified AttH-like fold of *Nha*-KHS due to similarity of NE1406 protein. **(A)** HHpred alignment of 3D-structures of *Nha*-KHS (grey) as well as highly similar NE1406 protein (salomon), originating *Nitrosomonas europaea* [33]. **(B)** The topology diagram of *Nha*-KHS predicted by Pro-origami.

When unwrapping the tertiary structure, a topology diagram can be produced. Therefore, the Pro-origami tool was applied. AttH-like folds are characterize by structural classification of proteins (SCOP) as:

Two flattened beta-barrels of lipocalin-like topology are orthogonally packed with a pseudo twofold symmetry [5]. Lipocalin-like structures overlap with the DUF2006 group (PF09410) and COG5621 family of predicted

secreted hydrolases, to which *Nha*-KHS most like would be categorized [33].

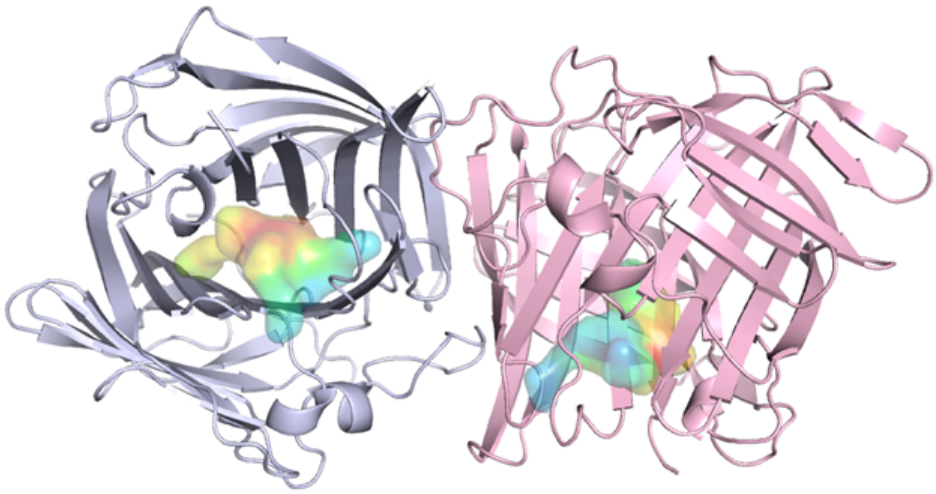

FIGURE 4.6: The prediction of the cavity of *Nha*-KHS for docking of substrate/ product by CASoX. Change of colors of the molecule indicate the change from hydrophobic (blue) to hydrophilic (red)areas of the molecules.

The topology contains two repeats of up-and-down beta barrel structures, whereas the first repeat continues to a common fold with its three strand. According to Flower [24], beta barrel fold proteins belong to so-called calycin superfamily and are commonly encountered as transmembrane proteins, which supports the localization of *Nha*-KHS in membrane fractions identified by Stefanie Gabriel [12]. Analysis with *PROFtmb* and *PPM* would give further indications of the accuracy of the prediction [41]. Typical features of the calycin superfamily are identified as antiparallel 8-stranded $\beta$-barrel and a short $3_{10}$-helix. The attributes are located in front of the first $\beta$-strand to close off the barrel at one side. [25]. The predicted structures can be found on the topology diagram as well as on the 3D-structure.

Calculations with CASoX software aided in visualization of isoflavonoid cavity docking studies with *Nha*-KHS (see FIGURE 4.6). Due to the dense structure, only limited space is given for entering the substrate. Therefore, it had been predicted that the loop, including the amino residue $N^{211}$, would allow sufficient flexibility for a bulky substrate. The mechanism of flavonoid (de)hydration by *Nha*-KHS still requires intensive investigation for precise conclusions. However, through the docking studies, conducted with PyMol (FIGURE 4.7), certain amino acid residues may play an important role in the hydration process.

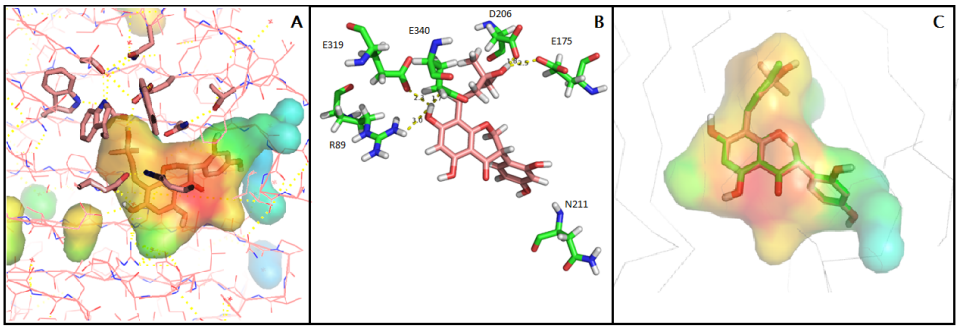


FIGURE 4.7: Visualization by PyMol of docking between *Nha*-KHS cavity with substrate/product and the involved amino acid residues. (**A**) Segment of the cavity of *Nha*-KHS, in which kievitone-hydrate is docked. (**B**) Amino acid residues surrounding kievitone(-hydrate), predicted to be involved in the hydration. (**C**) Spacial arrangement as well as colored changes in hydrophobicity of kievitone(-hydrate) in the cavity. Change of colors indicates the change from hydrophobic (blue) to hydrophilic (red) areas of the molecules.

In order to gain insight in the interaction between substrate and amino acid residues of *Nha*-KHS, the model of NE1406 will serve as a template. The docking studies of NE1406 suggested that the ligand interacts with conserved $W^{49}$, $W^{228}$ and $W^{230}$ as well as nonconserved residues [33]. However, in the cavity of *Nha*-KHS several tryptophanes, $W^{60}$, $W^{219}$, $W^{221}$ and $W^{236}$, and other residues can also be encountered in close proximity to the ligand, almost retaining the molecule with the aid of $N^{211}$. Furthermore, conserved residues proposed for playing a distinct role in the hydroxylation of the prenyl-group, detected in NE1406 and *Nha*-KHS, are $Y^{87}$, $E^{346}$ and $D^{213}$, respectively $D^{206}$, $E^{175}$ and $R^{89}$. For studies regarding the reaction mechanism, the conserved residues would be ideal targets for amino acid exchange and identification of residues involved in catalysis. Two more conserved and highly interesting targets for protein engineering located in immediate surrounding of the saturated hydroxyl-group are $E^{319}$ and $E^{340}$. Mutagenesis could be the method of choice for an attempt of cavity enlargement for bulkier substrates such as sterols (see FIGURE 4.8) to expand the substrate scope. Mutating the restraining tryptophanes such as $W^{221}$ to smaller amino acid residues, e.g. alanin, would be a possible approach to broaden the substrate scope.

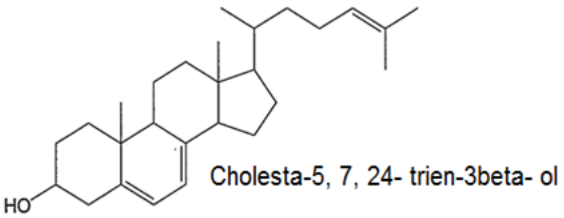


FIGURE 4.8: Chemical structure of cholesta-5, 7, 24- trien-3-beta-ol, a sterol.

# Chapter 5

# Conclusions and Outlook

Throughout this study, the successful conversion of the original and alternative substrates with KHS was achieved. Furthermore, model substrates were chosen for biochemical characterization of *Nha*-KHS-$His_{10}$ to confirm the hydration of the substrates and optimize the reaction conditions. The improvements implemented in the activity assay assured a reliable and reproducible analytics of XN and OH-XN. Therefore, kinetic parameters and screening of active clones as well as signal sequence and glycosylation variants were established. Additionally, expression as well as purification studies on bioreactor cultivations of *P. pastoris* strain expressing *Nha*-KHS-$His_{10}$ were successfully conducted.

As described by Turbek *et al.* [46] KHS catalyzes the hydration as well as the dehydration reaction. Therefore, exploring also the dehydration reaction could allow for a broader analysis of the enzyme. Testing the activity of the enzyme with OH-XN, in order to produce XN could be performed with diminutive effort by applying the freeze dried enzyme to an activity assay with XN-OH.

Due to the elucidation of the 3D-structure, enzyme engineering by creating muteins of amino acid residues potentially involved in the reaction mechanism, will be the next step. Furthermore, resting cells conversion in DWP as performed previously, would be an ideal medium througput screening system after further optimizations. Conversion of prenylated phenols as alternative substrates could aid in the identification of functional groups required for the reaction. Substrates as well as products will be provided by the company partner DSM Innovative Synthesis. Enzyme engineering could lead to the determination of the reaction mechanism as well as an enlarged active site cavity for broadening the substrate scope of *Nha*-KHS.

# Appendix A

# Appendix

## A.1 Instruments and devices

TABLE A.1: Instruments and devices.

| Task | Instrument/Device | Manufacturer |
|---|---|---|
| Absorbance measurement | FLUOstar Omega | BMG Labtec, Germany |
| | BioPhotometer Plus | Eppendorf, Germany |
| | Specord 210/205 dual-beam spectrophotometer | Analytik Jena, Germany |
| | DU® 800 UV-Visible Spectrophotometer | Bio-Rad, USA |
| | Microplate, 96-well, PS, U-bottom, MICROLON® | Greiner bio-one AG, Germany |
| | Semi-Micro-Cuvettes, PS, 10 x 10 x 45 mm | Greiner bio-one AG, Germany |
| Agarose gel electrophoresis | PowerPac™ Basic + Sub-Cell GT | Bio-Rad, USA |
| Cell harvest/ Centrifugation | Avanti™ centrifuge, JA-10, JLA-8.1 and JA-25.50 rotors | Beckman Coulter™, USA |
| | Microcentrifuge 5145R | Eppendorf, Germany |
| | Tabletop centrifuge 5810R | Eppendorf, Germany |
| Deep well plate shaker | Heidolph Titramax 1000 | Fisher Scientific, USA |
| Desalting/ buffer exchange | HiPrep26/10 Desalting column | GE Healthcare Life Sciences, USA |
| | PD-10 Desalting Column | GE Healthcare Life Sciences, USA |
| Determination of DNA concentration | NanoDrop 2000 UV-Vis Spectrophotometer | Thermo Scientific, USA |

Continuation of Table A.1

| **Task** | **Instrument/Device** | **Manufacturer** |
|---|---|---|
| Electrotransformation | MicroPulser™ | Bio-Rad, USA |
| | Electrocorporation Cuvettes (2 mm gap) | Life Technologies, USA |
| Bioreactor cultivation | DASGIP® benchtop parallel bioreactor system (0.7 L-2.7 L working volume) | Eppendorf, Germany |
| | 2x pitched-blade impellers (30-1,250 rpm agitation speed) | |
| | DASGIP® Monitoring System 220mm | |
| | T-sensors Pt100 RTD | |
| | dissolved oxygen sensors, K9, 325 mm | Bradley-James Corporation, USA and Canada |
| | pH 0.0-12.0 405-OPAS-SC-K3S/325 | Mettler TOLEDO, USA |
| | DASware® control | |
| Concentration of culture SN | Quattro Flow Fluid System | Pall Corporations, USA |
| Gel filtration | HiLoad 16/600 Superdex 200 pg | GE Healthcare Life Sciences , USA |
| HPLC-MS (Biocatalysis) | Agilent 1200 series, G1312B, BinPumpSL | Agilent Technologies, USA and Canada |
| | Agilent 1200 series, G1314C, VWD SL | |
| | Agilent 1200 series, G1316B, TCC SC | |
| | Agilent 1200 series, G13167C, HiP-ALS SL | |
| | Agilent Technoolgies, LC/MS SL | |
| | LC/MS Genimini-NX5u C18 110A 250mm column | Phemomenex, USA |
| HPLC-MS (Chemistry) | Agilent 1200 series, G1312B, BinPumpSL | Agilent Technologies, USA and Canada |
| | Agilent 1200 series, G1314C, VWD SL | |

| Continuation of Table A.1 | | |
|---|---|---|
| **Task** | **Instrument/Device** | **Manufacturer** |
| | Agilent 1200 series, G1316B, TCC SC<br>Agilent 1200 series, G13167C, HiP-ALS SL<br>Agilent Technoolgies, LC/MS SL<br>Poroshell 120 EC-C18, 2.7 $\mu$m, 100x3mm | |
| HPLC-UV (Biokatalysis) | Agilent 1100 series, G1311A, QuatPump<br>Agilent 1100 series, G1315B, DAD<br>Agilent 1200 series, G1316A, COLCOM<br>Agilent 1260 Infinity, G13121B, 1260 FLD<br>Agilent 1100 series, G1367A, WPALS<br>Agilent 1100 series, G1379A Degasser<br>LC/MS Genimini-NX5u C18 110A 250mm column<br>Phurospher® STAR RP-18 endcapped (5 $\mu$m) LiChroCART®250-4.6 | Agilent Technologies, USA and Canada<br><br>Phemomenex, USA<br><br>Merck Millipore, Ireland |
| HPLC vials | 1.5 ml Rollrandflasche, 32 x 11.6 mm, Klarglas, 1. hydrolytische Klasse, enge Öffnung 11 mm Verschluss: Aluminium Bördelkappe, farblos lackiert, mit Loch; PTFE rot/Silicon weiß/PTFE rot, 45◦ shore A, 1,0 mm | Markus Bruckner Analysentechnik, Austria |
| Immunoblotting (Western Blot) | PowerEase500 XCell SureLock™ Electrophoresis *SureLock*® cell and module | Life Technologies, USA<br><br>Thermo Scientific, USA |

| Continuation of Table A.1 | | |
|---|---|---|
| **Task** | **Instrument/Device** | **Manufacturer** |
| | Nitrocellulose Blotting Membrane, 0.45 $\mu$m<br>Bioimager G:Box HR16 | GE Healthcare Life Sciences , USA<br>SynGene, UK |
| Incubator<br>(28 °C and 37 °C) | Binder<br>Kühlbrutschränke | Binder GmbH, Germany |
| Mixing | Magnetic stirrer- IKA-MAG RCT | IKA, Germany |
| Mixing (small volumes) | Vortex- Genie 2 | Scientific Inductries Inc., USA |
| NMR | Varian Inova-500 nmr spectrometer | Varian Inc., USA |
| PCR reaction | GeneAmp® PCR System 2700 | Applied Biosystems, USA |
| Real time PCR reaction for thermo stability assays | CFX Connect™ Real-Time System<br><br>nanoDSF Prometheus NT.48 | Bio-Rad, USA<br><br>NanoTemper Technologies, Germany |
| pH- meter | inoLab WTW 720 pH meter | WTW GmbH, Germany |
| Protein concentration | Ultrafiltration with Amicon® Ultra-15 Centrifugal filter devices, 15 mL, 30 kDa molecular weight cutoff | Merch Millipore, Ireland |
| Protein electrophoresis | NuPAGE® SDS-PAGE Gel System<br>NuPAGE® Novex® 4-12% Bis-Tris Mini Gels 1.0 mm, 15 well | Life Technologies, USA |
| Protein purification | Äkta prime<br><br>Fraction collector F9-R<br>HisTrapFF Crude column, 5 mL<br>Ni-Sepharose® 6 Fast flow columns | GE Healthcare Life Sciences , USA |
| Protein storage | Lyophilisator alpha 1-4 LSC<br>-20°C freezer | Christ, Germany<br><br>Liebherr, Germany |

| Continuation of Table A.1 | | |
|---|---|---|
| **Task** | **Instrument/Device** | **Manufacturer** |
| | 4 °C fridge | Liebherr, Germany |
| Reaction tubes for activity assay | PYREX® culture tubes | SciLabware, UK |
| Shaker (small volumes) | Thermomixer comfort | Eppendorf, Germany |
| Shaker for cultivation/ activity assay | Multitron Standard | Infors AG, Switzland |
| Sonication | Sonifier 2501 | Branson, USA |
| Sterile work | UNIFLOW KR130 biowizard | UNIQUIP, USA |
| Balancing | Lab Scale: SI-202<br>Practum® Precision Balance | Denver Instruments, USA<br>Sartorius AG, Germany |

## A.2 Reagents

TABLE A.2: Reagents.

| **Reagent** | **Supplier** |
|---|---|
| 8-prenylnaringenin | Sigma-Aldrich, Germany |
| Acetic Acid | Roth GmbH, Germany |
| Acetonitrile | VWR, USA |
| Acrylamide/BIS | Sigma-Aldrich, Germany |
| Agar Agar | Roth GmbH, Germany |
| Agarose LE | Biozyme, Germany |
| Ammonium persulfate | Roth GmbH, Germany |
| Anti-mouse IgG (A4416) | Sigma-Aldrich, Germany |
| Antifoam | Acepol Chemicals, India |
| Aqua bidest. | Fresenius Kabi GmbH, Austria |
| Bacto™ | BD, USA |
| Bovine Serum Albumin | Roth GmbH, Germany |
| Biorad Protein Assay dye reagent (5x) | Bio-Rad, USA |
| Biotine | Roth GmbH, Germany |
| Boric acid | Roth GmbH, Germany |
| Calcium sulphate dihydrate | Roth GmbH, Germany |
| Chloroform | Roth GmbH, Germany |
| Citric Acid | Roth GmbH, Germany |
| Coomassie Blue | Sigma-Aldrich, Germany |

Continuation of Table A.2

| **Reagent** | **Supplier** |
|---|---|
| Cobalt chloride hexahydrate | Roth GmbH, Germany |
| Cupric sulphate | Roth GmbH, Germany |
| D-Glucose | Roth GmbH, Germany |
| Deutarated Methanol | Roth GmbH, Germany |
| Di-potassium hydrogen phosphate | Roth GmbH, Germany |
| Dimethylsulfoxide | Roth GmbH, Germany |
| DNA loading dye (6x) | Thermo Scientific, USA |
| Dodecane | Roth GmbH, Germany |
| EDTA | Roth GmbH, Germany |
| Enzymes and adequate buffer, various | Thermo Scientific, USA |
| Ethanol | Roth GmbH, Germany |
| Ethidium bromide | Roth GmbH, Germany |
| Ferrous sulphate heptahydrate | Roth GmbH, Germany |
| Formic Acid | Roth GmbH, Germany |
| GeneRuler$^{TM}$ DNA Ladder | Thermo Scientifc, USA |
| Glycerol | Roth GmbH, Germany |
| Histidine | Roth GmbH, Germany |
| Hydrochloric Acid | Roth GmbH, Germany |
| Hops-extract capsules | Allcura Lebensmittel GmbH, Germany |
| Imidazole | Sigma-Aldrich, Germany |
| Isopropyl-$\beta$-D-thiogalactopyranosid | Peqlab Biotechnologies GmbH, Germany |
| Kanamycin | Sigma-Aldrich, Germany |
| Kievitone | DSM, Netherlands |
| LB (Lennox) | Roth GmbH, Germany |
| Magnesium sulphate heptahydrate | Roth GmbH, Germany |
| Manganese sulphate monohydrate | Roth GmbH, Germany |
| Methanol | Roth GmbH, Germany |
| Monoclonal anti-polyhistidine antibody in mouse (H1029) | Sigma-Aldrich, Germany |
| n-Hexane | Roth GmbH, Germany |
| Ni-Sepharose$^{TM}$ beads | GE Healtchcare Life Sciences, USA |
| Nickel sulfate | Sigma-Aldrich, Germany |
| Novex®Sharp Pre-Stained Protein Standard | Thermo Scientific, USA |
| NuPage® LDS Sample Buffer (4x) | Life Technologies, USA |
| NuPage® Mes SDS Running Buffer (20x) | Life Technologies, USA |

| Continuation of Table A.2 | |
|---|---|
| **Reagent** | **Supplier** |
| NuPage® Sample reducing agent (10x) | Life Technologies, USA |
| Peptone | Roth GmbH, Germany |
| Phenylmethylsulfonyl fluoride | Sigma-Aldrich, Germany |
| Phosphoric Acid 85% | Roth GmbH, Germany |
| PonceauS | Sigma-Aldrich, Germany |
| Potassium dihydrogen phosphate | Roth GmbH, Germany |
| Potassium hydroxide | Roth GmbH, Germany |
| Potassium sulphate | Roth GmbH, Germany |
| Sodium chloride | Roth GmbH, Germany |
| Sodium citrate | Roth GmbH, Germany |
| Sodium dodecyl sulfate | Life Technologies, USA |
| Sodium iodide | Roth GmbH, Germany |
| Sodium molybdate dihydrate | Roth GmbH, Germany |
| Sulphuric acid conc. (69%) | Roth GmbH, Germany |
| SuperSignal® WestPico Chemiluminescent Substrate | Thermo Scientific, USA |
| SYPRO® Orange | Thermo Scientific, USA |
| TEMED | Roth GmbH, Germany |
| Tris | Roth GmbH, Germany |
| Tween®20 | Roth GmbH, Germany |
| Xanthohumol | BioVision Incorporate, USA |
| Yeast Extract | Bacto Laboratories Pty Ltd, Australia |
| Zeocin | InvivoGen, USA |
| Zinc chloride | Roth GmbH, Germany |

## A.3 Kits and enzymes

TABLE A.3: Kits and enzymes.

| **Kits/enzymes** | **Supplier** |
|---|---|
| Endo$H_f$ deglycosylation enzyme mix | Thermo Scientific, USA |
| FastDigest™ restriction enzymes | Thermo Scientific, USA |
| Gene Jet™ Plasmid Miniprep Kit | Thermo Scientific, USA |
| Phusion® DNA Polymerase | Thermo Scientific, USA |
| Restriction enzymes | Thermo Scientific, USA |
| T4 DNA Ligase | Thermo Scientific, USA |
| Wizard® SV Gel and PCR Clean Up System | Promega Corporation, USA |

| Continuation of Table A.3 | |
|---|---|
| **Kits/enzymes** | **Supplier** |

## A.4 Media and buffers

TABLE A.4: Medium and Buffer.

| **Medium/Buffer** | **Composition** |
|---|---|
| BEDS solution | 1 mL 0.1 M bicine NaOH (10x), pH 8.3, 300 $\mu$L ethylene glycol, 500 $\mu$L DMSO, 2 mL 5 M sorbit (5x), 6.2 mL $ddH_2O$ |
| BMGY/BMMY- medium | 1% yeast extract, 2% peptone, 100 mM potassium phosphate, pH 6.0, 1.34% YNB, $4x10^{-5}$% biotin, 1% glycerol or 1% MeOH |
| Binding Buffer for protein purification | 50 mM $NaH_2PO_4$, pH 7.0, 300 mM NaCl, 10 mM imidazole |
| modified Basal Salt Medium (BSM), pH 2.0 (*P. pastoris* bioreactor cultivation) | 33 g of glucose monohydrate, 0.17 g of $CaSO_4 \cdot 2H_2O$, 2.32 g of $MgSO_4$, 2.86 g of $K_2SO_4$, 4.25 g of $H_3PO_4$, 0.64 g of KOH, 0.22 g of NaCl, 0.6 g of EDTA, 40 mL of $NH_4Cl$ stock solution (250 g $L^{-1}$),10 mL of 4% of histidine stock solution, 4.35 mL of PTM1 trace salt solution, 4.35 mL of 500x biotin stock solution and adjusted to a final volume of 1 L with $ddH_2O$ |
| 50 mM Citrate buffer, pH 4.0, 5.0, 6.0 | mixture of 50 mM citric acid and 50 mM sodium citrate |
| Coomassie Brilliant Blue G-250 staining solution | 1 g of Coomassie Blue in 1 L of: methanol (50% w/v), acetic acid (10% v/v), $ddH_2O$ (40%) |
| Desalting Buffer for protein purification | 50 mM citrate buffer, pH 6.0 |
| Elution Buffer for protein purification | 50 mM $NaH_2PO_4$, pH 7.0, 300 mM NaCl, 250 mM imidazole |
| Glucose-Feed (*P. pastoris* bioreactor cultivation) | 632.3 g of glucose monohydrate dissolved in 367.7 mL of $ddH_2O$, 12 mL of PTM1 trace solution, 10 mL 4% histidine and 12 mL of biotin 500x stock |
| IPTG stock (100 mM) | 1.19 g IPTG dissolved in 50 mL $ddH_2O$ |
| Kanamycin stock, 40 mg $mL^{-1}$ | 40 mg Kanamycin dissolved in 1 mL $ddH_2O$ |

Continuation of Table A.4

| **Medium/Buffer** | **Composition** |
|---|---|
| LB-agar | LB-Medium + 20 g $L^{-1}$ of Agar |
| LB-Medium | 10 g $L^{-1}$ tryptone, 5 g $L^{-1}$ yeast extract, 5 g $L^{-1}$ NaCl |
| Methanol-Feed (*P. pastoris* bioreactor cultivation) | 1 L of MeOH, 12 mL of PTM1 trace solution and 12 ml biotin (500x stock) |
| 50 mM Potassium phosphate buffer pH 7.0, 8.0 | mixture of 50 mM potassium dihydrogen phoshphate and di-potassium hydrogen phosphate |
| Primary antibody solution (H1029) | 1:2000 dilution of H1029 in 1% BSA, 50 mL TBST, 0.5 g BSA and 25 $\mu$L antibody |
| PTM1 trace salt solution | 5 mL of conc. $H_2SO_4$, 0.02 g of $H_3BO_3$, 3.84 g of $CuSO_4$, 0.92 g of $CoCl_2 \cdot 6H_2O$, 65.0 g of $FeSO_4 \cdot 7H_2O$,3.0 g of $MnSO_4 \cdot H_2O$, 1.18 g of KJ,0.20 g of $Na_2MoO_4 \cdot 2H_2O$ and 20.0 g of $ZnSO_4$ dissolved in 1 L $ddH_2O$ and sterile filtered |
| SDS-Running Buffer for handmade gels $(10x)$ | 28 g Tris, 144 g glycine, 10 g SDS and adjusted to 1 L with $ddH_2O$ |
| Secondary antibody solution (A4416) | 50 mL TBST, 2.5 g milk powder and 5 $\mu$L of antibody |
| SOC-Medium | 20 g $L^{-1}$ tryptone, 0.58 g $L^{-1}$ NaCl, 5 g $L^{-1}$ yeast extract, 2 g $L^{-1}$ $MgCl_2$, 0.16 g $L^{-1}$ KCl, 2.46 g $L^{-1}MgSO_4$, 3.46 g $L^{-1}$ dextrose |
| TAE buffer, 50 x | 242 g $L^{-1}$ Tris, 14.6 g $L^{-1}$ EDTA, 57.1 mL $L^{-1}$ acetic acid, adjust to final volume with $ddH_2O$ |
| TBS (10X) | 30.3 g Tris, 87.9 g NaCl, pH 7.5 (HCl), filled to 1 L with $ddH_2$ |
| TBST (1 L ) | 100 mL of 10x TBS-buffer, 300 $\mu$L of Tween®, filled to 1 L with $ddH_2O$ |
| TBST-milk | 50 mL of TBST and 2.5 g milk powder |
| Transfer buffer (20x) | 29 g of 12M Tris, 144 g of 96 M Glycine, filled to 1 L with $ddH_2O$ |
| Transfer buffer (1 L) | 50 mL of 20x Transfer buffer, 100 mL of methanol, 850 mL of $dH_2O$ |
| 50 mM Tris buffer, pH 9.0 | 6.057 g of Tris dissolved in 1 L of $ddH_2O$ and adjusted to pH 9.0 |
| YPD-medium | 1% of yeast extract, 2% of peptone, 2% of glucose |

| Continuation of Table A.4 | |
|---|---|
| **Medium/Buffer** | **Composition** |
| Zeocine stock, 100 mg $L^{-1}$ | 100 mg of Zeocin dissolved in 1 mL of $ddH_2O$ |

## A.5 Strains, plasmids and genes

TABLE A.5: *E. coli* strains.

| Strain | Genotype | Source |
|---|---|---|
| TOP 10F' | F'{*lac*I$^q$ Tn*10* (Tet$^R$)} *mcr*A Δ(*mrr-hsd*RMS-*mcr*BC) Φ80 *lac*ZΔM 15 Δ*lac*X74 *rec*A1 *ara*D139 Δ(*ara-leu*)7697 *gal*U *gal*K *rps*L *end*A1 *nup*G | Thermo Scientific, USA |
| BL21 Star$^{TM}$(DE3) | F$^-$ *omp*T *hsd*$S_B$($r_B^-m_B^-$) *gal dcm rne*131 (DE3) | Thermo Scientific, USA |

TABLE A.6: *P. pastoris* strains.

| ***P. pastoris* strains** | | |
|---|---|---|
| **Strain** | **Genotype** | **Source** |
| *P. pastoris* CBS7435 | Accession: PRJEA62483 | Centraalbureau voor Schimmelcultures, Netherlands |
| *P. pastoris* CBS7435 Δ*his4* | Accession: PRJEA62487 | Institute of Molekulare Biotechnology, Graz University of Technology, Ao.Univ.-Prof. Mag.rer.nat. Dr.rer.nat. Anton Glieder |

TABLE A.7: *E. coli* expression plasmids.

| Plasmid | Features | Source |
|---|---|---|
| pET26b(+) | N-terminal $His_6$-tagging bacterial expression vector with T7 promotor, lac operon, signal sequence and kanamycin resistence marker for periplasmic protein expression via pelB leader sequence. | EMD Millipore, USA |

TABLE A.8: *P. pastoris* expression plasmids.

| Plasmid | Features | Source |
|---|---|---|
| pPpB1_S | *E. coli-P. pastoris* shuttle vector harboring replication origin (pUC ORI), promotors (P_ADH1 and P_EM72_Syn) and selection marker (Zeocin_Syn). | Institute of Molecular Biotechnology, Graz University of Technology, Austria |
| pPpT4_$\alpha$ _S | | Institute of Molecular Biotechnology, Graz University of Technology, Austria |

TABLE A.9: Kievitone hydratase genes, sequence-optimized for expression in *P. pastoris* and *E.coli*.

| Gene | Organism | Gene length [bp] | Protein size [kDa] | Accession |
|---|---|---|---|---|
| *Ate*-KHS-$His_{10}$ | *Aspergillus terreus* | 1152 | 41.2 | XP_ 001217367.1 |
| *Fso*-KHS-$His_{10}$ | *Fusarium solani* | 1104 | 40.3 | AAA87627 |
| *Nha*-KHS-$His_{10}$ | *Nectria haematococca* | 1098 | 39.9 | XP_ 003041184.1 |

## A.6 Nucleotide sequences and amino acid sequences of*Nha*-KHSs

TABLE A.10: Nucleotide sequences of *Nha*-KHS. Sequence optimized for expression in *E.coli* (5′→ 3′).

| ***Nha*-KHS (1057 bp)** |
|---|
| 1 CATATGCGTG CATCTTTTCT TTTGACGGCA GGTTTAGCAA CGGCGGCAGT AGGTAGAGCG |
| 61 AAGTCCGTCC CAAAGAAGTT TCCGTTTAAG CCGGAGAACA GCAAAACGAC TGGCACCAAT |
| 121 GCGATCCCTA TCGTCTATGG TCTGAGCGAA AGCCAACCGA ATAGCGTTGG TGGTTCTTGG |
| 181 TGGTCTAGCA GCTACATTAC CACTACCAAC AACGAGCAAT ACGTCGTGCT GGCGCACTAT |
| 241 CTGGACAACC CGGTTTATAC GTATTTTCGC GCGAGCACCC TGAACCTGGA GACTAACGAA |
| 301 TACCACCAGT ACGTGACCGT GGGTTCCAGC ACGCCGAACA TCACCACCCT GGATGTCAGC |
| 361 GTCGGCAACA ACGGTATCAA GAGCGAGAGC GAGGATAACC TGTCGAAATT GCGCAGCTAC |
| 421 AGCAATCATG ACAATGTGAC CTTCGATATT ACTTACGACG CTACCACGGG TGCGGTGGCC |
| 481 AATGGCGGTG CAGGCACCTT CCAGTTTGGT GAGGGCCTGA CCTGGGAGTT TGGCCTGCCA |
| 541 AGCGCCAAAA CCGAGGGTAG CTTGACCGTT CACGGTGAAA AACTGGCGAT TGATCCGGCG |
| 601 AAATCGCATA CGTGGTACGA CCGTCAATGG GGTAACACGG CAGCAATTCC GTCTAATTGG |
| 661 ACGTGGTTCC AGCTGCACAT CCCGTCCACC GAATACAAGA TCTCCGCGTG GATTTTCAGC |
| 721 GATCCGTTCC GTAATACCGA AACCCGTTTT GCGACGATTC GCGGTGCGAA TGACGAAACC |
| 781 CTGGTTCTGC CGTTGGAATT TACGCCGATC TATAAACGTA CCTATGAGAG CGCGACGGGT |
| 841 CGTGTAACGT ACCCGCTGGA CTGGAAACTG AAGATTTCTG GCTTCGGCGA TTTCAAACTG |
| 901 AGCAGCTATA CCGAGGACCA GGAATTGGTT GGCGAGGACG CTCTGCAAAC CGCCTACGAG |
| 961 GGTTTCATCA CGTTCAGCGG CAATGTCCAT AGCAAGCCGG TGCAGGGTTA TGGCCTGGTT |
| 1021 GAAATTGTGT ACAGCACGTG GGATGTTTAA TAAGCTT |

TABLE A.11: Nucleotide sequence of *Nha*-KHS. Sequence optimized for expression in *P. pastoris* (5′→ 3′).

| ***Nha*-KHS (1098 bp)** |
|---|
| 1 GAATTCCGAA ACGATGAGAG CTTCCTTTCT TCTGACCGCC GGTTTGGCTA CCGCAGCCGT |
| 61 GGGACGTGCT AAGTCTGTGC CTAAGAAATT TCCTTTCAAG CCAGAAAATT CTAAGACCAC |
| 121 AGGAACAAAT GCAATTCCCA TAGTATATGG CCTGAGTGAA TCCCAACCAA ATTCTGTCGG |
| 181 TGGATCTTGG TGGTCATCTT CCTATATCAC TACCACTAAT AACGAACAAT ACGTCGTTTT |
| 241 GGCTCATTAT TTGGACAATC CTGTCTACAC TTACTTCCGT GCTTCCACTT TGAATCTTGA |
| 301 GACTAATGAG TACCACCAGT ACGTTACAGT GGGTTCTTCC ACTCCTAATA TAACTACCTT |
| 361 GGATGTTTCT GTGGGTAACA ATGGCATTAA AAGTGAGTCC GAAGATAATC TTTCTAAGCT |
| 421 GAGATCATAC TCTAACCATG ATAATGTGAC CTTCGATATT ACTTACGACG CCACCACTGG |
| 481 AGCTGTCGCT AATGGAGGCG CCGGAACTTT CCAATTCGGA GAAGGTTTGA CATGGGAGTT |
| 541 CGGTTTGCCT TCTGCTAAAA CAGAGGGCTC CCTGACCGTT CATGGTGAAA AACTTGCTAT |
| 601 CGACCCTGCT AAATCCCATA CATGGTATGA TCGTCAGTGG GGAAATACTG CCGCTATCCC |
| 661 CTCTAACTGG ACTTGGTTCC AACTTCATAT TCCATCCACA GAATACAAAA TTAGTGCATG |
| 721 GATTTTCTCC GACCCATTCA GAAACACAGA AACCCGTTTT GCAACTATTA GAGGTGCAAA |

TABLE A.11: Nucleotide sequence of *Nha*-KHS. Sequence optimized for expression in *P. pastoris* (5′→ 3′).

| |
|---|
| 781 TGATGAAACA CTGGTACTAC CTTTGGAATT TACACCAATC TACAAAAGAA CCTACGAATC |
| 841 TGCCACCGGA AGAGTTACAT ATCCTCTTGA TTGGAAATTG AAGATTTCCG GATTCGGTGA |
| 901 TTTCAAACTT AGTTCTTATA CAGAAGATCA AGAGCTAGTT GGTGAAGATG CCCTTCAAAC |
| 961 AGCATACGAG GGATTCATTA CCTTCAGTGG TAATGTGCAC TCTAAACCCG TGCAGGGGTA |
| 1021 TGGCCTTGTG GAAATCGTTT ACAGTACTTG GGATGTCCAT CACCATCACC ATCACCATCA |
| 1081 CCATCACTAA GCGGCCGC |

TABLE A.12: Amino acid sequence of *Nha*-KHS. (N-terminus → C-terminus).

| ***Nha*-KHS-His$_{10}$ (39.9 kDa), ACCESSION: XP_003041184.1** |
|---|
| M R A S F L L T A G L A T A A V G R A K S V P K K F P F K P E N S K T T G |
| T N A I P I V Y G L S E S Q P N S V G G S W W S S S Y I T T T N N E Q Y V |
| V L A H Y L D N P V Y T Y F R A S T L N L E T N E Y H Q Y V T V G S S T P |
| N I T T L D V S V G N N G I K S E S E D N L S K L R S Y S N H D N V T F D |
| I T Y D A T T G A V A N G G A G T F Q F G E G L T W E F G L P S A K T E |
| G S L T V H G E K L A I D P A K S H T W Y D R Q W G N T A A I P S N W T |
| W F Q L H I P S T E Y K I S A W I F S D P F R N T E T R F A T I R G A N D E |
| T L V L P L E F T P I Y K R T Y E S A T G R V T Y P L D W K L K I S G F G D |
| F K L S S Y T E D Q E L V G E D A L Q T A Y E G F I T F S G N V H S K P V |
| Q G Y G L V E I V Y S T W D V H H H H H H H H H H |

## A.7 Primers

TABLE A.13: List of primers used for amplification of target genes. Green: *Hind*III restriction side. Gray: *Nde*I restriction side. Blue: *Xho*I restriction side. Brown: *Not*I restriction side. Red: *Eco*RI, restriction side.

| **Primer** | **Sequence** |
|---|---|
| Fw_*Nha*_KHS_*Nde*I | 5′-TATA CATATG CGTGCATCTTTTC-3′ |
| Rw_*Nha*_KHS-His10_*Hind*III | 5′-GCC AAGCTT ATTAGTGATGGTGATGGTGATGGTGAT-GGTGATGAACATCCCACGTGCTG-3′ |
| Fw_*Nha*_KHS-His10_*Nde*I | 5′-ATATA CATATG AGAGCTTCCTTTCTTCTGAC-3′ |
| Rv_*Not*I_Pp_HisOHYs | 5′-GA GCGGCC GCCCTTTAGTGATGGTGATGGTGATG-3′ |
| Fw_alpha_*Xho*I_*Nha*_KHS | 5′-TCT CTCGAG AAGAGAGAGGCCGAAGCTATGAGAG-CTTCCTTTCTTCTG-3′ |
| Rv_*Not*I_Pp_HisOHYs | 5′-GA GCGGCC GCCCTTTAGTGATGGTGATGGTGATG-3′ |
| Fw_nosig_*Eco*RI | 5′- GAAA GAATTC CGAAACGATGAAGTCTGTGCCTAA-GAAATTTC-3′ |
| Rv_*Nha*_*Not*I_Pp_HisOHYs | 5′-GA GCGGCC GCCCTTTAGTGATGGTGATGGTGATG-3′ |
| Fw_Flag_*Nha*_*Eco*RI | 5′-GAAA GAATTC CGAAACGATGGATTACAAAGACGAT-GACGATAAGGAGCTTCCTTTCTTCTGAC-3′ |

TABLE A.13: List of primers used for amplification of target genes. Green: *Hind*III restriction side. Gray: *Nde*I restriction side. Blue: *Xho*I restriction side. Brown: *Not*I restriction side. Red: *EcoRI*, restriction side.

| **Primer** | **Sequence** |
|---|---|
| Rv_*Nha*_*Not*I_Pp_HisOHYs | 5′-GA GCGGCC GCCCTTTAGTGATGGTGATGGTGATG-3′ |

TABLE A.14: List of primers used for site-directed mutagenesis. Green: Codon of alanine. Orange: Reverse complement codon of alanine.

| **Primer** | **Sequence** |
|---|---|
| Fw_N112A_*Nha* | 5′-TTCTTCCACTCCT GCT ATAACTACCTTGG-3′ |
| Rv_N112A_*Nha* | 5′-CCAAGGTAGTTAT AGC AGGAGTGGAAGAA-3′ |
| Fw_N132A_*Nha* | 5′-GAGTCCGAAGAT GCT CTTTCTAAGCTG-3′ |
| Rv_N132A_*Nha* | 5′-CAGCTTAGAAAG AGC ATCTTCGGACTC-3′ |
| Fw_N144A_*Nha* | 5′-TCTAACCATGAT GCT GTGACCTTCGAT-3′ |
| Rv_N144A_*Nha* | 5′-ATCGAAGGTCAC AGC ATCATGGTTAGA-3′ |
| Fw_N219A_*Nha* | 5′-CTATCCCCTCT GCT TGGACTTGGTT-3′ |
| Rv_N219A_*Nha* | 5′-AACCAAGTCCA AGC AGAGGGGATAG-3′ |

## A.8 Amino acid alignments by BLAST®

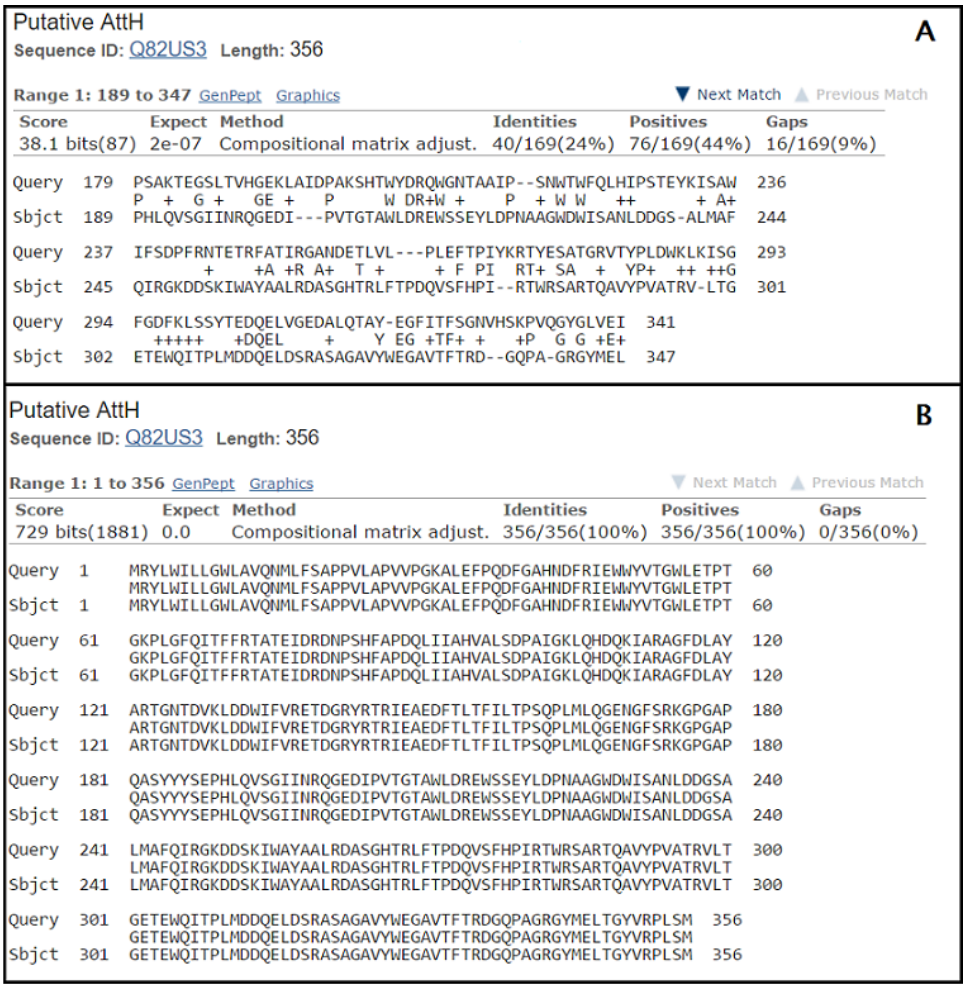


FIGURE A.1: Protein alignments by BLAST®. **(A)** BLAST® Alignment of amino acid sequence of *Nha*-KHS (ACCESSION: XP_003041184.1) as well as highly similar NE1406 protein (ACCESSION: Q82US3), originated in *Nitrosomonas europaea* [33]. **(B)** Identical BLAST® alignment of amino acid sequence of NE1406 protein with carotenoid 1,2-hydratase from *Nitrosomonas europaea*(ACCESSION: WP_011111974.1)

# Bibliography


[1] Lehrman M. A. "Oligosaccharide-based information in endoplasmic reticulum quality control and other biological systems." In: *J. Biol. Chem.* 276 (2001). DOI: 10.1074/jbc.R100002200.

[2] McPhersona A. and Gavirab J. A. "Introduction to protein crystallization." In: *Akta Crys.* 70 (2014). DOI: 10.1107/S2053230X13033141.

[3] Ahmad M. *et al.* "Protein expression in *Pichia pastoris*: recent achievements and perspectives for heterologous protein production." In: *Appl Microbiol Biotechnol.* 98.12 (2014). DOI: 10.1007/s00253-014-5732-5.

[4] Chain P. *et al.* "Complete Genome Sequence of the Ammonia-Oxidizing Bacterium and Obligate Chemolithoautotroph *Nitrosomonas europaea*." In: *J. Bacteriol.* 185.9 (2003). DOI: 10.1128/JB.185.9.2759-2773.2003.

[5] SCOP database. *Entry of AttH-like proteins*. 2009. URL: http://scop.mrc-lmb.cam.ac.uk/scop/data/scop.b.c.bai.b.b.A.html (visited on 09/02/2016).

[6] Dovala D. *et al.* "Rapid analysis of protein expression and solubility with the SpyTag–SpyCatcher system.." In: *Proteins* 117 (2016). DOI: 10.1016/j.pep.2015.09.021.

[7] Cleveland T. E. and Smith D. A. "Partial purification, and further characterization, of kievitone hydratase from cell-free culture filtrates of *Fusarium solani f. sp. phaseoli*". In: *Physiological Plant Pathology* 22 (1983).

[8] El-Heliebi A. "Improving esterases for activity towards alternative substrates." MA thesis. Graz University of Technology, 2009.

[9] Nising C. F. and Bräse S. "Recent developments in the field of oxa-Michael reactions." In: *Chem. Soc. Rev.* 41.3 (2012). DOI: 10.1039/c1cs15167c.

[10] Stevens J. F., Taylor A. W., and Deinzer M. L. "Quantitative analysis of xanthohumol and related prenylflavonoids in hops and beer by liquid chromatography-tandem mass spectrometry." In: *Journal of Chromatography A.* 832 (1999).

[11] Agnihotri G. and Liu H. W. "Enoyl-CoA hydratase. reaction, mechanism, and inhibition." In: *Bioorg. Med. Chem.* 11.1 (2003). DOI: 10.1016/S0968-0896(02)00333-4.

[12] Gabriel S. "Expression, Purification and Initial Characterization of Fungal Hydratases." MA thesis. Graz University of Technology, 2016.

[13] Haid A. and Suissa M. "Immunochemical identification of membrane proteins after sodium dodecyl sulfate-polyacrylamide gel electrophoresis." In: *Methods Enzymology* 96 (1983).

[14] Hellwig S. *et al.* "Analysis of single-chain antibody production in *Pichia pastoris* using on-line methanol control in fed-batch and mixed-feed fermentations." In: *Biotechnology and Bioengineering* 74.4 (2001). DOI: 10.1002/bit.1125.

[15] Horvath A. and Riezman H. "Rapid Protein Extraction from *Saccharomyces cerevisiae*." In: *Yeast* 10 (1994).

[16] Drenth J., ed. *Principles of Protein X-ray Crystallography.* 2nd edition. Vol. A: Space Group Symmetry. 1999. ISBN: 978-0-387-33746-3.

[17] Jin J. and Hanefeld U. "The selective addition of water to C=C bonds; enzymes are the best chemists." In: *ChemComm* 47 (2011). DOI: 10.1039/c0cc04153j.

[18] Junker M. and Clark P. L. "Slow formation of aggregation-resistant beta-sheet folding intermediates.." In: *Proteins* 78.4 (2010). DOI: 10.1002/prot.22609.

[19] Näätsaari L. and *et al.* "Deletion of the Pichia pastoris *KU70* Homologue Facilitates Platform Strain Generation for Gene Expression and Synthetic Biology." In: *PLoS ONE* 7.6 (2012). DOI: 10.1371/journal.pone.0039720.

[20] Balabin R. M. "Polar (Acyclic) Isomer of Formic Acid Dimer: Gas-Phase Raman Spectroscopy Study and Thermodynamic Parameters." In: *J. Phys. Chem. A.* 113.17 (2009).

[21] Engleder M. MA thesis. Graz University of Technology, 2014.

[22] Engleder M. et al. "Structure-Based Mechanism of Oleate Hydratase from Elizabethkingia meningoseptica." In: *Chembiochem.* 16.12 (2015). DOI: 10.1002/cbic.201500269.

[23] Novagen by Merck Millipore. *pET26b(+) Vector and Restriction Map*. 1998. URL: http://www.synthesisgene.com/vector/pET-26b.pdf (visited on 08/27/2016).

[24] Flower D. R. "Structural relationship of streptavidin to the calycin protein superfamily." In: *FEBS Lett.* 333 (1993).

[25] Flower D. R., North A. C., and Sansom C. E. "The lipocalin protein family: structural and sequence overview." In: *Biochim Biophys Acta.* 1482 (2000).

[26] Gurdeep R. and Chatwal A. M., eds. *Synthetic Dyes For B.Sc. and M.Sc. Students of Indian Universities 3rd Revised.* 2007. ISBN: 9788183187701.

[27] Waterham H. R.*et al.* "Peroxisomal Targeting, Import, and Assembly of Alcohol Oxidase in *Pichia pastoris*." In: *J Cell Biol.* 139.6 (1997).

[28] Schwartz T. U. *et al.* "Homodimerization of the G protein SR$\beta$ in the nucleotide-free state involves proline cis/trans isomerization in the switch II region." In: *Proceedings of the National Academy of Sciences of the United States of America (PNAS)* 103.18 (2006).

[29] Hahn T., ed. *International Tables for Crystallography.* 5th edition. Vol. A: Space Group Symmetry. 2002. ISBN: 978-0-7923-6590-7. DOI: 10.1107/97809553602060000100.

[30] Artimo P. *et al.* "ExPASy: SIB bioinformatics resource portal." In: *Nucleic Acids Res.* 40 (2012).

[31] Athmaram T. N. *et al.* "A simple *Pichia pastoris* fermentation and downstream processing strategy for making recombinant pandemic Swine Origin Influenza a virus Hemagglutinin protein." In: *J. Ind. Microbio. Biotechnol.* 40 (2013). DOI: 10.1016/S0968-0896(02)00333-4.

[32] Boersma A. J. *et al.* "Catalytic enantioselective syn hydration of enones in water using a DNA-based catalyst." In: *Nat. Chem.* 2 (2010). DOI: 10.1038/nchem.819.

[33] Chiu H.-J. *et al.* "Structure of the first representative of Pfam family PF09410 (DUF2006) reveals a structural signature of the calycin superfamily that suggests a role in lipid metabolism." In: *Acta Crystallogr Sect F Struct Biol Cryst Commun.* 66 (2010). DOI: 10.1107/S1744309109037749.

[34] Coulton A. T. *et al.* "The recruitment of acetylated and unacetylated tropomyosin to distinct actin polymers permits the discrete regulation of specific myosins in fission yeast." In: *J. Cell. Sci.* 123 (2010).

[35] Dwek R.A. *et al.* "Targeting glycosylation as a therapeutic approach." In: *Nat. Rev. Drug Discov.* 1 (2002). DOI: 10.1074/jbc.R100002200.

[36] Gerhauser C. *et al.* "Cancer Chemopreventive Activity of Xanthohumol, a Natural Product Derived from Hop." In: *Molecular Cancer Therapeutics* 1 (2002). DOI: 10.1016/j.chroma.2006.08.019.

[37] Goto Y. *et al.* "N-glycosylation is required for secretion and enzymatic activity of human hyaluronidase1." In: *FEBS Open Bio.* 4 (2014). DOI: 10.1016/j.fob.2014.06.001.

[38] Hiramatsu N. *et al.* "Secreted protein-based reporter systems for monitoring inflammatory events: critical interference by endoplasmic reticulum stress." In: *J. Immunol. Methods.* 315 (2006). DOI: 10.1016/j.jim.2006.07.003.

[39] Li D. *et al.* "The *Fusarium solani* gene encoding kievitone hydratase, a secreted enzyme that catalyzes detoxification of a bean phytoalexin." In: *Mol. Plant Microbe Interact.* 8 (1995).

[40] Liu W.-C. *et al.* "Scaling-up Fermentation of *Pichia pastoris* to demonstration-scale using new methanol-feeding strategy and increased air pressure instead of pure oxygen supplement." In: *Nature Scientific Reports* 6 (2016). DOI: 10.1038/srep18439.

[41] Lomize M. A. *et al.* "OPM: orientations of proteins in membranes database." In: *Bioinformatics* 22.5 (2006). DOI: 10.1093/bioinformatics/btk023.

[42] Magalhaes P. J. *et al.* "Analysis of xanthohumol and isoxanthohumol in different hop products by liquid chromatography-diode array detection-electrospray ionization tandem mass spectrometry." In: *Journal of Chromatography A.* 1150 (2007). DOI: 10.1016/j.chroma.2006.08.019.

[43] Maurer M. *et al.* "Versatile modeling and optimization of fed batch processes for the production of secreted heterologous proteins with *Pichia pastoris*." In: *Microb. Cell* 5 (2006). DOI: 10.1038/srep18439.

[44] Milligan S. R. *et al.* "The endocrine activities of 8-prenylnaringenin and related hops *(Humulus lupulus L.)* flavanoids." In: *JCE and M* 85.12 (2000). DOI: 10.1210/jcem.85.12.7168.

[45] Rezaee M. *et al.* "Determination of organic compounds in water using dispersive liquid–liquid microextraction." In: *Journal of Chromatography A.* 1116.1-2 (2006). DOI: 10.1016/j.chroma.2006.03.007.

[46] Turbek C. S. *et al.* "Induction and purification of kievitone hydratase from *Fusarium solani f. sp. phaseoli*." In: *Phytochemistry.* 29 (1990).

[47] Van Damme P. *et al.* "NatF Contributes to an Evolutionary Shift in Protein N-Terminal Acetylation and Is Important for Normal Chromosome Segregation." In: *PLoS Genetics* 7.7 (2011). DOI: :10.1371/journal.pgen.1002169.

[48] Tolner B. *et al.* "Production of recombinant protein in *Pichia pastoris* by fermentation." In: *Nature Protocols* 1.2 (2006). DOI: 10.1038/nprot.2006.126.

[49] Resch V. and Hanefeld U. "The selective addition of water". In: *Catal. Sci. Technol.* 5 (2015).

[50] Ruddock L. W. and Molinari M. "N-glycan processing in ER quality control." In: *J. Cell Sci.* 119 (2006). DOI: 10.1242/jcs.03225.

[51] Feng X. and Yung J. "Catalytic enantioselective boron conjugate addition to cyclic carbonyl compounds: a new approach to cyclic beta-hydroxy carbonyls." In: *Chem. Comm. (Camb.)* 43 (2009). DOI: 10.1039/b914207j.